"New Insights in Black Hole Physics from Holography", IFT
Madrid, 19 June, 2025

Holographic QFTs on constant curvature manifolds and phase transitions

Elias Kiritsis

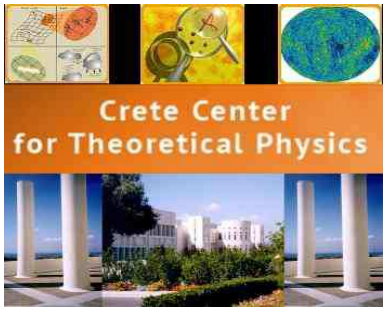

Bibliography

Work with:

Ahmad Ghodsi, Francesco Nitti, Parisa Mashayekhi,
Published in ArXiv:2505.23366

Francesco Nitti, Jean-Loup Raymond
Published in ArXiv:2505.10703

Jani Kastikainen, Francesco Nitti
Published in ArXiv:2502.04036

Ahmad Ghodsi, Francesco Nitti
Published in ArXiv:2409.02879
Published in ArXiv:2309.04880

Ahmad Ghodsi, Francesco Nitti, Valentin Noury
Published in ArXiv:2209.12094

Introduction-I

- Most of the time we analyze QFT on flat space.

- There are, however, many good reasons to analyze QFT on fixed curved spaces.

♠ QFT on spheres:

- It is standard in order to introduce a mass gap and avoid IR divergences.

- It is important in the computation of susy indices.

- It is important in order to define F-functions in three dimensions.

♠ The analytic continuation of the above is QFT On de Sitter space.

• It seems that both during a period of inflation and today we are living in parts of de Sitter.

• QFT has many secrets when it is on de Sitter:

• Massless particles make perturbation theory break-down.

• It is not yet clear how to define useful diff-invariant quantities in de Sitter.

• There are many very different representations of the de Sitter group that can be realized. It is not clear which ones exist in a given QFT.

QFT on AdS

• It was suggested so that it can cure IR problems in gauge theories while still staying at infinite volume.

Callan+Wilczek

• Major differences can appear in the dynamics of confining theories.

Aharony+Marolf+Rangamani

• CFT on AdS can be mapped via a conformal transformation to Boundary CFT.

• Conformal Holographic defects are described by CFT on AdS×S.

• QFT$_d$ on AdS$_d$ gives rise to "rigid" Holography as its boundary S-matrix carries the symmetry of AdS: O(2,d-1), and can be identified with the correlation functions of a (non-local) CFT in d-1 dimensions.

Fitzpatrick+Katz+Poland+Simmons-Duffin,Penedones

• One reason this is useful, is that it can be used to study S-matrix elements both in AdS and flat space by using the boundary bootstrap.

Paulos+Penedones+Toledo+van Rees+Viera

The holographic picture

• A natural (d+1)-dimensional metric anzatz for the ground state of a QFT$_d$ on a constant curvature manifold M_d is

$$ds^2 = du^2 + e^{2A(u)}\zeta_{\mu\nu}dx^\mu dx^\nu \tag{1}$$

where $\zeta_{\mu\nu}$ is the constant curvature metric on M_d.

• The asymptotics of e^A near the boundary $u \to -\infty$ control the source for the radius of the constant curvature slice metric.

• The ansatz enforces that the source that defines the boundary metric is $\zeta_{\mu\nu}$.

• The ansatz is expected to give us the ground states of this holographic theory.

Interfaces

- The BCFT is a special case of an interface between two CFTs

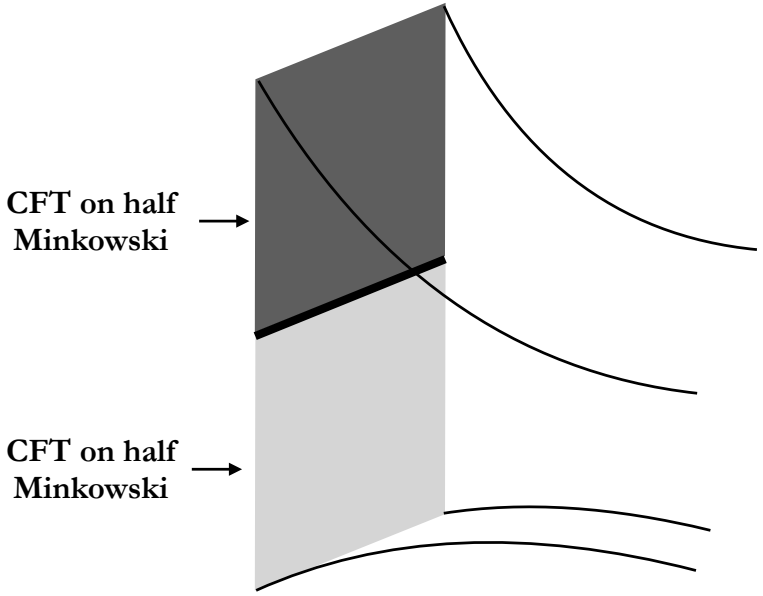

- We may do a conformal transformation on each of the pieces to map it to AdS in Poincaré coordinates with the boundary at the interface.

$$dy^2 - dt^2 + dx^i dx^i \rightarrow \frac{dy^2 - dt^2 + dx^i dx^i}{y^2}$$

- Clearly the two boundaries touch on the interface.

- If the interface is conformal, we expect a O(d,1) symmetry.

Holographic Interfaces

• When the slice manifold has negative constant curvature (like AdS) then the bulk scale factor e^A is not monotonic.

• Such solutions may have "two boundaries"

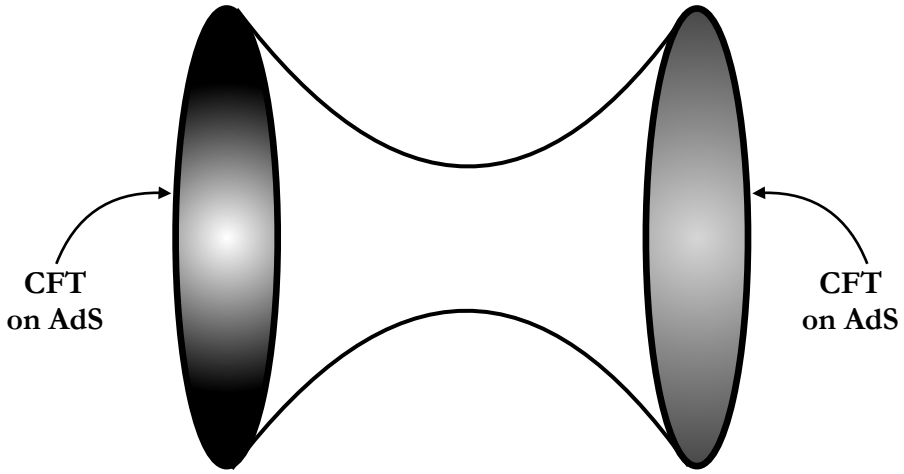

• However, if the slice manifold has infinite volume, the two boundaries are connected

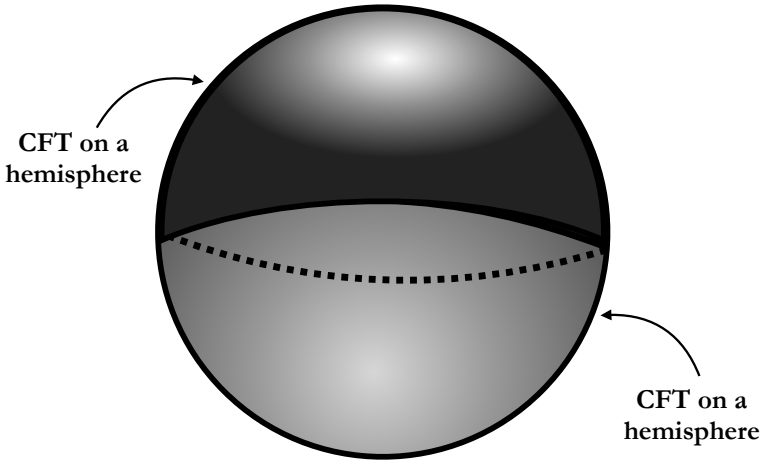

• The simplest example of this is global AdS_{d+1}, sliced with AdS_d slices and

$$e^A = \cosh \frac{u}{\ell} \quad , \quad -\infty < u < +\infty$$

• This is a non-monotonic scale factor.

• In such a case the metric has two (apparent) AdS boundaries. One, B_+, at $u = -\infty$ and another B_- at $u = +\infty$.

• In the bulk AdS case, corresponding to a CFT on AdS_d, the gravitational solution is interpreted as two copies of the (same) CFT: one on $B^+ \sim AdS_d$ and the other on $B_- \sim AdS_d$.

• However, we may turn on more fields and in general the two UV CFTs can be different.

• If the negative curvature manifold M_ζ is compact ($g > 2$ Riemann surface in $d = 2$ or Schottky manifolds in $d > 2$) then the solution describes a wormhole with negative curvature slices.

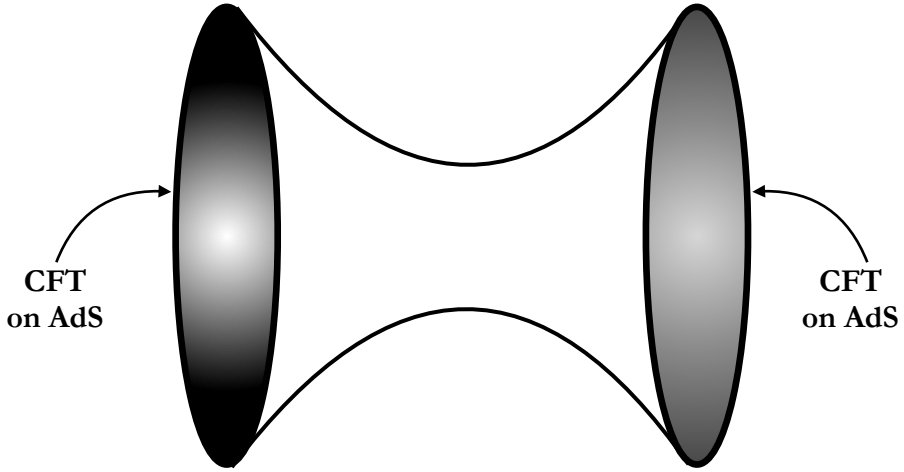

The curved-sliced RG flows

• We assume an Einstein-dilaton theory in order to simplify our explorative task.

• Our finding generalize to themultiscalar case.

$$S_{Bulk} = M_P^{d-1} \int du\, d^d x \sqrt{-g} \left(R - \frac{1}{2} g^{ab} \partial_a \Phi \partial_b \Phi - V(\Phi) \right).$$

$$ds^2 = du^2 + e^{2A(u)} \zeta_{\mu\nu} dx^\mu dx^\nu, \qquad \Phi = \Phi(u)$$

• The slice is a manifold M_ζ whose metric ζ is any (constant) curvature Einstein metric.

$$R^{(\zeta)}_{\mu\nu} = \kappa \zeta_{\mu\nu}\,, \qquad R^{(\zeta)} = d\kappa\,, \qquad \kappa = \pm \frac{(d-1)}{\alpha^2}\,.$$

• The solution is characterized by the scalar field profile $\Phi(u)$ and by the scale factor $A(u)$, which are related via the bulk Einstein equations.

• We systematically study the solutions to these equations for any sign of $R^{(\zeta)}$.

• The regular solutions have generically one boundary except in the case of negative curvature that can have two boundaries $B_\pm$ at $u = \pm\infty$.

• The boundaries are conformal to M_ζ.

• The end-points of the solution depend crucially on $R^{(\zeta)}$ and the scalar bulk potential $V(\Phi)$.

• For $R^{(\zeta)} \geq 0$ they look like

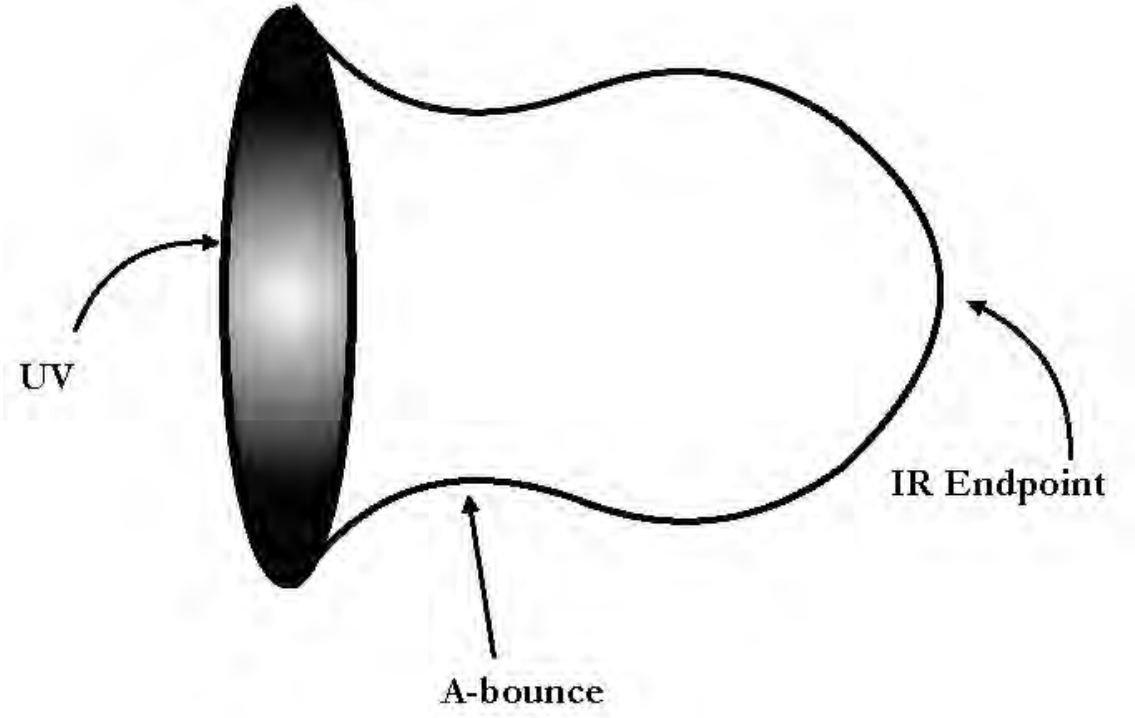

- For $R^{(\zeta)} < 0$

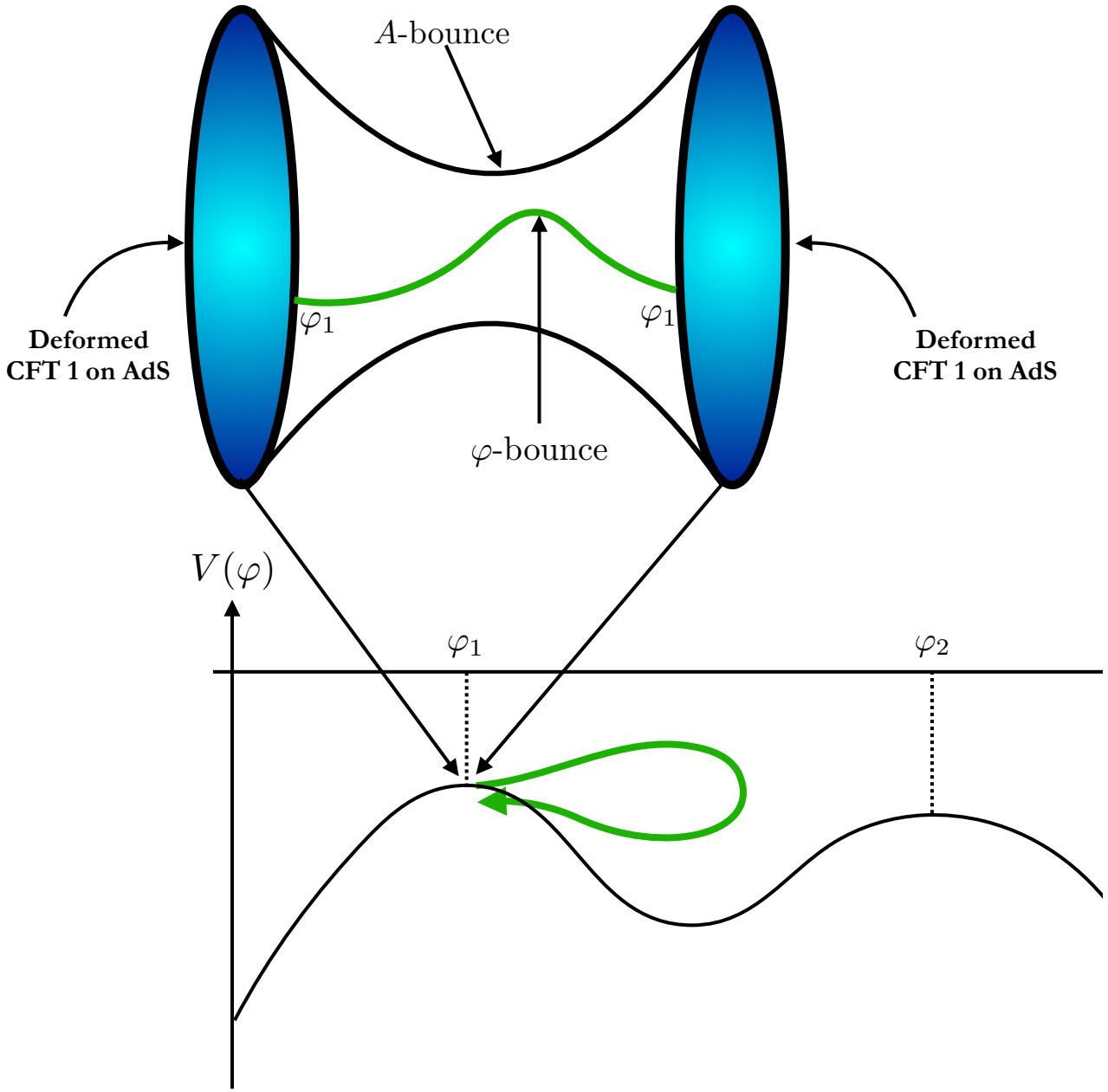
A-bounce
Deformed
CFT 1 on AdS
φ_1
φ_1
Deformed
CFT 1 on AdS
φ-bounce
$V(\varphi)$
φ_1
φ_2

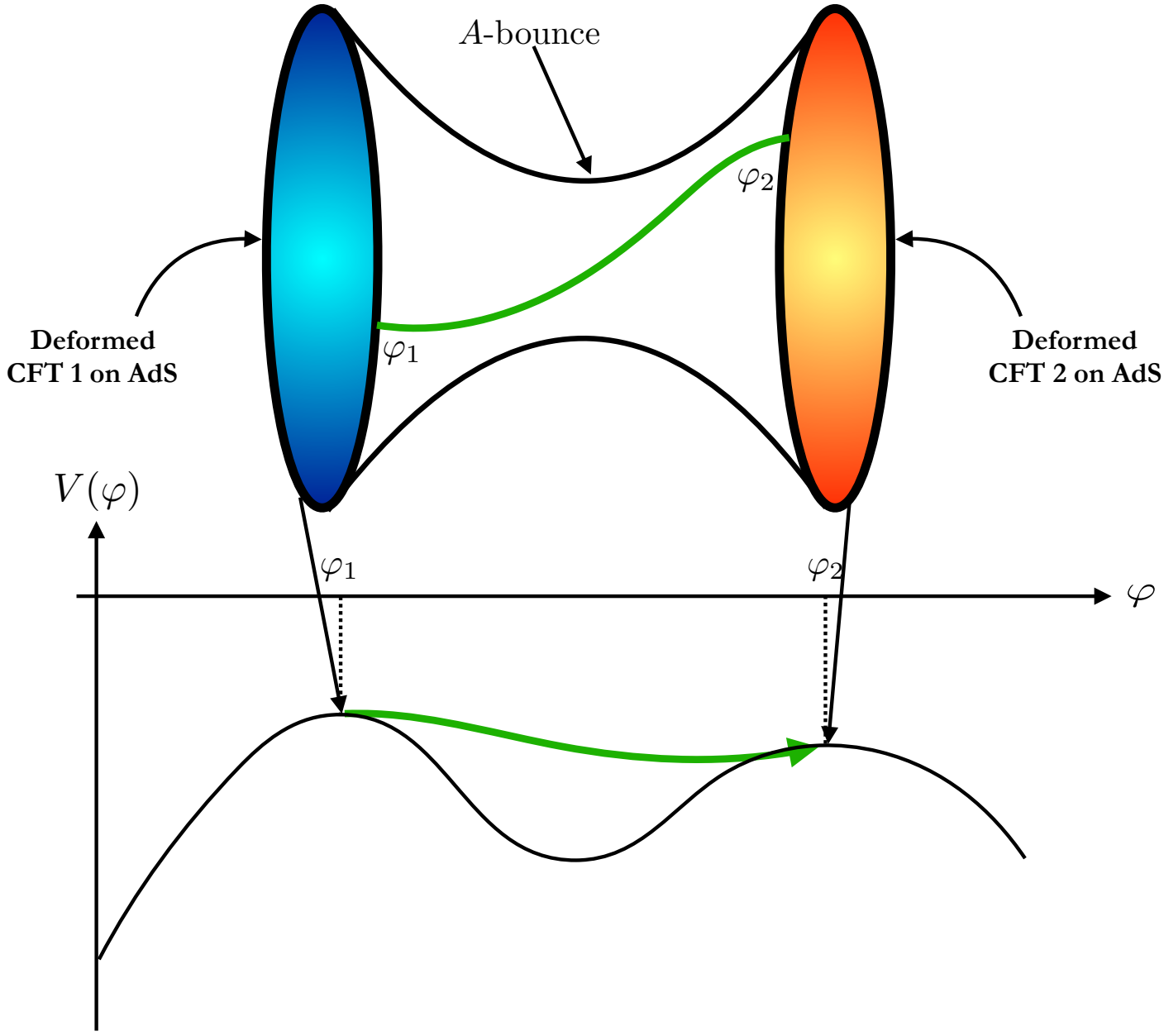

- There are extra rules when we go to $\Phi \to \pm\infty$.

The bulk Einstein Equations

• The solution is characterized by the scalar field profile $\Phi(u)$ and by the scale factor $A(u)$, which are related via the bulk Einstein equations.

$$2(d-1)\ddot{A} + \dot{\Phi}^2 + \frac{2}{d}e^{-2A}R^{(\zeta)} = 0$$

$$d(d-1)\dot{A}^2 - \frac{1}{2}\dot{\Phi}^2 + V(\Phi) - e^{-2A}R^{(\zeta)} = 0$$

$$\ddot{\Phi} + d\dot{A}\dot{\Phi} - V(\Phi)' = 0\,,$$

The first order formalism

- We define the "superpotentials" (no supersymmetry)

$$\dot{A} \equiv -\frac{1}{2(d-1)} W(\Phi)\,, \quad \dot{\Phi} \equiv S(\Phi)\,, \quad R^{(\zeta)} e^{-2A(u)} \equiv T(\Phi)\,.$$

- The equations of motion become

$$\frac{d}{2(d-1)} W^2 + (d-1) S^2 - d S W' + 2V = 0\,,$$

$$S S' - \frac{d}{2(d-1)} S W - V' = 0\,.$$

- Once a solution is found we can evaluate

$$T(\Phi) = \frac{d}{4(d-1)} W^2(\Phi) - \frac{S(\Phi)^2}{2} + V(\Phi)$$

The bulk integration constants vs QFT parameters

• For the flows that describe spaces with a single boundary, they are dual to a single QFT on a constant curvature metric with a relevant coupling, m.

• The bulk equations have three (dimensionless) integration constants.

• One corresponds to the dimensionless curvature $\mathcal{R}$:

$$\mathcal{R} \equiv m^2 \ \alpha_{UV}^2$$

• The second corresponds to the (dimensionless) scalar vev $\langle O \rangle$. It must be tuned for regularity.

• The third is not physical as it can be removed by a radial translation.

♠ In the first order formalism the (W,S) equations have two integration constants: one is $\mathcal{R}$, and the second is the scalar vev.

• The scalar vev, $\sim \mathcal{C}(\mathcal{R})$ is tuned in terms of $\mathcal{R}$ by regularity.

• There is another vev: that of the energy momentum tensor on the constant curvature manifold

$$\langle T_{\mu\nu} \rangle \sim \mathcal{B}(\mathcal{R})\ \zeta_{\mu\nu}$$

• $\mathcal{B}(\mathcal{R})$ is related in a non-trivial way to $\mathcal{C}(\mathcal{R})$

♠ Therefore, for the one-boundary solutions, there is one free parameter (source) $\mathcal{R}$ and two vev parameters $\mathcal{B}(\mathcal{R})$ and $\mathcal{C}(\mathcal{R})$.

Asymptotics near potential extrema

• Regular solutions START (AND SOMETIMES END) at extrema of the potential.

• Near a maximum of the potential, there are two branches of solutions known as the $-$ and the $+$ branch.

$$\ell\, W_{\pm} = 2(d-1) - \frac{\Delta_{\pm}}{2}(\phi - \phi_0)^2 + \cdots$$

♠ The $-$ branch contains the generic solutions that contain both source and vev.

♠ The $+$ branch contains only the special solution for which the source vanishes (relevant vev-driven flow).

• For both types of solutions above, the metric has an AdS boundary at the maximum.

• We denote these asymptotics as $Max_{\pm}$.

• Near a minimum of the potential we also have the $+$ and $-$ branches of solutions.

♠ The $-$ branch contains the generic solution.

• It does not exist for non-zero slice curvature. It exists only for flat slices and in that case it describes the IR-end of an RG flow.

♠ The $+$ branch contains the special solution. The bulk metric has an AdS BOUNDARY in this case

• The $+$ solution describes a UV fixed-point perturbed by the vev of an irrelevant operator.

• In principle, it can exist for both flat and curved slices.

• We denote these asymptotics as $Min_{\pm}$.

- $Max_{\pm}$ and Min_{+} are associated to AdS boundaries and therefore to QFT UV fixed points.

- Min_{-}, to a shrinking slice geometry and therefore to an IR Fixed point.

- The $+$ branch solutions, as they contain less integration constants, exist only in fine-tuned cases.

- The Min_{-} solution does not exist, when the (dimensionless) curvature of the slice $\mathcal{R} \neq 0$.

• When $\mathcal{R} > 0$, here is the possibility that the flow stops at a generic value of $\Phi = \Phi_0$, away from an extremum of the potential.

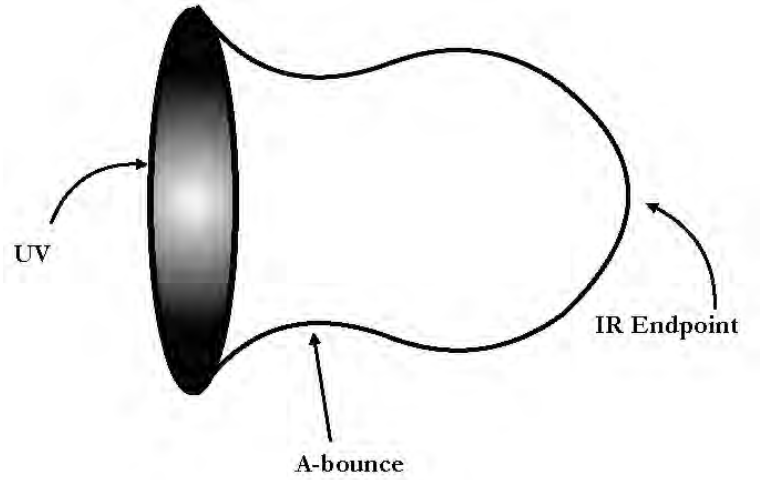

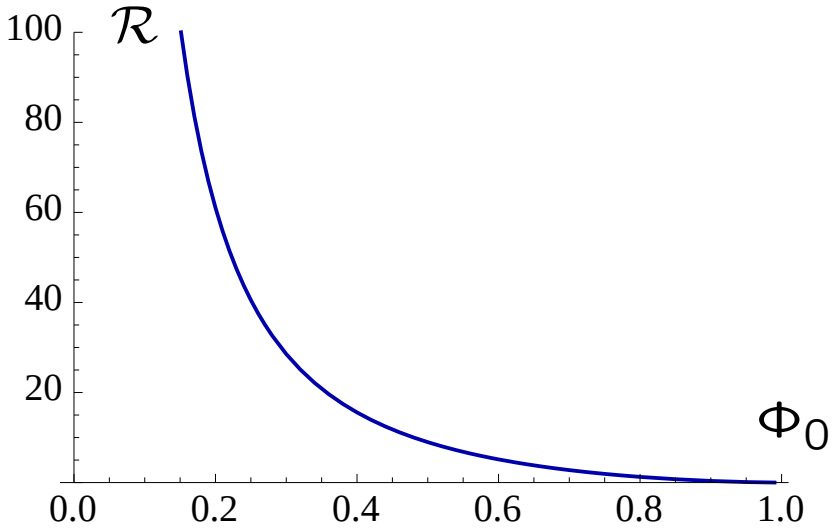

• If Φ_0 is not an extremum of $V(\Phi)$ this is not possible when $\mathcal{R} \leq 0$

• The above classify ALL endpoints where Φ is finite.

Classification of complete flows when $\mathcal{R} = 0$

♠ All flows start and end at extrema of the potential.. They have a single aAdS boundary.

- (Max_-, Min_-). This is the generic flow driven by the coupling of a relevant operator.

- (Max_+, Min_-). This is a flow driven by the vev of a relevant operator.

- (Min_+, Min_-). This is a flow driven by the vev of an irrelevant operator.

Classification of complete flows when $\mathcal{R} > 0$

• In this case, although flows can start at extrema of the potential, (both maxima as $Max_{\pm}$ and minima as Min_{+}), they always end at intermediate points, not at extrema.

• (Max_{-}, Φ_0). This is the generic flow driven by the coupling of a relevant operator.

• (Max_{+}, Φ_0). This is a flow driven by the vev of a relevant operator.

• (Min_{+}, Φ_0). This is a flow driven by the vev of an irrelevant operator.

Classification of complete flows when $\mathcal{R} < 0$

- It is not possible for a flow to be regular and end at intermediate points (non-extrema of the potential).

- Therefore, all regular flows must start and end at extrema of the potential.

- As the asymptotic solution Min_- does not exist when $\mathcal{R} \neq 0$, we have in total the following $3 \times 3 = 9$ options,

$$(Max_- \ , \ Max_+ \ , \ Min_+) \ \otimes \ (Max_- \ , \ Max_+ \ , \ Min_+)$$

all of them having two AdS boundaries.

- (Max_-, Max_-), (Max_+, Max_+).

- (Max_-, Max_+) and its reverse (Max_+, Max_-).

- (Max_-, Min_+) and its reverse, (Min_+, Max_-).

- (Max_+, Min_+) and its reverse, (Min_+, Max_+)

- (Min_+, Min_+).

• As mentioned the Max_+ and Min_+ asymptotics are fine-tuned (they have half the adjustable integration constants).

• Therefore the generic solutions will be of the (Max_-, Max_-) type.

• Single fine-tuning of the potential or the integration constants is needed for the (Max_-, Max_+) and (Max_-, Min_+) solutions to exist.

• Double fine-tuning is needed for (Max_+, Max_+), (Max_+, Min_+) and (Min_+, Min_+) to exist.

Classifying the solutions, $\mathcal{R} < 0$

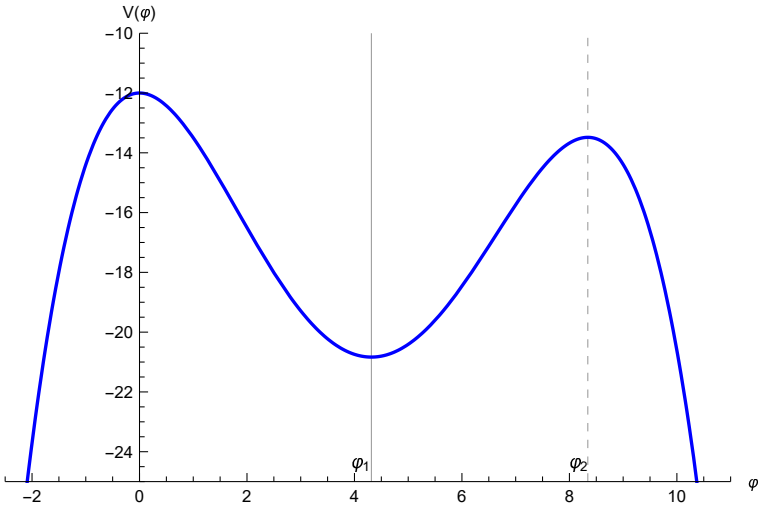

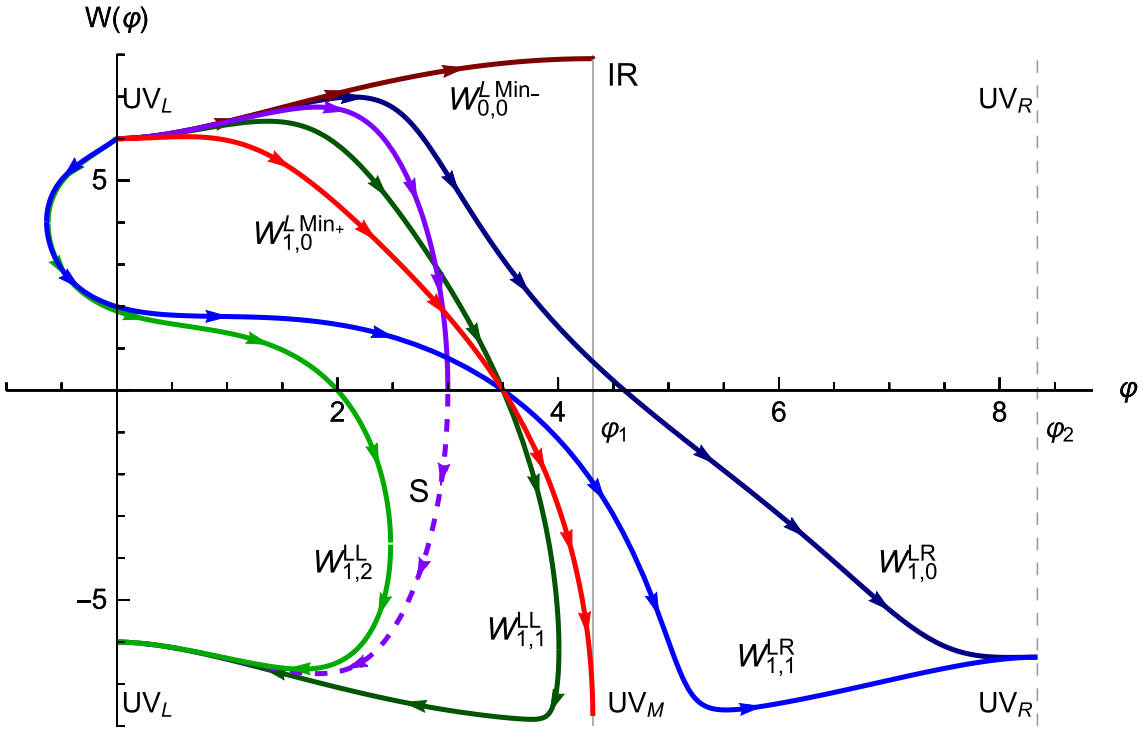

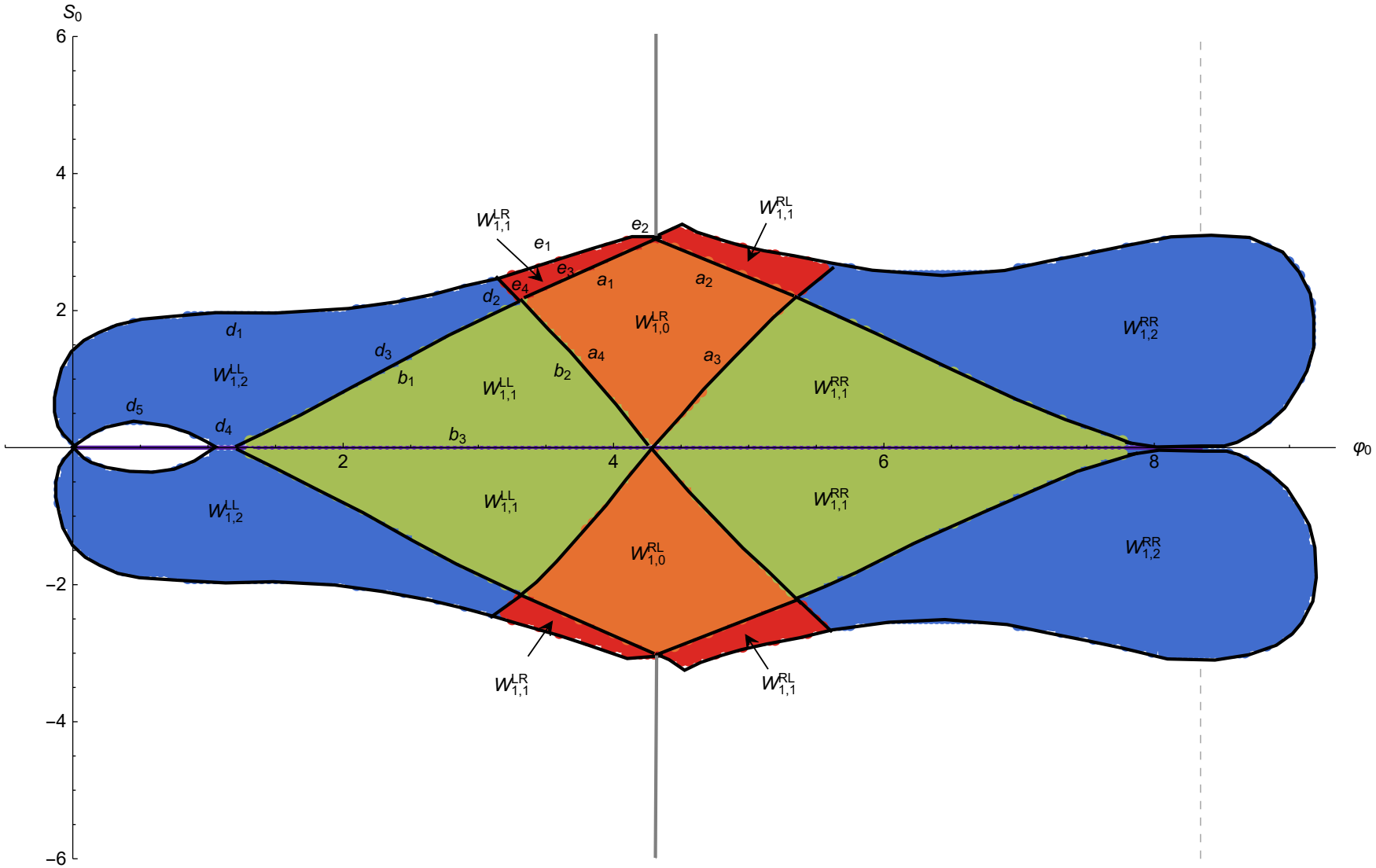
S_0
6
4
2
−2
−4
−6
2
4
6
8
φ_0
$W^{LR}_{1,1}$
e_1
e_2
e_3
e_4
$W^{RL}_{1,1}$
a_1
a_2
a_3
a_4
$W^{LR}_{1,0}$
d_1
d_2
d_3
d_4
d_5
$W^{LL}_{1,2}$
b_1
b_2
b_3
$W^{LL}_{1,1}$
$W^{RR}_{1,1}$
$W^{RR}_{1,2}$
$W^{RL}_{1,0}$

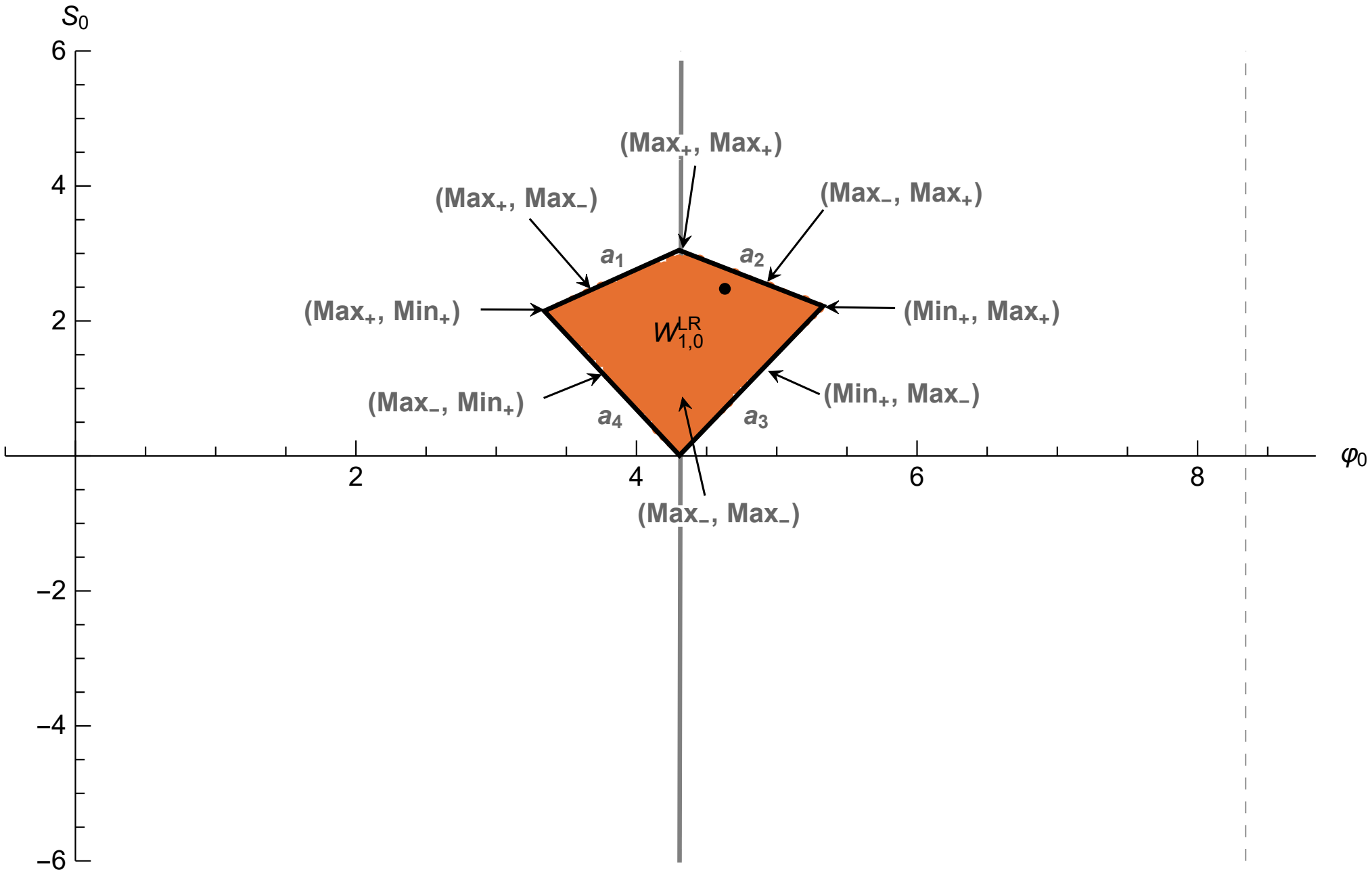
S_0
6
4
2
−2
−4
−6
2
4
6
8
φ_0
(Max$_+$, Max$_+$)
(Max$_+$, Max$_-$)
(Max$_-$, Max$_+$)
a_1
a_2
(Max$_+$, Min$_+$)
(Min$_+$, Max$_+$)
$W^{LR}_{1,0}$
(Max$_-$, Min$_+$)
(Min$_+$, Max$_-$)
a_4
a_3
(Max$_-$, Max$_-$)

Flow fragmentation

• In this limiting region we have an explicit example of solution fragmentation.

• There are two phenomena visible in this example.

♠ Walking. This the phenomenon when an intermediate AdS region appears between the UV and IR, or between UV and UV as is the case here

♠ The emergence of a new boundary.

$$(Max_-, Max_-) \quad \rightarrow \quad (Max_-, Min_-) \quad \oplus \quad (Min+, Max_-)$$

• Such flows can be rotated into cosmological solutions with a cosmological bounce, no singularity and "inflation" at the place of big bag.

The dS RG Flows

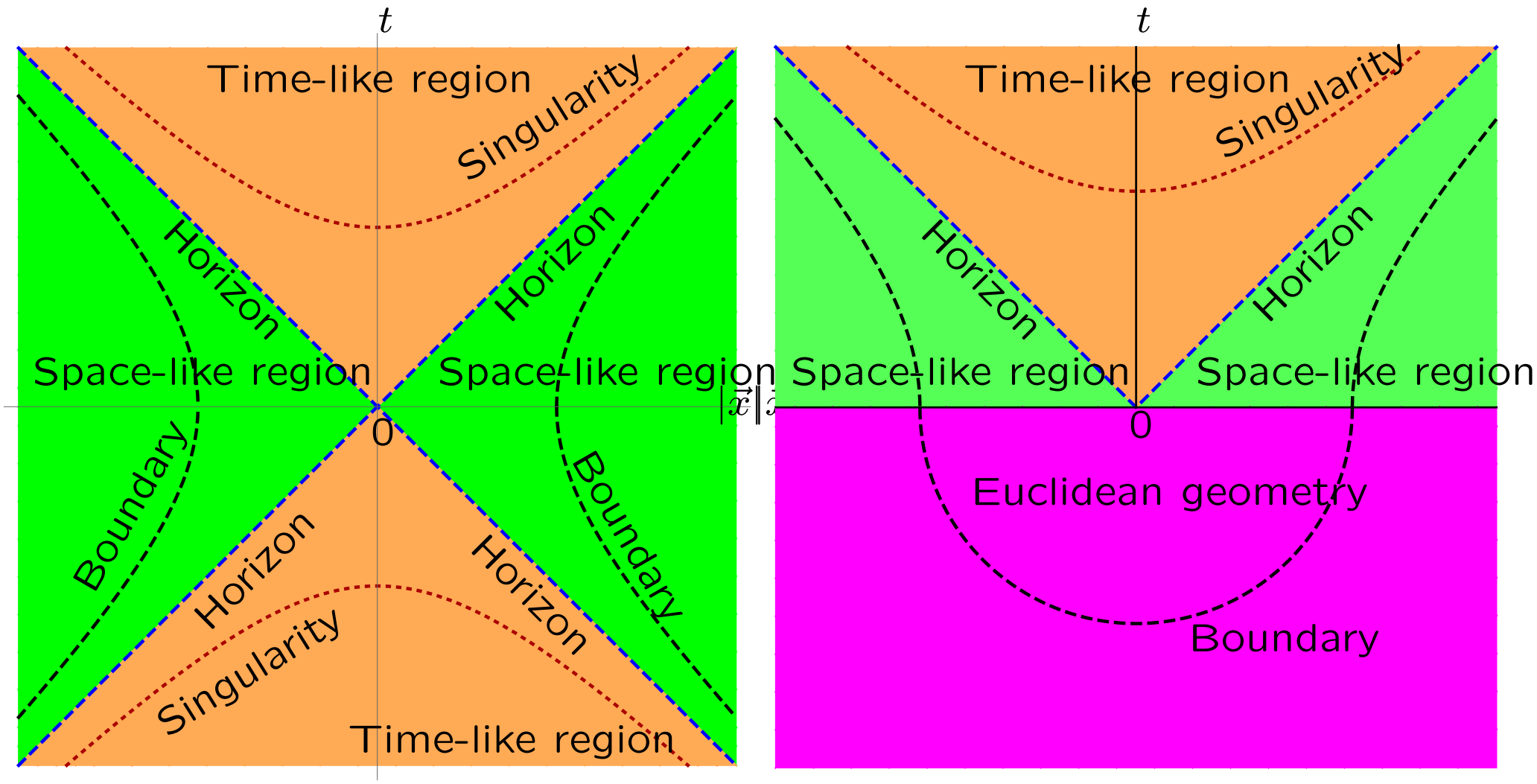

Ghosh+Kiritsis+Nitti+Witkowski

Confining Theories on curved manifolds

• In a single scalar setup, the confining solutions are solutions where the scalar runs off to infinity.

• These are singular solutions (naked singularities)

• But one out of the one-parameter family of solutions is "less" singular.

• This corresponds to a resolvable singularity and can be resolved by KK states.

Gubser: the good, the bad and the naked

• Such solutions correspond to confining ground states in flat space.

Gursoy+Kiritsis+Nitti

• All of their aspects (with flat slices) have been studied extensively in the past and are well known and controllable.

• In the case of curved slices new phenomena appear.

Confining theories on curved manifolds, II

- We study Einstein Dilaton theory with a potential.

- We parametrize the boundary behavior of the potential (as $\Phi \to +\infty$), as

$$V \simeq -V_\infty e^{2a\Phi} + \cdots ,$$

where V_∞ and a are two positive constants.

- The non-confining range:

$$0 \quad \leq \quad a \quad < \quad a_C \equiv \sqrt{\frac{1}{2(d-1)}}.$$

- The confining range:

$$a_C \quad < \quad a \quad < \quad a_G \equiv \sqrt{\frac{d}{2(d-1)}}$$

- The Gubser-violating range:

$$a \quad > \quad a_G$$

- We are interested in the confining range.

- There are three types of asymptotic solutions:

♠ **Type 0** solutions. These have all the integration constants but are too singular to be acceptable

♠ **Type I** asymptotics ($S = S_0 e^{a\Phi} + \cdots$)

$$S_0 = \sqrt{\frac{2V_\infty}{d-1}}, \quad W_0 = a\sqrt{8(d-1)V_\infty},$$

They exist only for $\mathcal{R} > 0$.

♠ **Type II** asymptotics:

$$S_0 = a\sqrt{\frac{2V_\infty}{a_G^2 - a^2}}, \quad W_0 = \sqrt{\frac{2V_\infty}{a_G^2 - a^2}},$$

They exist for all real values of $\mathcal{R}$.

Confining Theories on AdS-The space of solutions

• We choose a simple potential with the required asymptotics and a single maximum.

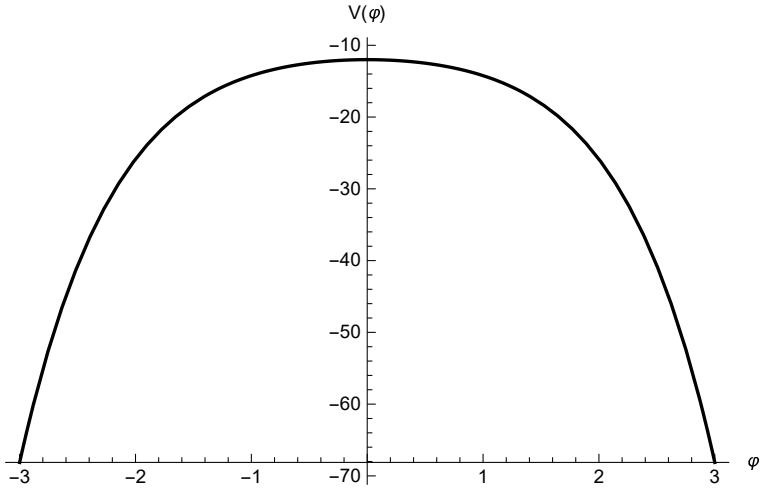

• The theory sitting at the maximum is the UV of the confining QFT.

• With flat metric slices, that solution runs from the maximum to $\Phi \to +\infty$ via a "regular" solution and this is the confining ground-state on flat $\mathbb{R}^d$.

• We now consider solutions with AdS_d slices.

• There are three classes of "regular" solutions

♠ Two-boundary Solutions: They start at $\Phi = 0$ (boundary) and end at $\Phi = 0$ (boundary). These are interface solutions of confining theories.

♠ One-boundary solutions: They start at $\Phi = 0$ (boundary) and end at $\Phi = \pm\infty$ (IR-end point). These are dual to confining theories on AdS_d.

♠ No-boundary solutions: Start at $\Phi = -\infty$ and end at $\Phi = +\infty$ or start at $\Phi = -\infty$ and return back to $\Phi = -\infty$. Topological theories ?

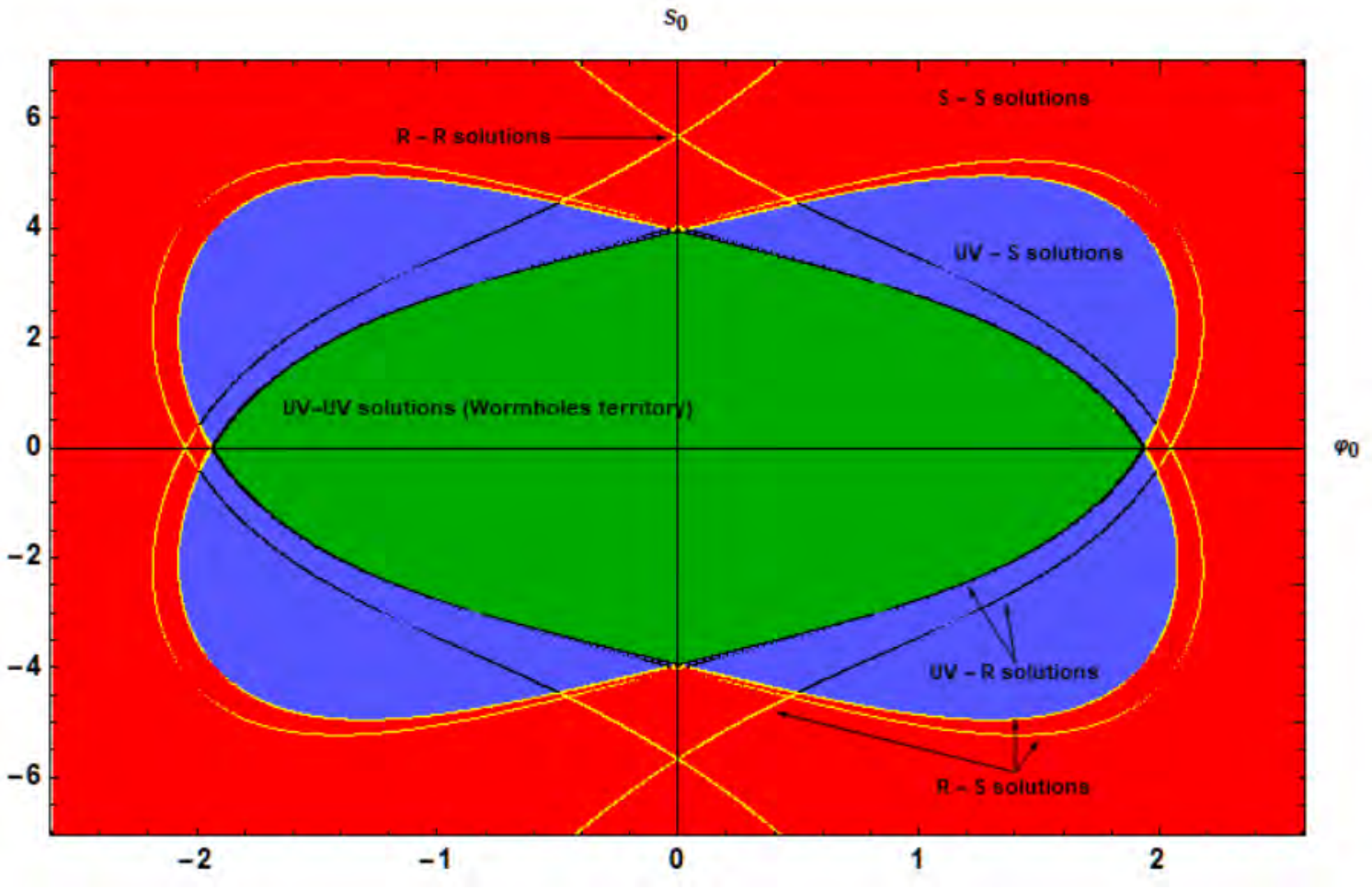
s_0
S – S solutions
R – R solutions
UV – S solutions
UV–UV solutions (Wormholes territory)
UV – R solutions
R – S solutions
φ_0
6
4
2
0
−2
−4
−6
−2
−1
0
1
2

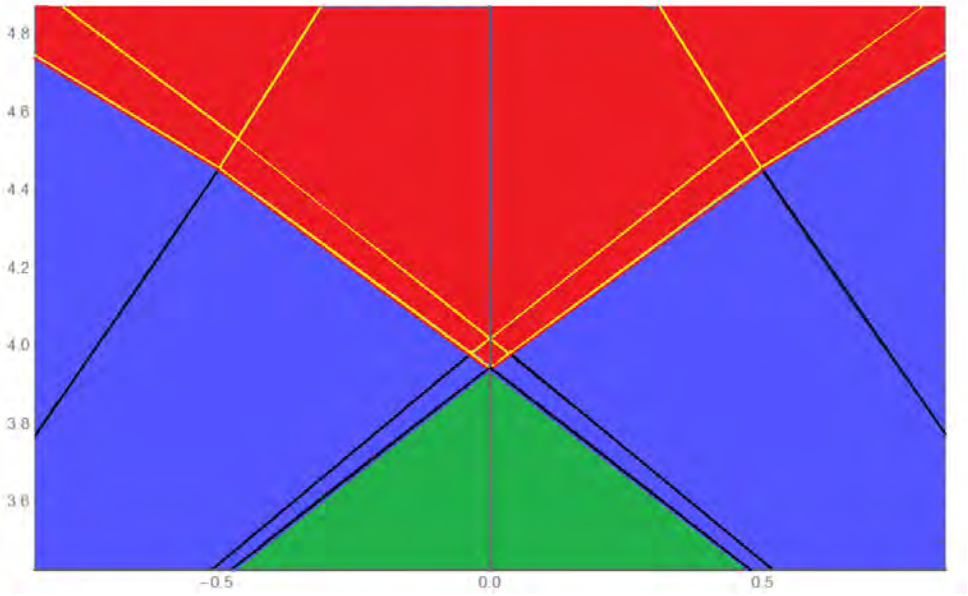
4.8
4.6
4.4
4.2
4.0
3.8
3.6
−0.5
0.0
0.5

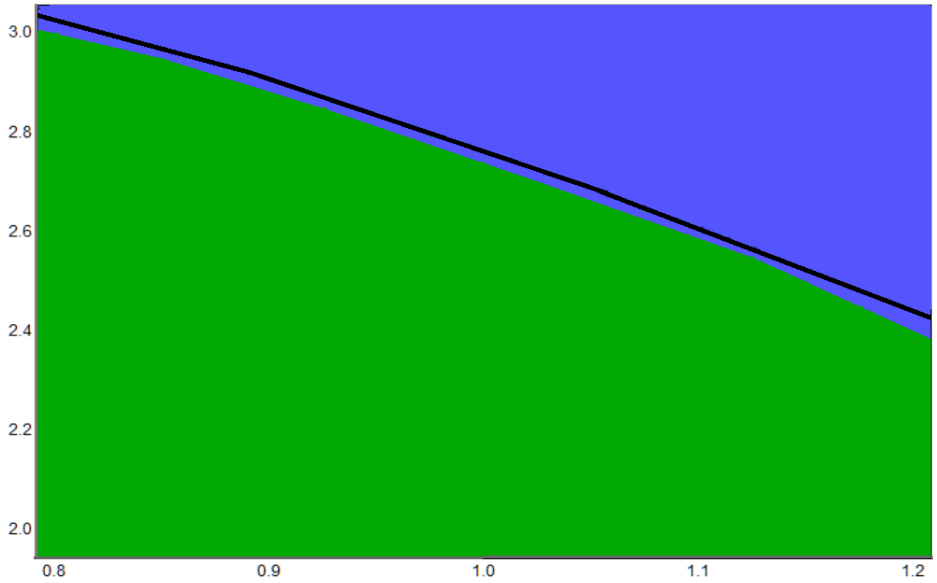
3.0
2.8
2.6
2.4
2.2
2.0
0.8
0.9
1.0
1.1
1.2

AdS: relation to sources

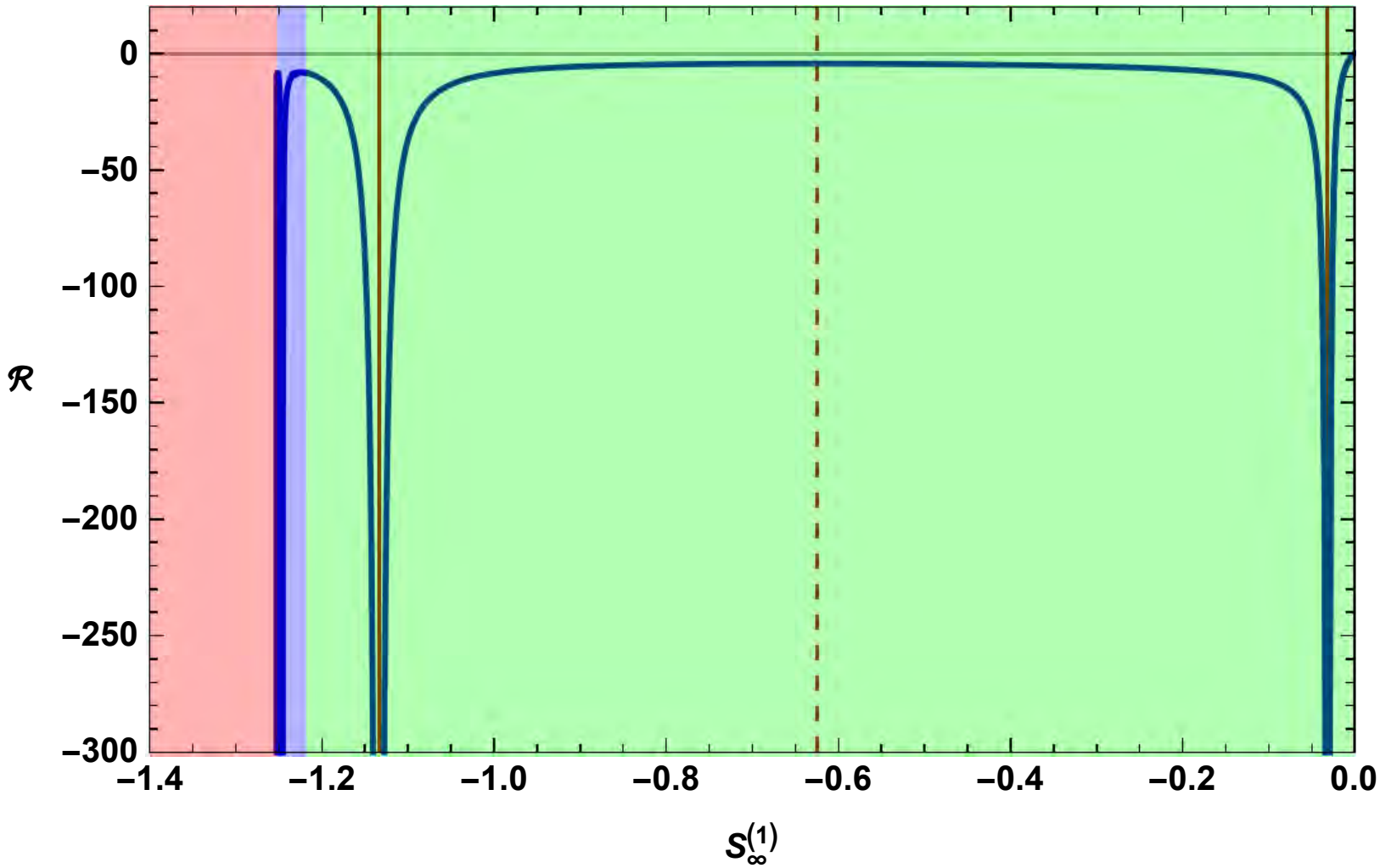

$\mathcal{R}$, the dimensionless curvature, for UV-Reg solutions.

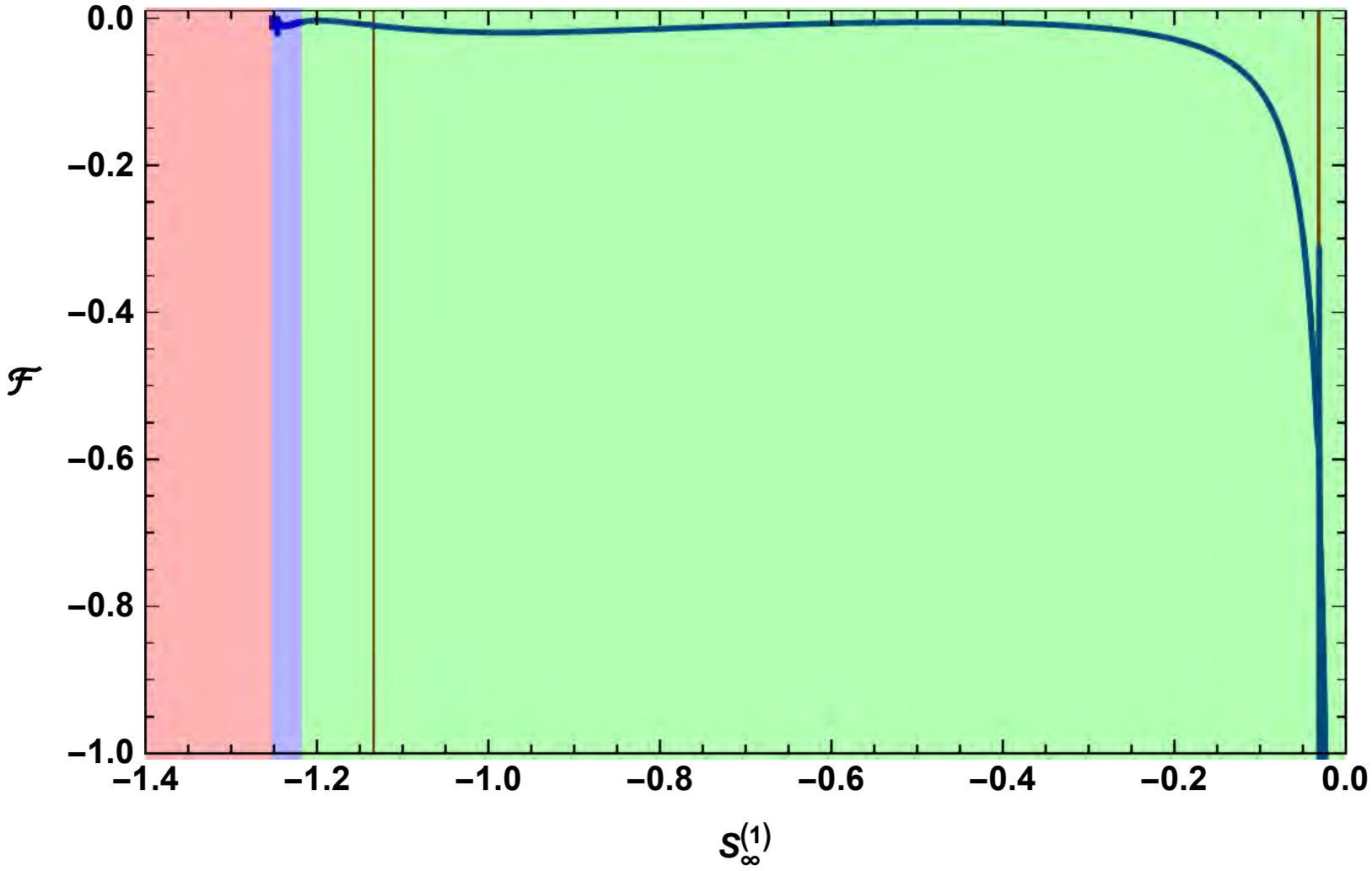

(a): The free energy for UV-Reg solutions living on the black curves. The vertical red lines show the location of Φ-bounces.

The free energy

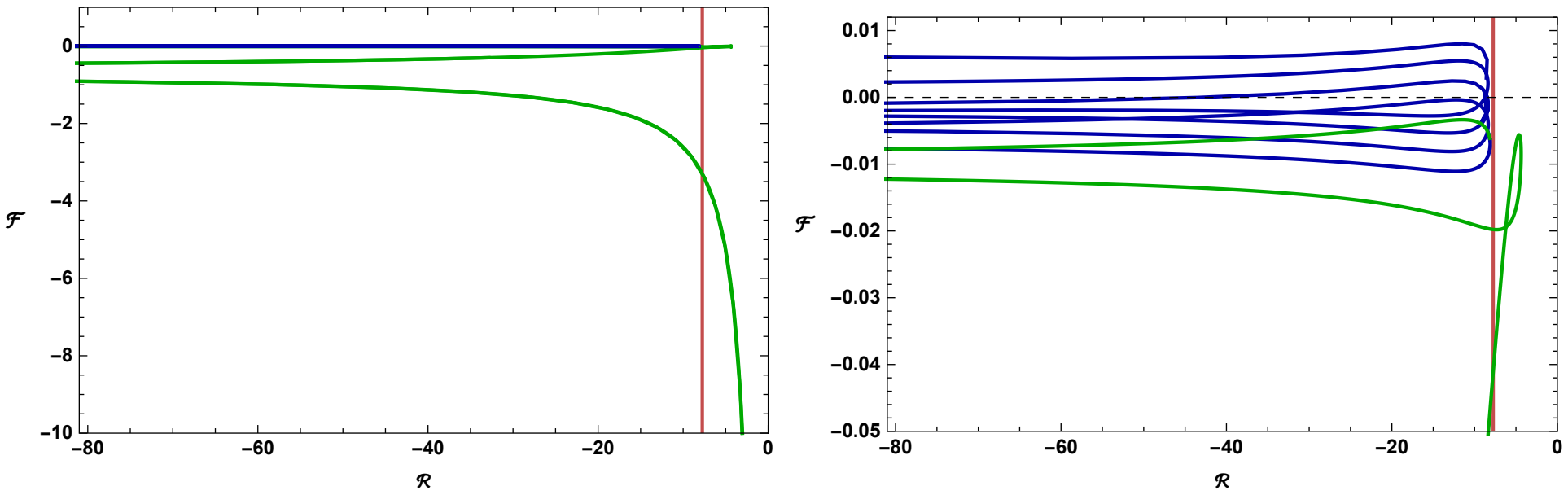

(a): Free energy in terms of dimensionless curvature. The green/blue curves correspond to the green/blue region in previous plots. Figure (b) is the zoomed region near $\mathcal{F} = 0$. The vertical red line shows for $\mathcal{R} \gtrsim -7.7$ only solutions without A-bounce exist.

- The solution with no oscillations has the lowest free energy.

- Is there Efimov scaling here?

Curvature-driven phase transitions and confinement

- We review the possible types of relevant solutions

- $\mathcal{R} > 0$

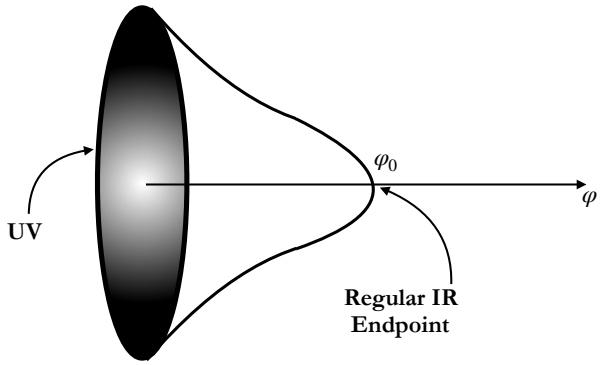

Type III

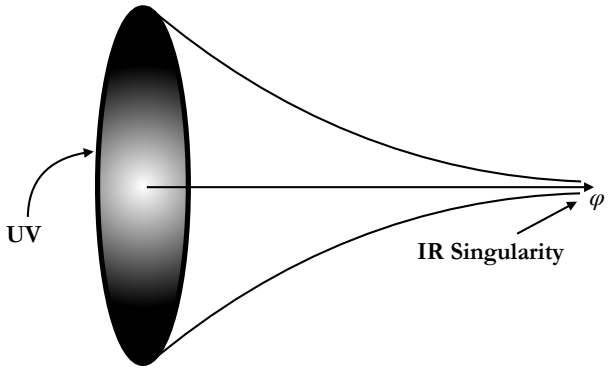

Type I-II

- $\mathcal{R} = 0$: Only type -II

- $\mathcal{R} < 0$: An infinite number of type II solutions competing. No transition here.

- Therefore the transition can happen only at $\mathcal{R} \geq 0$.

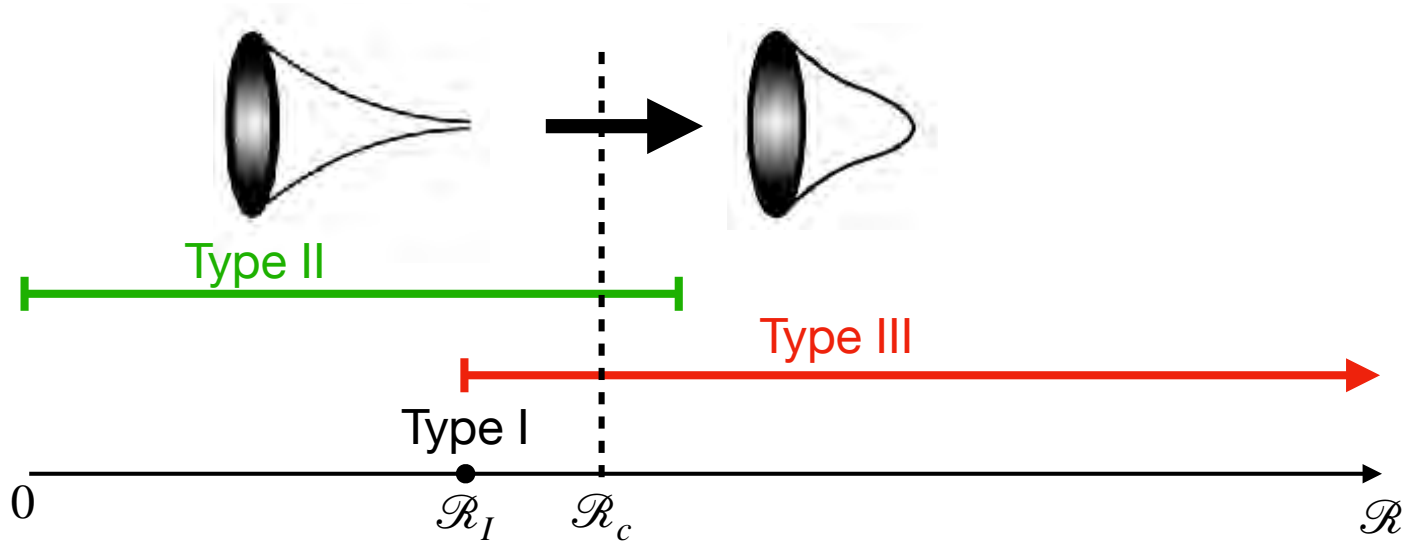

1st order transition

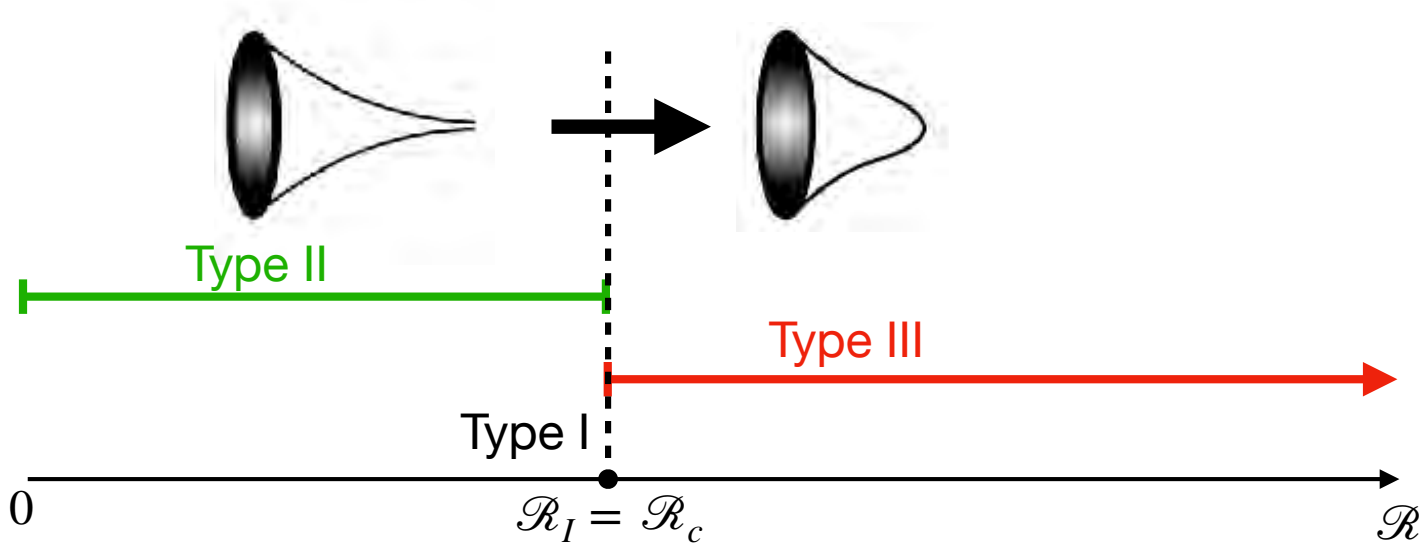

2nd or higher order transition

IHQCD-like theories

$$\varphi \to +\infty : \quad V_\alpha(\varphi) \sim -V_\infty \varphi^\alpha e^{2a_C\varphi} \qquad a_C = \sqrt{\frac{1}{2(d-1)}},$$

• For $\alpha > 0$, the model displays a mass gap, a discrete spectrum of "glueball" excitations and confinement.

• It **does not** have scaling IR asymptotics.

• For $\alpha < 0$ the model has a mas gap, continuous spectrum and is deconfined.

• The asymptotic masses of the (discrete) spectrum behave as

$$m_n^2 \sim n^{N_\alpha} \quad , \quad N_\alpha \equiv \begin{cases} 2\alpha, & 0 < \alpha < 1, \\ \\ 2, & \alpha > 1. \end{cases}$$

• The special value $\alpha = \frac{1}{2}$ leads to Regge-like behavior for the mass eigenstates, $m_n^2 \sim n$.

• This corresponds to the model of IHQCD, that is the bottom model that fits best YM_4 lattice data.

Gursoy+Kiritsis+Nitti

• The models with $a = a_c$ correspond to a bifurcation in the space of confining potentials.

• The model of IHQCD, $a = a_c$ and $\alpha = \frac{1}{2}$ is a double bifurcation on the space of potentials.

• In order to find the phase diagram of this theory as a function of $\mathcal{R}$ we had to use dynamical system methods and in particular "Center Manifold Theory".

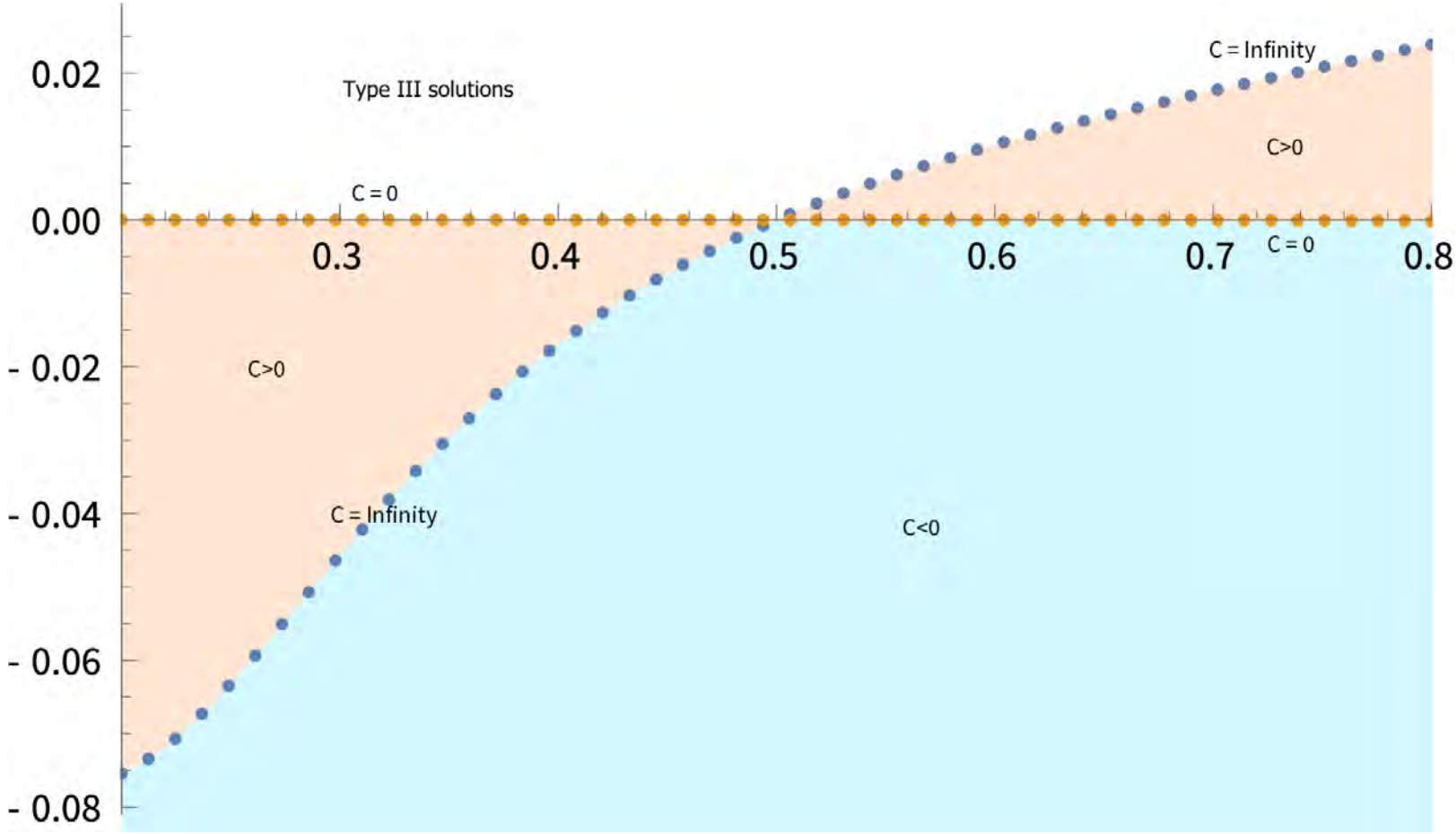

The orange area corresponds to type I/II solutions with $C_\alpha > 0$. The blue area corresponds to type I/II solutions with $C_\alpha < 0$.

Conclusions

- We have studied (RG) flow solutions with slices that have constant curvature manifolds.

- Such solutions have one, two or zero boundaries.

- We have analysed in detail several types of examples.

- There is a rich pattern of dynamical phenomena, including different types of phase transitions.

- We found also many limiting cases where one obtains all possible exotic RG flows.

- Other phenomena found include flow (multi)-fragmentation, walking behavior, and the generation of new boundaries.

- In the $\mathcal{R} < 0$ case, we have found an infinite number of saddle points for confining theories.

- We found phase transitions as a function of curvature for confining theories.

- We have developed the formalism to compute the mass spectra with $\mathcal{R} \neq 0$.

Open Ends

- The case of constructing a single non-confining holographic theory on AdS is still open.

- The study of interface correlators is an open problem.

- The Wilson loops of QFTs on AdS are currently under study, especially considering the fate of confinement.

- The spectra of holographic theories on de Sitter are extremely interesting to investigate.

- Entanglement in single theories as well as interfaces is interesting to compute and decipher.

- The fate of the instanton gas in AdS can be studied with holographic methods.

- There are general results in 2d that state that entanglement transmission is faster than energy transmission. Can they be generalized?

Ooguri+Karch, Bachas+Chen

THANK YOU!

QFT on AdS

- This problem was first seriously adressed by Callan and Wilczek in 1990.

- Their interest was in IR physics.

- Their motivation were the IR divergences that plagued QCD perturbation theory and which made perturbative calculations hard to control.

- The important property of AdS space for their purpose was that even massless fields, had propagators that vanished exponentially as large distances, like massive fields in flat space.

- The reason is that the Laplacian and other relevant operators have a gap in AdS.

- On the other hand, unlike the sphere, AdS has infinite volume.

- Critical systems are described by mean field theory above the upper critical dimension. But AdS acts as an infinite-dimensional space. Therefore critical fluctuations should be weak in any dimension.

- Generically speaking, AdS is expected to "quench" strong IR physics.

- An extra ingredient is that the QFT on AdS must realize the AdS symmetry that is like conformal invariance in one-less dimension.

Callan+Wilczek

- The structure of instantons is also expected to be different:

♠ In flat space, in QCD we expect to have an instanton liquid rather than a (dilute) instanton gas.

Witten

♠ Above the deconfinement phase transition, we expect an instanton gas instead.

- In AdS an instanton gas is generically expected.

Callan+Wilczek

- Chiral invariance for fermions is broken by boundary conditions in AdS.

- An important ingredient for QFT in AdS: boundary conditions.

Conformal Theories on AdS

- The prime example, N=4 SYM was analyzed in some detail in the past.

Gaiotto+Witten,Aharony+Marolf+Rangamani, Aharony+Berdichevsky+Berkooz+Shamir

- Boundary conditions on R^4_+ that preserve supersymmetry have been classified, and there are many.

Gaiotto+Witten

- Upon a conformal transformation the theory can be put on AdS_4 in Poincaré coordinates.

- This is true in general when the AdS metric is with Poinaré coordinates:

$$\mathrm{CFT_d - on - AdS_d} \quad = \quad \mathrm{CFT_d - on - R^d_+} \quad \mathrm{with \quad a \quad flat \quad boundary}$$

- At weak coupling the theory is generically non-confining.

- But at strong coupling some boundary conditions induce confinement.

• For example, using S-duality, the $g >> 1$ theory with a Higgs condensate is mapped to a $g << 1$ theory with a magnetic condensate that should be confining.

• In particular, S-duality interchanges (among others) Dirichlet and Neumann bc.

• With Neumann bc no order parameter exists that distinguishes a confining from a non-confining phase.

• Therefore, no sharp transition is expected in accordance with the large susy.

A confining gauge theory on AdS_4

• There are two types of boundary conditions: electric (Dirichlet) and magnetic (Neumann)

Aharony+Marolf+Rangamani

♠ With electric: gluons are allowed in AdS, they are gapped, and there is an $SU(N)$ global symmetry at weak coupling. Only boundary currents possible.

♠ With magnetic: electric charges are not allowed in bulk, there are O(1) degrees of freedom, and there is confinement (imposed by the bcs).

• There are also many other boundary conditions associated to subgroups.

• For asymptotically free gauge theories with Dirichlet boundary conditions a confinement/deconfinement phase transition is expected

Aharony+Berkooz+Tong+Yankielowicz

♠ $\Lambda L_{Ads} \gg 1$ Confining phase.

♠ $\Lambda L_{AdS} \ll 1$ Deconfined phase.

• With magnetic boundary conditions one expects confinement at all scales, and a free energy of $O(1)$. This is a kind of trivial confinement as no electric charges are allowed in the bulk.

• Wilson loops do not provide an easy criterion for confinement, as for large Wilson loops, the area and the perimeter scale the same way, in global coordinates.

• It is possible that subleading differences may tell the difference.

• But in Poincaré coordinates there are two classes of loops with different behavior for length and area.

• However QFT on AdS in different coordinates gives rise to a different quantum theory.

Rigid Holography

• In standard holography, the flat limit of the bulk AdS_5 gives on one hand the flat space string theory S-matrix and on the gauge theory side a specific correlator at $N \to \infty$.

Polchinski

• A QFT_d on rigid AdS_d provides also a kind of holography.

Fitzpatrick+Katz+Poland+Simmons-Duffin

• All correlation functions have automatically $O(1,d)$ invariance, due to the geometry.

• One may compute scattering amplitudes in the QFT_d-on-AdS_d and write them as CFT_{d-1} correlation functions.

Penedones

• This provides a novel "rigid" holography (without a graviton in the bulk and without energy-momentum tensor in the boundary).

• There is, however, a 1-to-1 correspondence between boundary and bulk operators. This is realized most clearly in the flat CFT with a boundary picture.

• This leads to the idea that one can use this correspondence and the standard bootstrap for the boundary CFT_{d-1} to study the S-matrix constraints in the bulk.

Paulos+Penedones+Toledo+van Rees+Viera

• This can be done at finite bulk curvature constraining the AdS S-matrix.

• Or by taking the curvature to zero, to constraint the flat space S-matrix giving rise to the S-matrix bootstrap.

• Therefore one can use the boostrap on CFT_{d-1} to study the S-matrix constraints in the bulk.

Paulos+Penedones+Toledo+van Rees+Viera, van Rees, Carmi+Di Pietro+Komatsu Giombi+Khanchiandani, Komatsu+Paulos+van Rees+Zhao, Cordova+He+Paulos, Gadde+Sharma, Meineri+Penedones+Spirig

• The zero curvature limit involves a $\Delta \to \infty$ limit in the boundary CFT.

• An important ingredient in rigid holography is that the QFT$_d$-on-AdS$_d$ has generically both UV and IR divergences.

• The IR divergences map in the standard way to UV divergences in the boundary CFT$_{d-1}$.

• The UV divergences in the bulk need to be renormalized in the standard way.

• This entails the renormalization of both bulk coupling constants and boundary conditions.

Banados+Bianchi+Munoz+Skenderis

• In the process the O(1,d) symmetry can be preserved.

• The whole setup can be generalized by adding new dynamical degrees of freedom on the boundary interacting with the bulk degrees of freedom.

BCFT

- A single QFT$_d$-on-AdS$_d$ does not lead to a single rigid holography.

- The reason is that a QFT$_d$-on-AdS$_d$ needs boundary conditions and there are many possibilities compatible with the symmetries.

- Taking the AdS$_d$ metric in Poincaré coordinates, and assuming QFT$_d \to$ CFT$_d$, we can map this problem to BCFT$_d$.

- For a given CFT$_d$, there are many boundary conditions that preserve the O(1,d) conformal symmetry.

- Even in d=2, not all of them are known except in some free field theories.

- When CFT$_d \to$ QFT$_d$, the problem is much more complicated.

Proximity in QFT

• One possible definition of the notion of proximity among CFTs is : can QFT_1 and QFT_2 live in the same Hilbert space?

• If there is flow connecting CFT_1 to CFT_2 we can claim that the two theories can live in the same Hilbert space

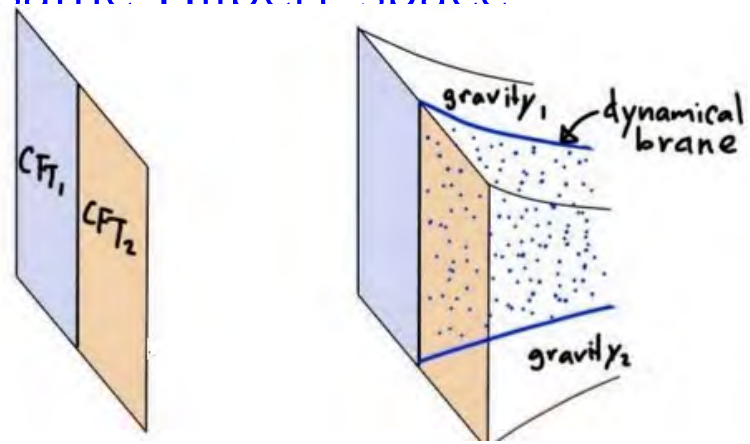

• Proximity can be defined in terms of the possibility for two theories to share an interface.

• They may be generating a bulk brane or

Takayanagi

• They may be like Janus interface geometries.

Bak+Gutperle+Hirano, + many others

Holographic QFT$_d$ on AdS$_d$

• Such a theory is described by a solution in the same ansatz but with only one (not two) boundaries, B$_+$.

• We have therefore three possibilities: QFT$_d$ on AdS$_d$, interface between QFT$_d$ and QFT'$_d$. or a wormhole.

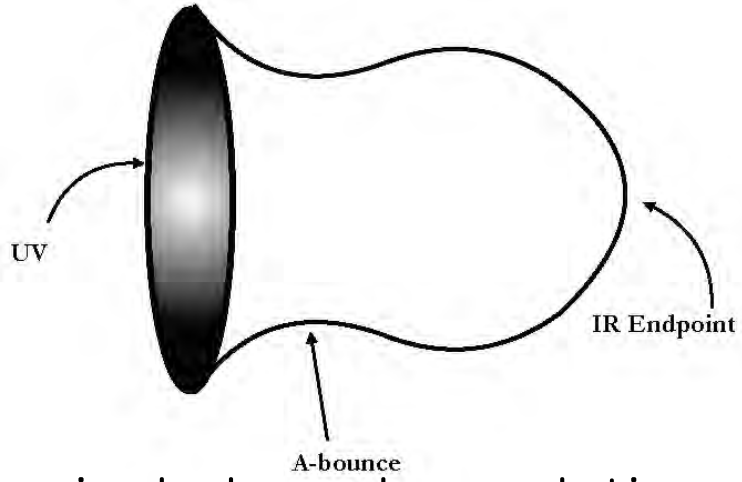

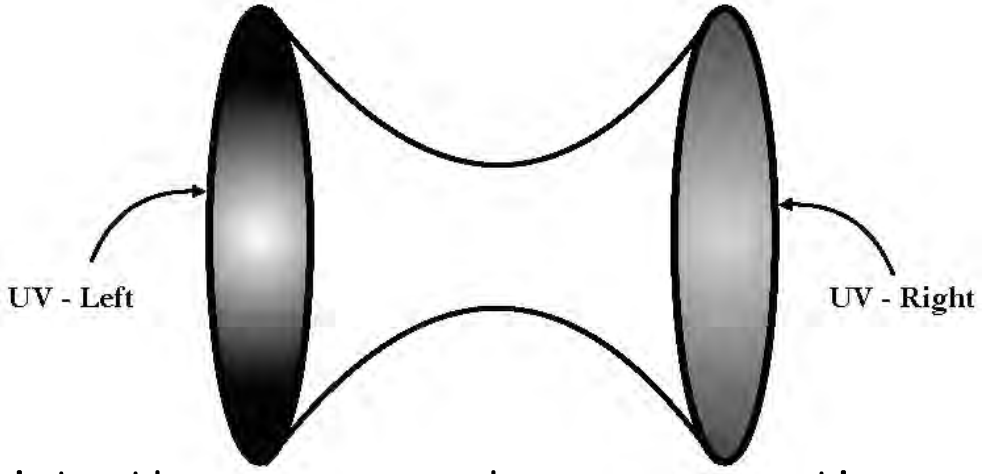

• If a single boundary solution exists then we can have competing saddle points for the two-boundary solutions

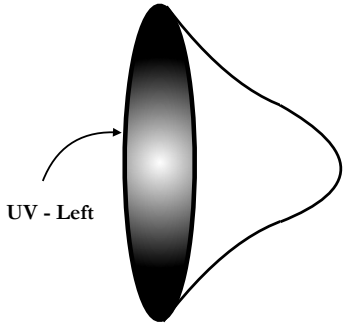

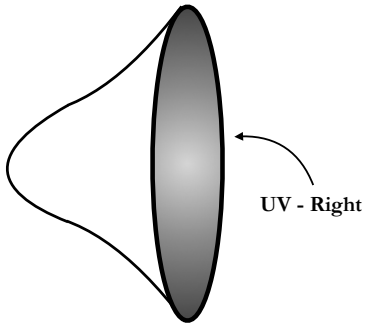

(Holographic) Conformal Defects

• Consider a D-dimensional flat-space QFT, and a $d < D$-dimensional localized (flat-space, non-dynamical) defect.

• This provides a transverse $O(D-d)$ symmetry in the theory.

• Consider also the possibility that the defect is conformal: The associated symmetry is $O(d+1,1)$ and commutes with $O(D-d)$.

• If there is a holographic realization of this, then the geometry should realize the $O(d+1,1) \times O(D-d)$ symmetry. It should therefore contain an $\mathrm{AdS}_{d+1} \times S^{D-d-1}$ manifold.

• The ground state of such holographic conformal defects, will be described by a conifold metric with $\mathrm{AdS}_{d+1} \times S^{D-d-1}$ slices.

• The boundary of such solutions has several components:

♠ One is the boundary of the total space, and this is conformal to $\mathrm{AdS}_{d+1}\times\mathrm{S}^{D-d-1}$, which is also conformal to flat space, $\mathbb{R}^d$.

♠ There is another piece of the boundary, namely the union of the boundaries of the AdS_{d+1} slices. Insertions on that boundary correspond to defect operators.

• Conifold solutions over $\mathrm{AdS}_d\times\mathrm{S}^n$ corresponding to conformal defects of flat space holographic CFTs have been thoroughly studied.

Ghodsi+Kiritsis+Nitti

They have two possible interpretations:

♠ As a holographic CFT$_{d+n}$ on AdS$_d$×S^n.

♠ As a (d-1)-dimensional defect in a $D = d + n$-dimensional CFT.

• This dual interpretation is compatible as the transverse radial distance to the defect can act as a RG scale.

• In the same vain, $\mathbb{R}^{d+n}$ is conformal to AdS$_d$×S^n

• Unlike the case of interfaces, the scale factors are always monotonic.

• The conformal interface corresponds to $d = D - 1$ and the remaining symmetry is realized by AdS$_D$. Also S^0 has two points and corresponds to the two sides of the interface.

The bulk integration constants in the two-boundary case

• The number of integration constants in the bulk equations is the same (3).

• Here, there is no regularity condition. The solutions are generically regular as the scale factor never vanishes.

• Therefore, the scalar vev is an independent parameter and does not depend on $\mathcal{R}$.

• The third constant is always redundant as usual.

• All parameters at the second boundary are determined from the solution, evolved from the first boundary.

• Overall our two-boundary solutions depend on two dimensionless independent parameters, $(\mathcal{R}_i, \mathcal{R}_f)$.

• This is one less from the three we would expect in the general case: $\mathcal{R}_{i,f}$ and

$$\xi \equiv \frac{m_i^2}{m_f^2}.$$

♠ We can recover the extra missing parameter by generalizing the solutions.

Classifying the solutions, II

- We picked $d = 4$ and a generic quartic potential that we parametrized as

$$V(\Phi) = -\frac{12}{\ell_L^2} + \frac{\Delta_L(\Delta_L-4)}{2\ell_L^2}\Phi^2 - \frac{(\Phi_1+\Phi_2)\Delta_L(\Delta_L-4)}{3\ell_L^2\Phi_1\Phi_2}\Phi^3 + \frac{\Delta_L(\Delta_L-4)}{4\ell_L^2\Phi_1\Phi_2}\Phi^4,$$

where Φ_1 and Φ_2 are defined as

$$\Phi_1 = \frac{12\ell_R^2\sqrt{\ell_R^2-\ell_L^2}\,\Delta_L(\Delta_L-4)}{\sqrt{\ell_R^2\Delta_L(\Delta_L-4)-\ell_L^2\Delta_R(\Delta_R-4)}\Big(\ell_R^2\Delta_L(\Delta_L-4)+\ell_L^2\Delta_R(\Delta_R-4)\Big)}$$

$$\Phi_2 = \frac{12\sqrt{\ell_R^2-\ell_L^2}}{\sqrt{\ell_R^2\Delta_L(\Delta_L-4)-\ell_L^2\Delta_R(\Delta_R-4)}}\,.$$

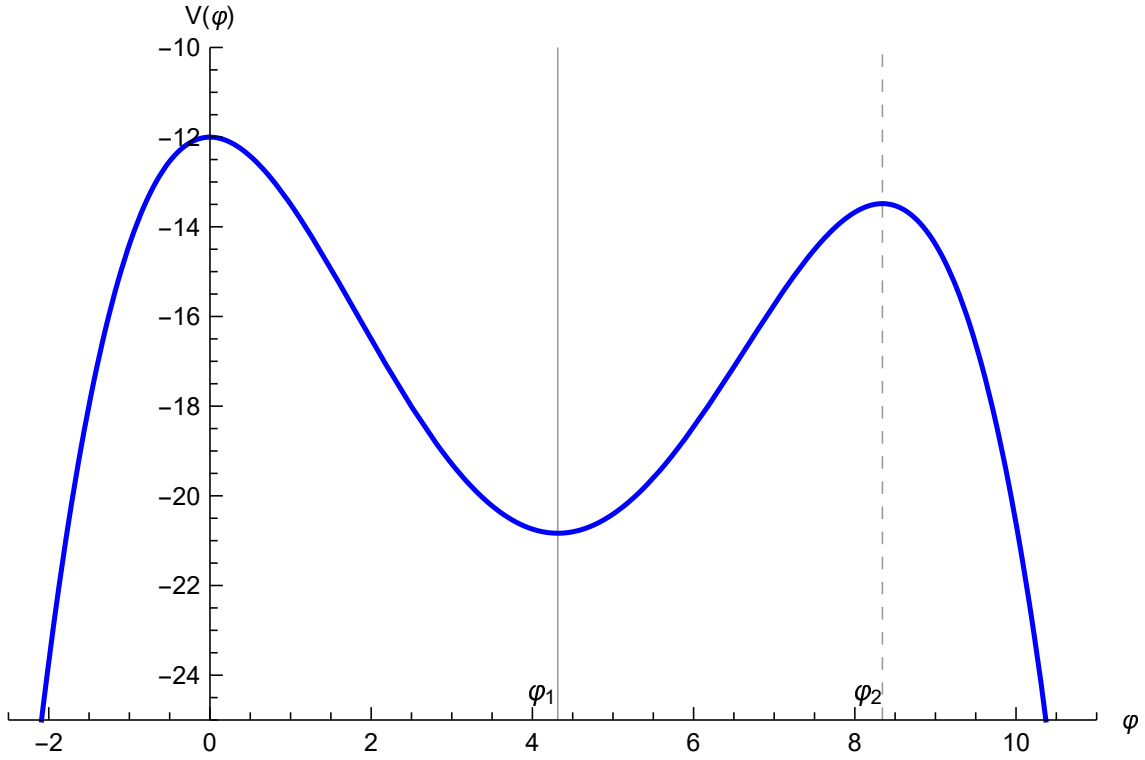

• The left maximum is at $\Phi = 0$. The AdS length is $\ell_L = 1$ and the scaling dimension $\Delta_L = 1.6$.

• The right maximum is at $\Phi = 8.34$. The AdS length is $\ell_R = 0.94$ and the scaling dimension $\Delta_R = 1.1$.

• The minimum is located at $\Phi_1 = 4.31$. It has $\Delta_+^{min} = 4.37$.

• "Technical" definitions:

♠ A-bounce is a point where $\dot{A} = 0 \rightarrow W = 0$. It always exists when the slice curvature is negative.

• Our solutions will have a single A-bounce. We shall denote its position by Φ_0.

♠ Φ-bounce is a point where $\dot{\Phi} = 0 \rightarrow S = 0$. It is a point where the first order equations break down but the second order equations do not.

♠ An IR-bounce is a point where both $\dot{A} = \dot{\Phi} = 0$.

• All bounces are defined AWAY from extremal points of V.

• We always start our solution at the (unique) A-bounce at $\Phi = \Phi_0$ and we solve the first order equations

$$\frac{d}{2(d-1)}W^2 + (d-1)S^2 - dSW' + 2V = 0\,,$$

$$SS' - \frac{d}{2(d-1)}SW - V' = 0\,.$$

• We only need an extra "initial" condition: $S_0 \equiv \dot{\Phi}|_{\Phi=\Phi_0} \equiv S(\Phi_0)$.

• The two parameters $(\Phi_0, S_0) \in R^2$ are the complete initial data of the first order system.

• For each pair (Φ_0, S_0) there is a unique solution.

• We then start solving the equations to the left and right of Φ_0 until we reach an AdS boundary on each side. Then our solution (W, S) is complete.

• We then solve the equations for Φ, A.

$$R^{(\zeta)}e^{-2A(u)} = \frac{d}{4(d-1)}W^2(\Phi) - \frac{S(\Phi)^2}{2} + V(\Phi) \quad , \quad \dot{\Phi} = S$$

The QFT couplings

• At each boundary, initial or final the metric asymptotes to M_ζ and the only parameter (source) is its curvature, $R_{i,f}$.

• The scalar will also have sources at the two boundaries:

$$\Phi(u) \to \Phi_-^{(i)} \quad , \quad u \to -\infty,$$

$$\Phi(u) \to \Phi_-^{(f)} \quad , \quad u \to +\infty,$$

• Therefore, we have four dimensionful couplings: $R_{i,f}$, $\Phi_-^{(i,f)}$.

• As the overall scale is irrelevant, the pair of theories is characterized by three dimensionless numbers which we take to be:

$$\mathcal{R}_i = \frac{R_i^{UV}}{\left(\Phi_-^{(i)}\right)^{2/\Delta_-^i}}, \quad \mathcal{R}_f = \frac{R_f^{UV}}{\left(\Phi_-^{(f)}\right)^{2/\Delta_-^f}}, \quad \xi = \frac{\left(\Phi_-^{(i)}\right)^{1/\Delta_-^i}}{\left(\Phi_-^{(f)}\right)^{1/\Delta_-^f}}$$

Three parameter solutions

- So far our ansatz missed one dimensionless parameter
- To recover it we modify it to:

$$A = \begin{cases} \bar{A}(u) & u < u_* \\ \\ \bar{A}(\tilde{u} - \delta) & u_* + \delta < \tilde{u} < +\infty \end{cases} ,$$

$$\Phi = \begin{cases} \bar{\Phi}(u) & u < u_* \\ \\ \bar{\Phi}(\tilde{u} - \delta) & u_* + \delta < \tilde{u} < +\infty \end{cases} ,$$

- This satisfies the Israel conditions at $u = u_*$ and A, Φ and their derivatives are continuous.

$$R_i^{UV} = \bar{R}_i^{UV}, \quad \Phi_-^i = \bar{\Phi}_-^i, \quad R_f^{UV} = e^{2\delta/\ell} \bar{R}_f^{UV}, \quad \Phi_-^f = e^{\delta \Delta_-^f/\ell} \bar{\Phi}_-^f$$

$W_{1,1}^{LL}$

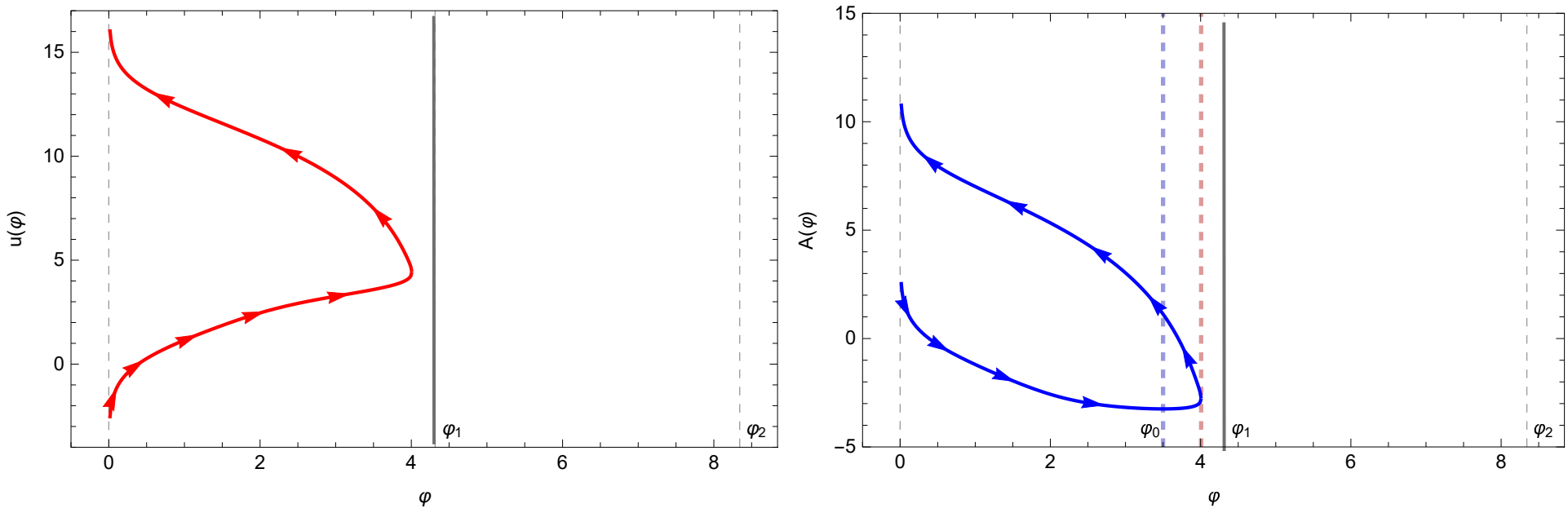

(a): The holographic coordinate at top UV_L tends to $-\infty$ and at bottom UV_L to $+\infty$.
(b): The scale factor has an A-bounce at $\Phi_0 = 3.5$ (blue dashed line) and a Φ-bounce at $\Phi = 4.0$ (red dashed line).

$W^{LL}_{1,2}$

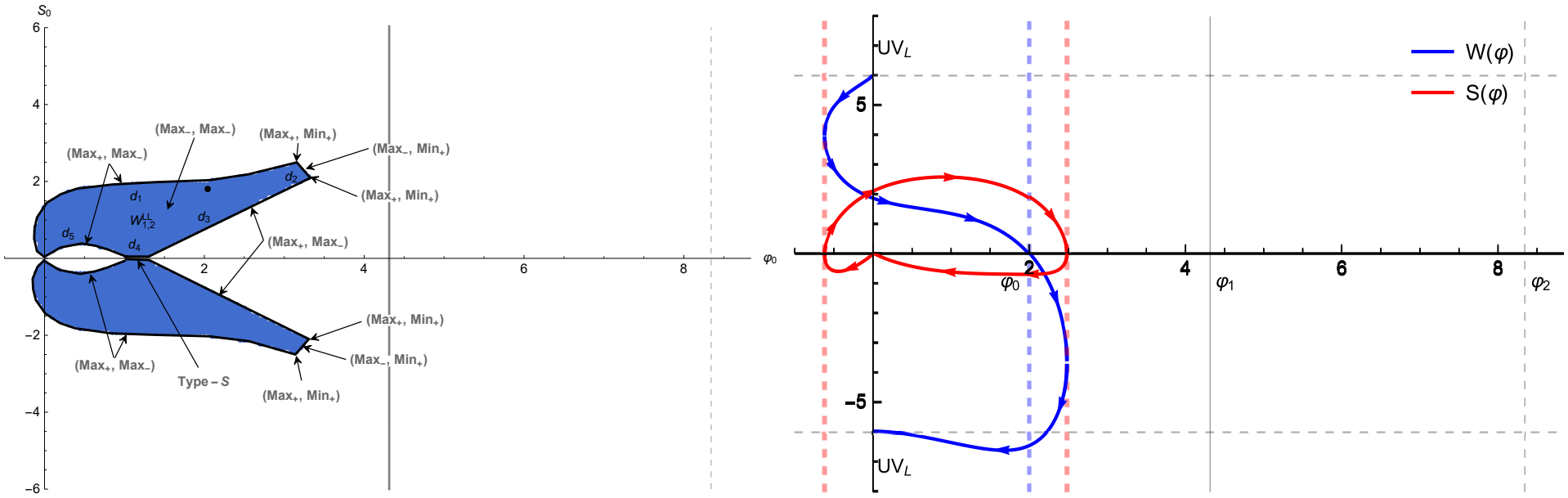

(a): The space of the $W^{LL}_{1,2}$ solutions is the upper blue region. The black dot represents the specific solutions of the diagram (b). The lower blue region corresponds to the solutions with an extra Φ-bounce near the bottom UV_L. (b): The blue and red curves for W, S, describe an RG flow that connects the UV_L fixed point to itself but after two Φ-bounces. The location of the Φ-bounces are indicated by red dashed lines.

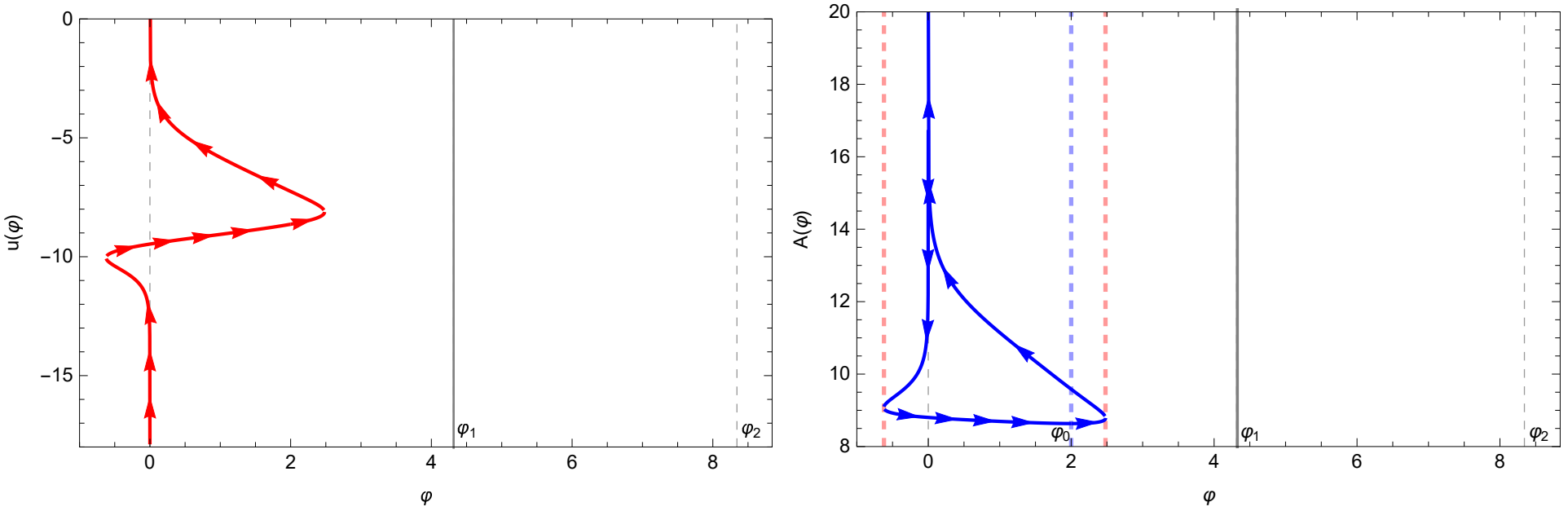

(a): The holographic coordinate at top UV_L boundary tends to $-\infty$ and for bottom UV_L to $+\infty$. (b): The scale factor has an A-bounce at $\Phi = 2.0$, the blue dashed line. The first Φ-bounce on the left occurs at $\Phi = -0.62$ and the second one at $\Phi = 2.48$, the red dashed lines.

$W^{LR}_{1,1}$

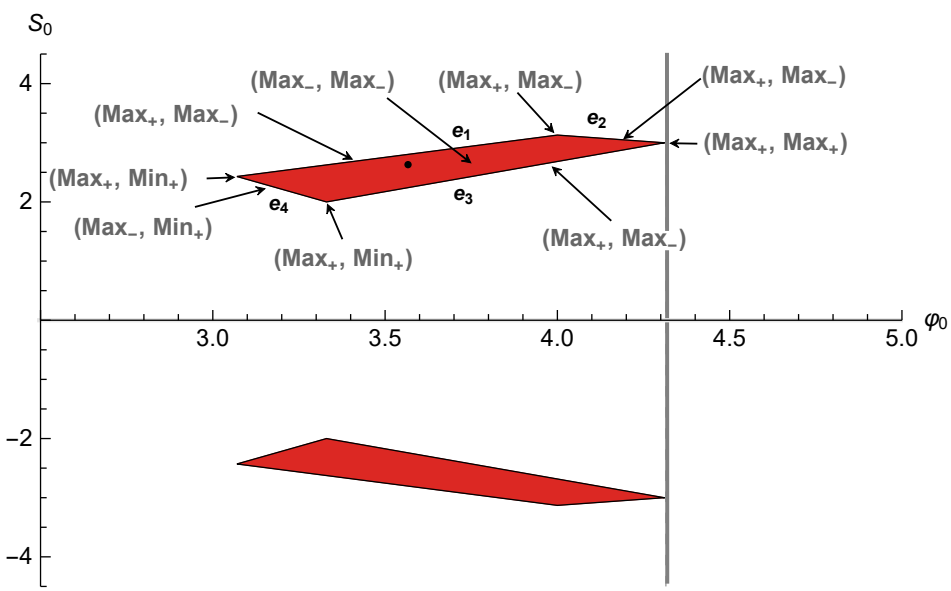

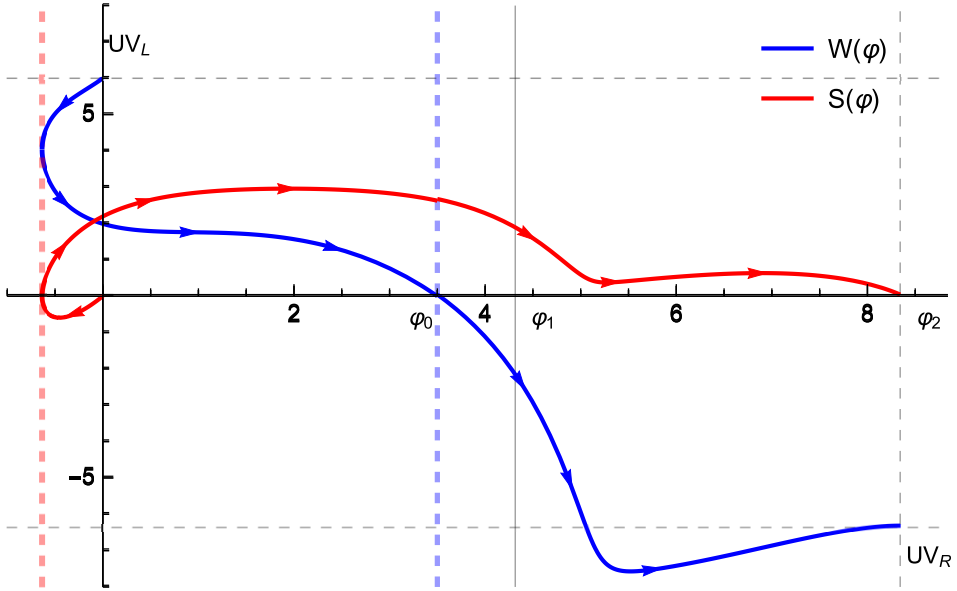

(a): A zoomed picture of the space of the $W^{LR}_{1,1}$ solutions. The black dot represents the RG flow in the diagram (b). (b): The RG flows of type $W^{LR}_{1,1}$ are between the UV_L boundary and UV_R. There is a Φ-bounce at $\Phi < 0$, the red dashed line. Notice that the red region at $S_0 < 0$ in figure (a) is the space of solutions with an extra Φ-bounce near UV_L but at $W < 0$.

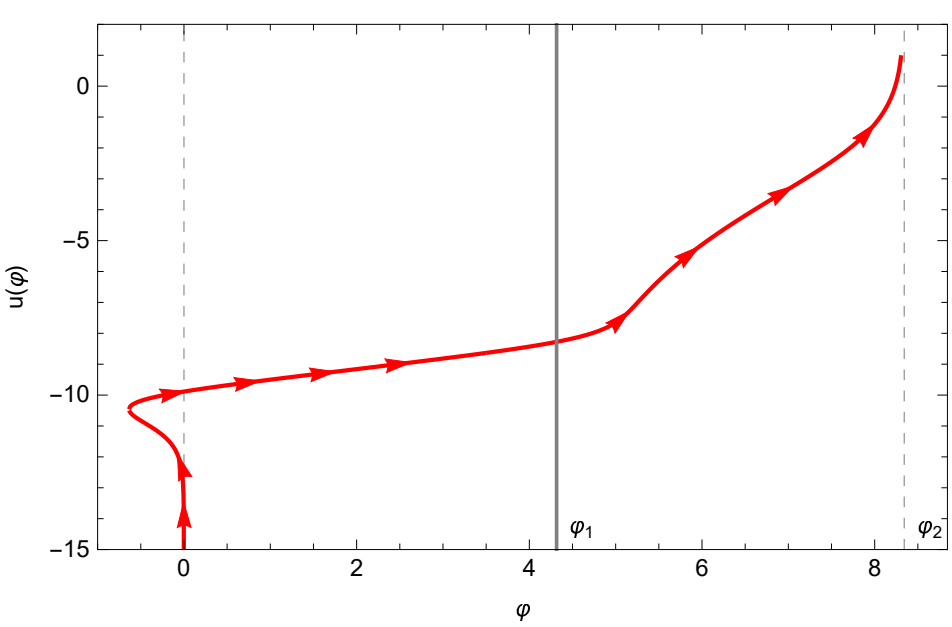

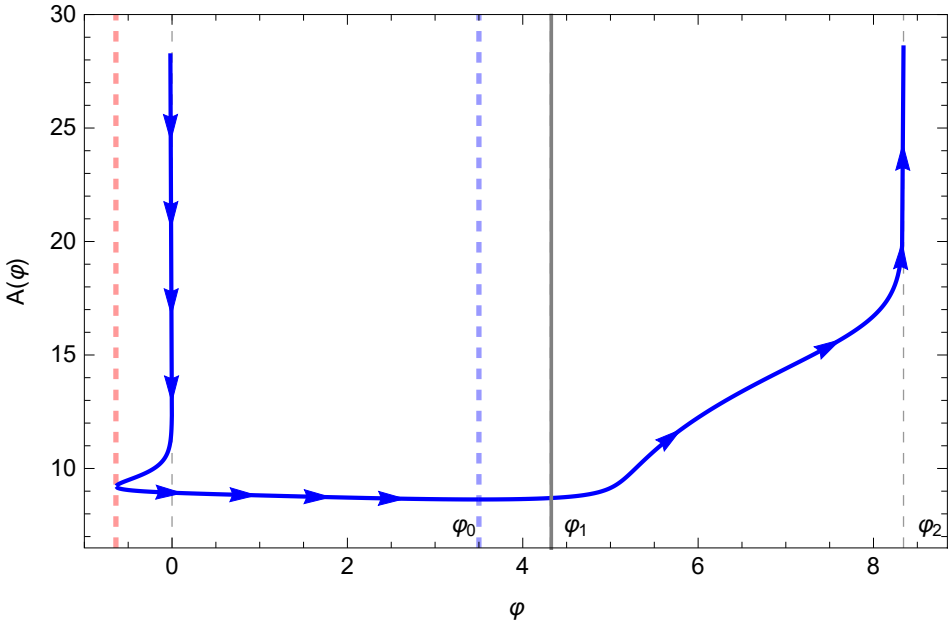

(a): The holographic coordinate at UV_L boundary tends to $-\infty$ and at UV_R to $+\infty$. (b): The scale factor has an A-bounce at $\Phi_0 = 3.5$, the blue dashed line. A Φ-bounce occurs at $\Phi = -0.64$, the red dashed line.

A (3,3) (A-bounce,Φ-bounce) solution

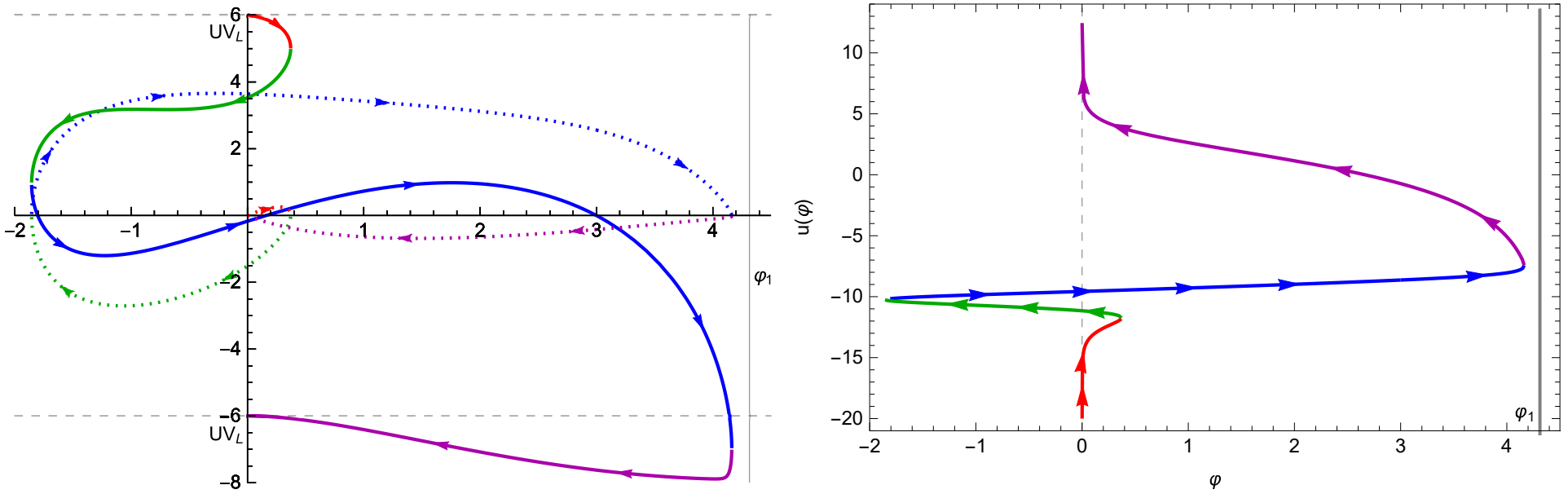

(a): An example of a multi-Φ-bounce solution, $W^{LL}_{3,3}$. The solid line is $W(\Phi)$ and dotted line is $S(\Phi)$. In this case an RG flow connects two UV boundaries on the left UV fixed point after three Φ-bounces. Unlike the previous cases the geometry here has three A-bounces.

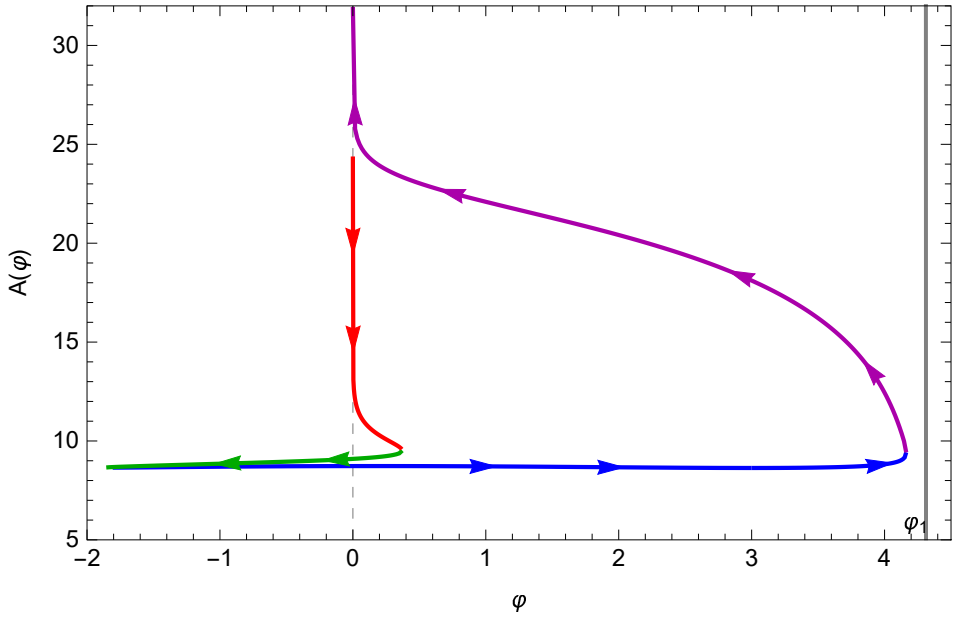

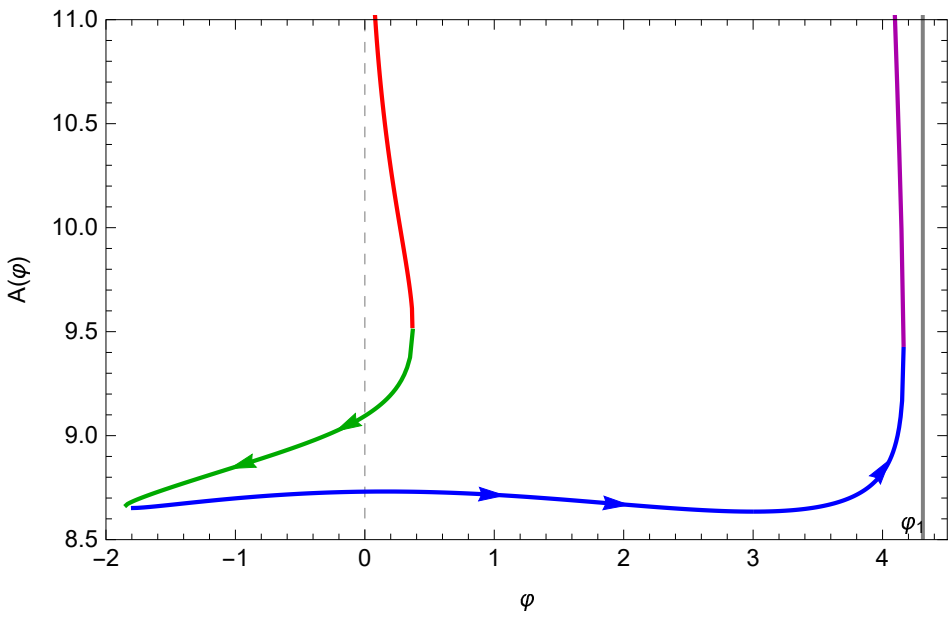

(b)and (c) show the behavior of holographic coordinate and scale factor in terms of Φ. Figure (d) is the magnification of the bottom of figure (c). It shows that there are three A-bounces for this RG flow.

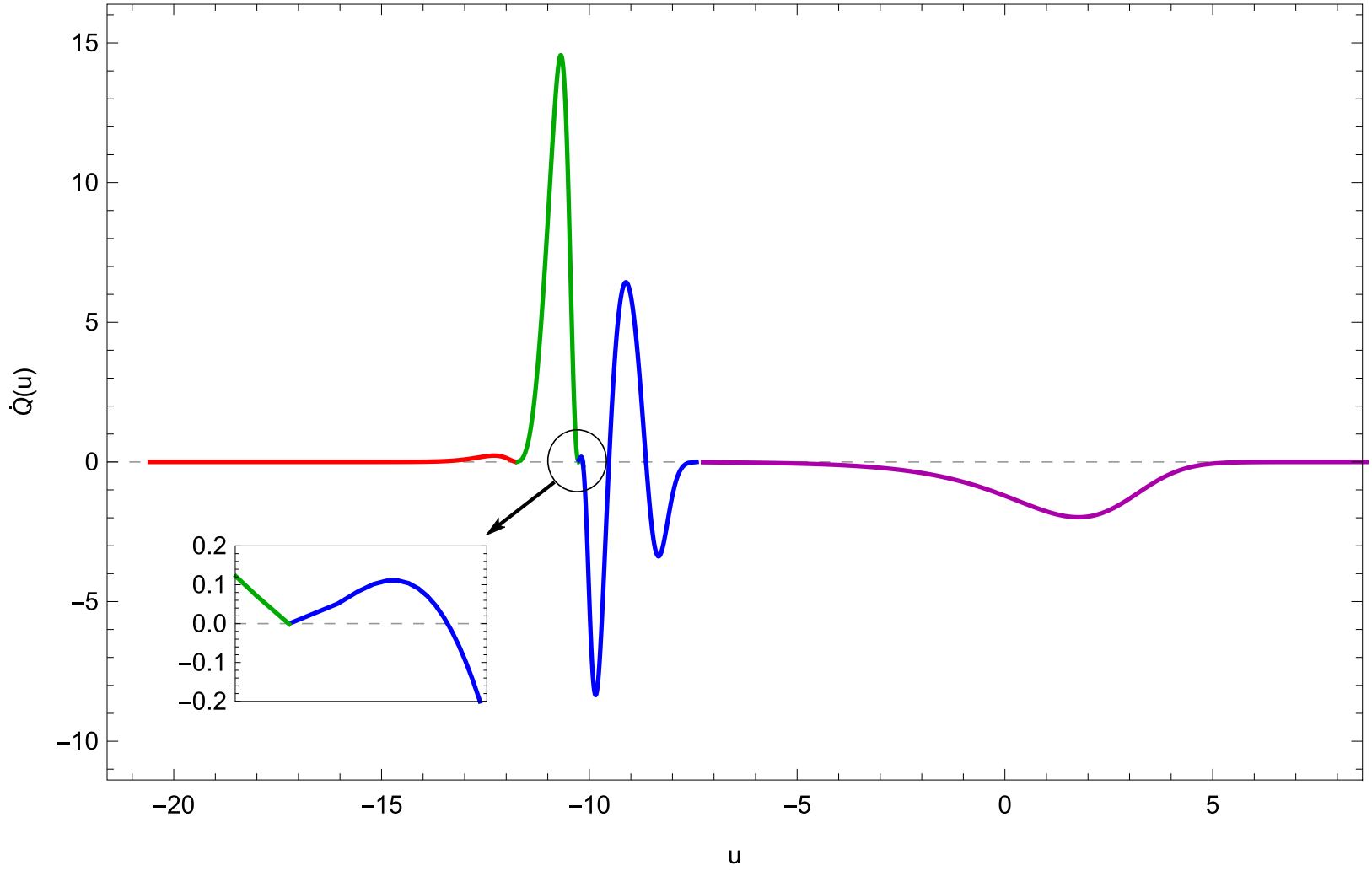

(e): The roots of $\dot{Q}$

$$Q(u) = \frac{1}{2}\dot{\Phi}^2 - V \geq 0\,, \qquad \dot{Q} = \frac{d}{2(d-1)} W S^2\,.$$

shows the location of Φ-bounces where the color of the graph is changed and location of A-bounces where the blue part of the curve crosses the u axis.

The behavior of relevant couplings

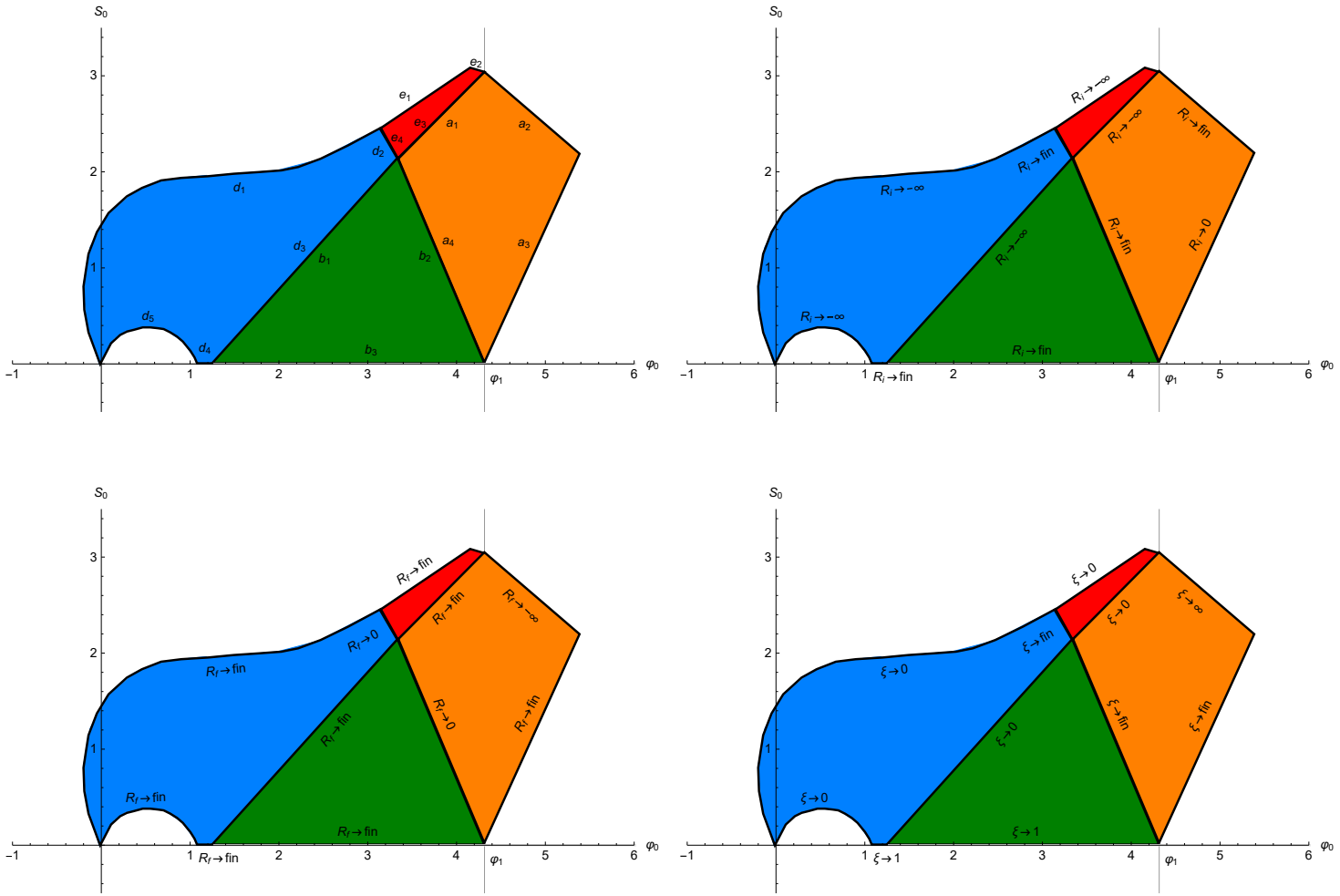

(a) Space of solution with its boundaries. (b) and (c): The behavior of $\mathcal{R}_i$ and $\mathcal{R}_f$ at boundaries. (d): The ratio of two relevant couplings, ξ, at boundaries.

The $a_3 \cup a_4$ solution: triple fragmentation

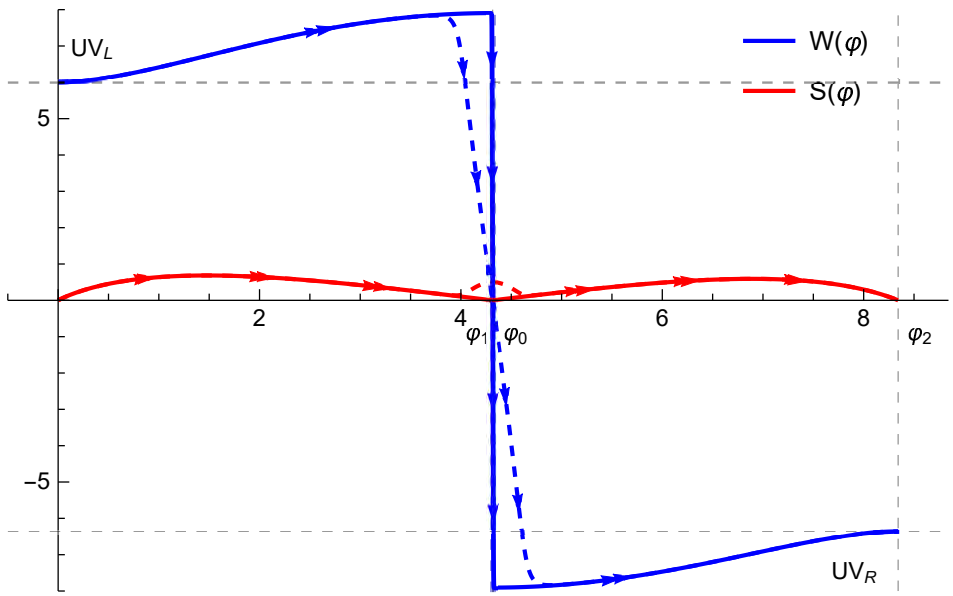

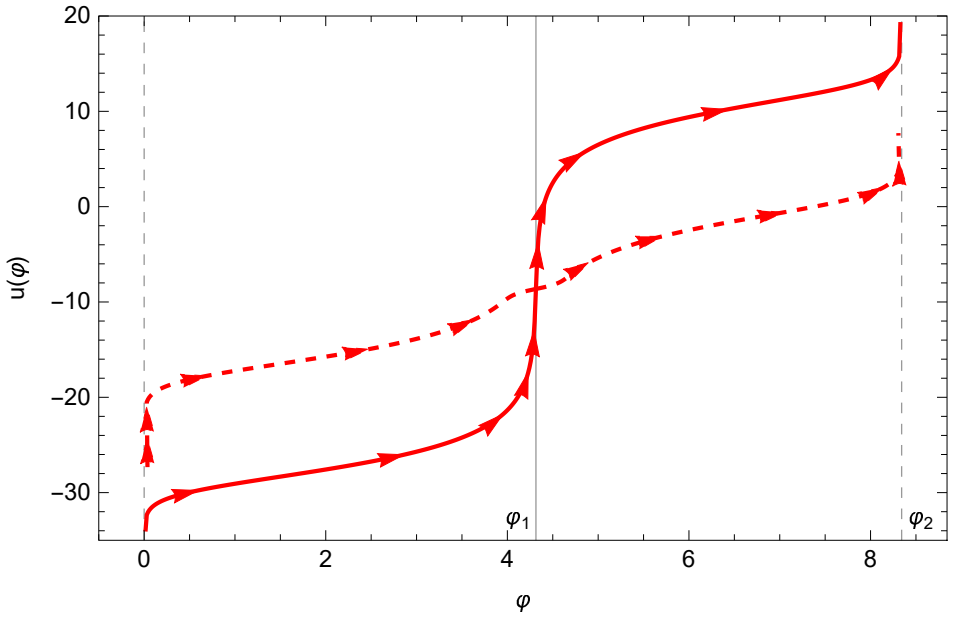

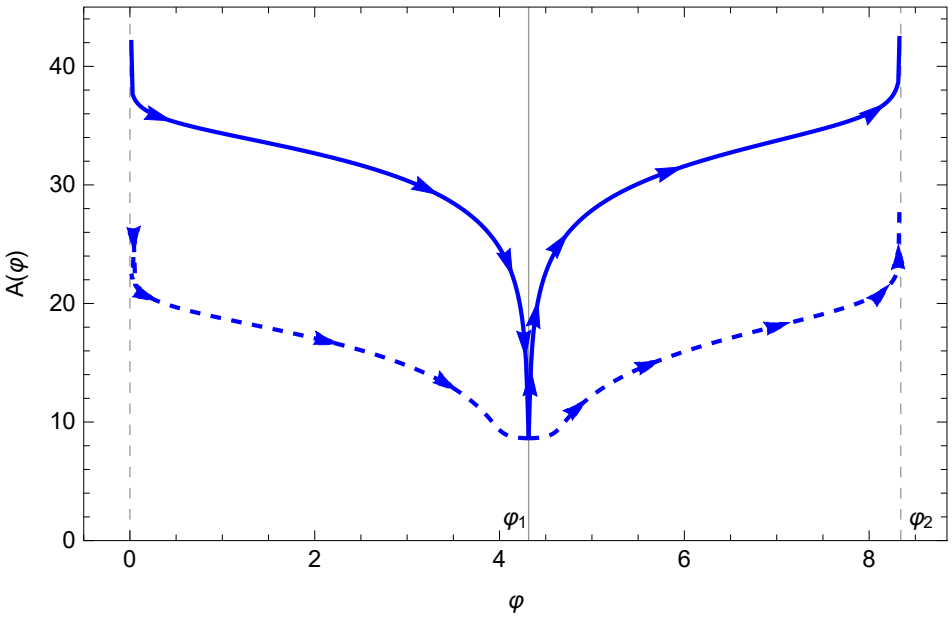

Along the fixed line $\Phi_0 = \Phi_1$ i.e. the minimum of the potential, if we decrease the value of S_0 down to zero, gradually the dashed curves in all figures above move toward the solid curves. In above curves the dashed curves have $S_0 = 0.5$ and the solid ones $S_0 = 0.01$.

Interface correlators

- The picture of overlapping boundaries in AdS-sliced flows is "singular".

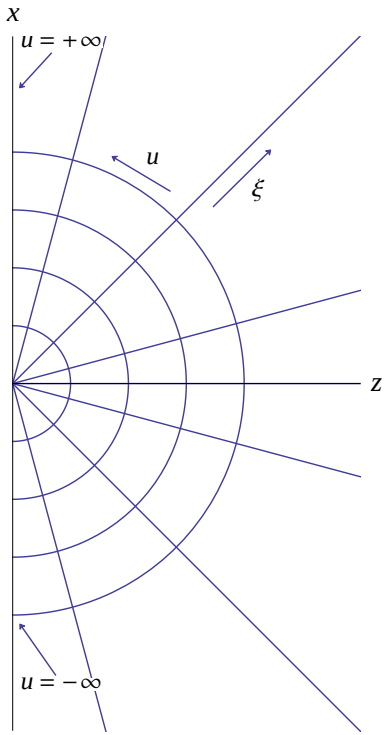

Relation between Poincaré coordinates (x, z) and AdS-slicing coordinates (ξ, u). Constant u curves are half straight lines all ending at the origin ($\xi \to 0^-$); Constant ξ curves are semicircle joining the two halves of the boundary at $u = \pm\infty$.

• The regular picture contains three boundaries:

♠ Two of them ($B_{1,2}$) are at $u = \pm\infty$.

♠ There is a third boundary, B_3, for all values of u that contains the boundaries of AdS slices.

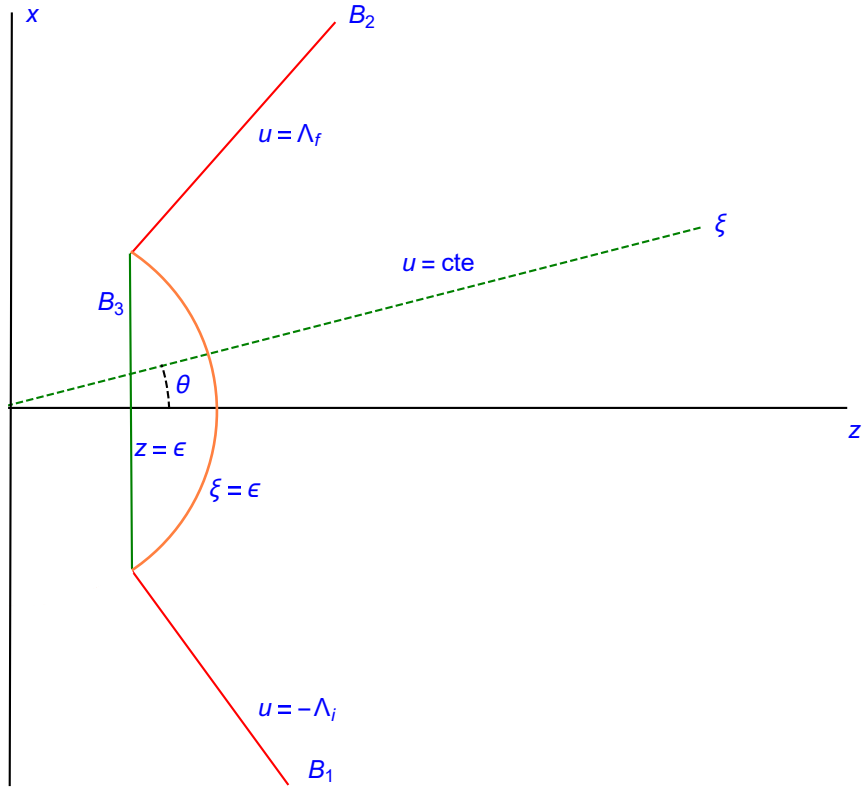

• For a well-defined variational problem apart from the GH term on $B_{1,2,3}$ one needs to add the Hayward term at the two corners, $B_1 \cup B_3$ and $B_2 \cup B_3$.

$$S_H = \frac{1}{8\pi G_N} \int d^{d-1}x \sqrt{-h}\, \arccos(n.\tilde{n})$$

• Correlators of insertions at the $B_{1,2}$ boundaries are done the same way as in standard AdS.

• Calculating correlators on the interface is problematic.

• We could not find a universal form of counterterms on a shifted boundary that removes all divergences from interface correlators.

• This is an open problem.

Details of the confining potential

We consider the following scalar potential

$$V(\Phi) = -\frac{d(d-1)}{\ell^2}\left(b\Phi^2 + \cosh^2(a\Phi)\right) \quad , \quad b = \frac{\Delta(d-\Delta)}{2d(d-1)} - a^2 \, . \tag{2}$$

As $\Phi \to \pm\infty$, the above potential diverges as

$$V(\Phi) \to -\frac{d(d-1)}{4\ell^2} e^{\pm 2a\Phi} \, , \tag{3}$$

where we assumed that $a < a_G$, the Gubser's bound.

This potential has a maximum at $\Phi = 0$ (UV fixed point) and near this point, it can be expanded as

$$V(\Phi) = -\frac{d(d-1)}{\ell^2} - \frac{1}{2}m^2\Phi^2 + \mathcal{O}(\Phi^4) \quad , \quad m^2 = \frac{\Delta(d-\Delta)}{\ell^2} \, . \tag{4}$$

ℓ determines the length scale of asymptotically AdS solutions, Δ determines m^2 and is the scaling dimension of the operator dual to the scalar Φ near

the UV fixed point. a determines the asymptotic behavior of the potential (confinement or deconfinement).

For the numerics we fix the constants of the theory as follows

$$d = 4 \quad , \quad \Delta = \frac{3}{2} \quad , \quad \ell = 1 \quad , \quad a = \sqrt{\frac{7}{24}} \quad , \quad b = -\frac{13}{96}. \tag{5}$$

For the specific choice $d = 4$ we have

$$a_C = \frac{1}{\sqrt{6}} \quad , \quad a_G = \frac{2}{\sqrt{6}}, \tag{6}$$

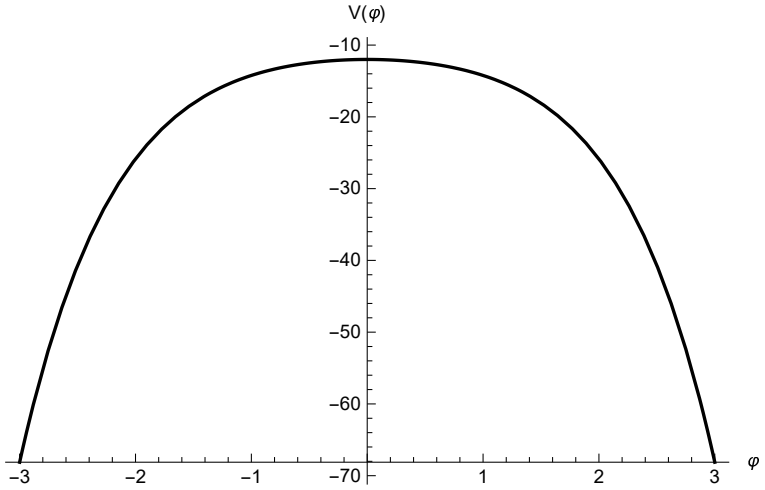

Vevs

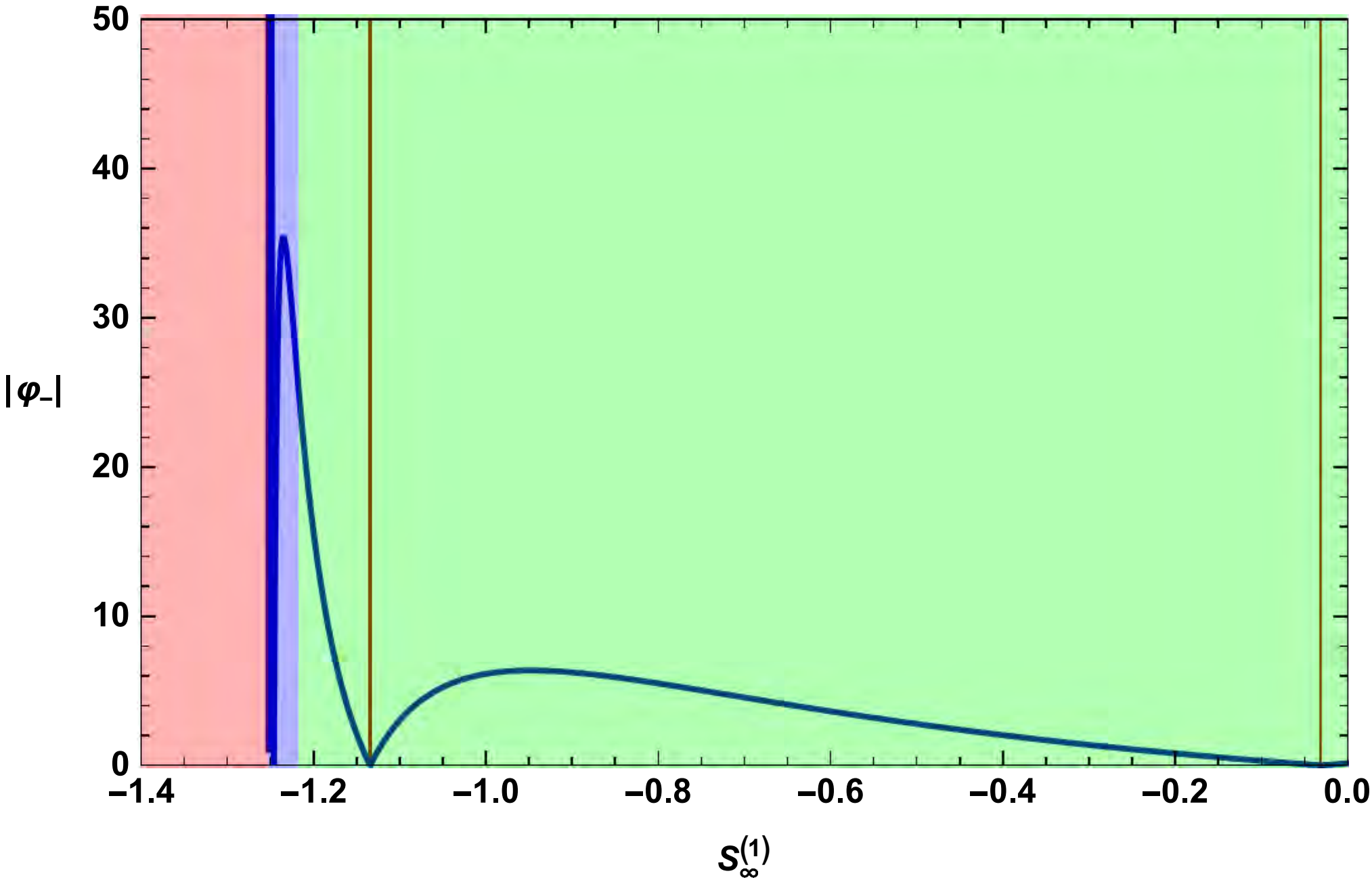

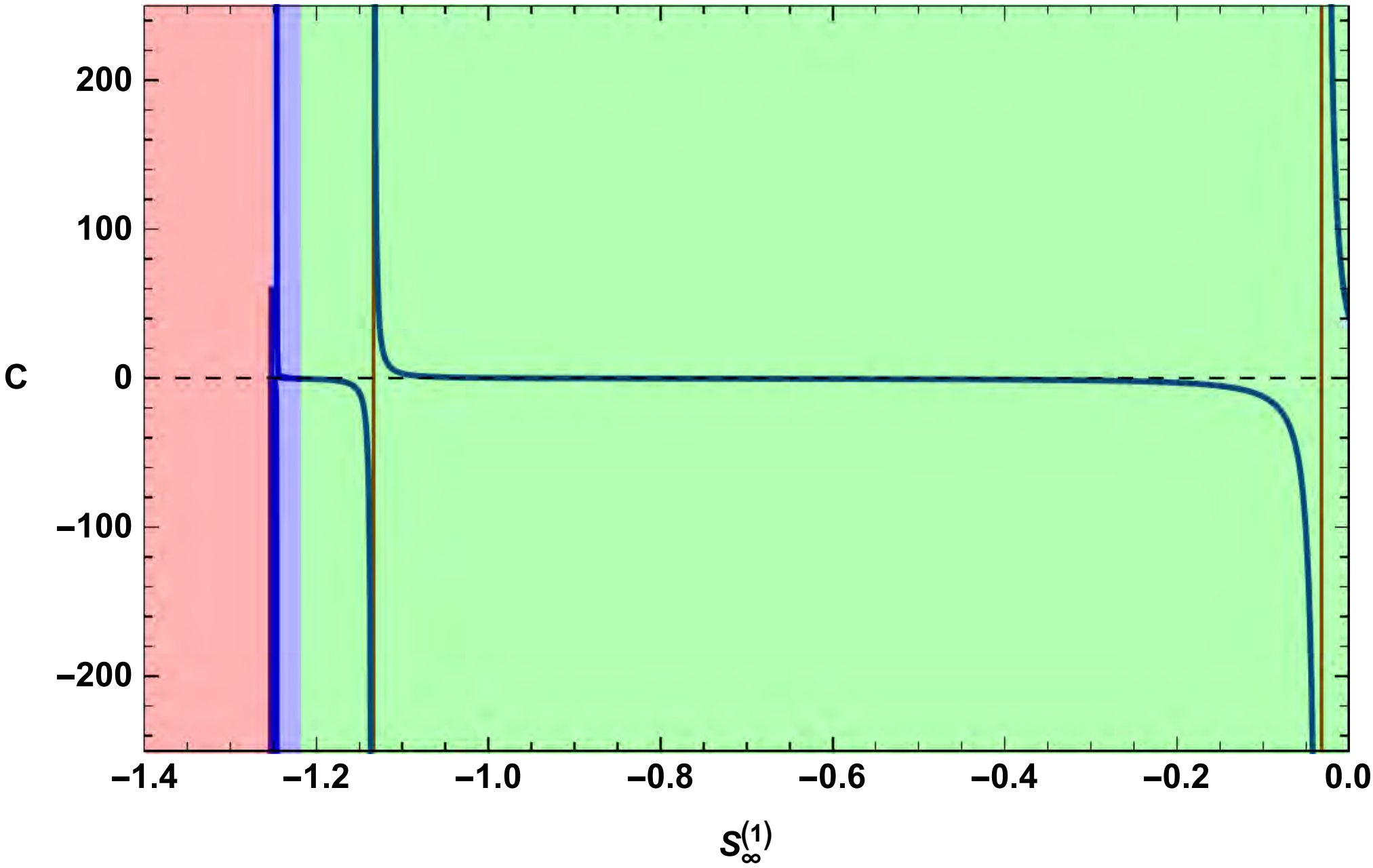
200
100
0
−100
−200
C
−1.4
−1.2
−1.0
−0.8
−0.6
−0.4
−0.2
0.0
$S_\infty^{(1)}$

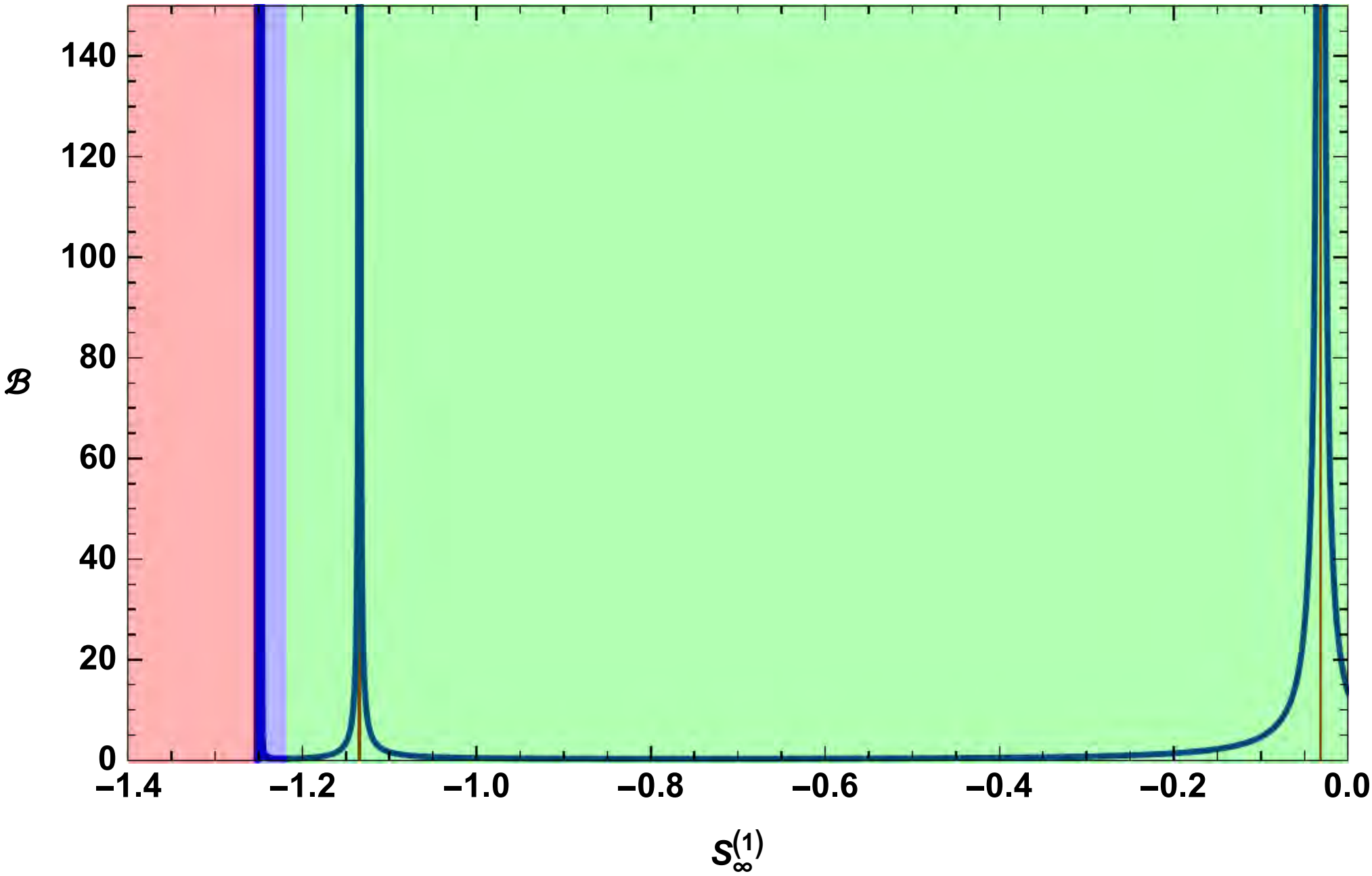
140
120
100
80
60
40
20
0
$\mathcal{B}$
−1.4
−1.2
−1.0
−0.8
−0.6
−0.4
−0.2
0.0
$S_\infty^{(1)}$

Φ_- the coupling of operator $\mathcal{O}$ at the UV boundary and C parameter of the UV boundary for UV-Reg solutions. All figures are plotted as a function of the free parameter $S_\infty^{(1)}$. In each graph, the green region belongs to the regular solutions without A-bounce and the blue region to solutions with at least one A-bounce. In the red region, we have not solutions with boundary. The vertical dashed line in figure (a) corresponds to the global AdS solution in the uplifted theory and the product solution is the solution right before the blue-red boundary. Figure (d) gives $\mathfrak{B}$ which we need to compute the free energy of the solutions.

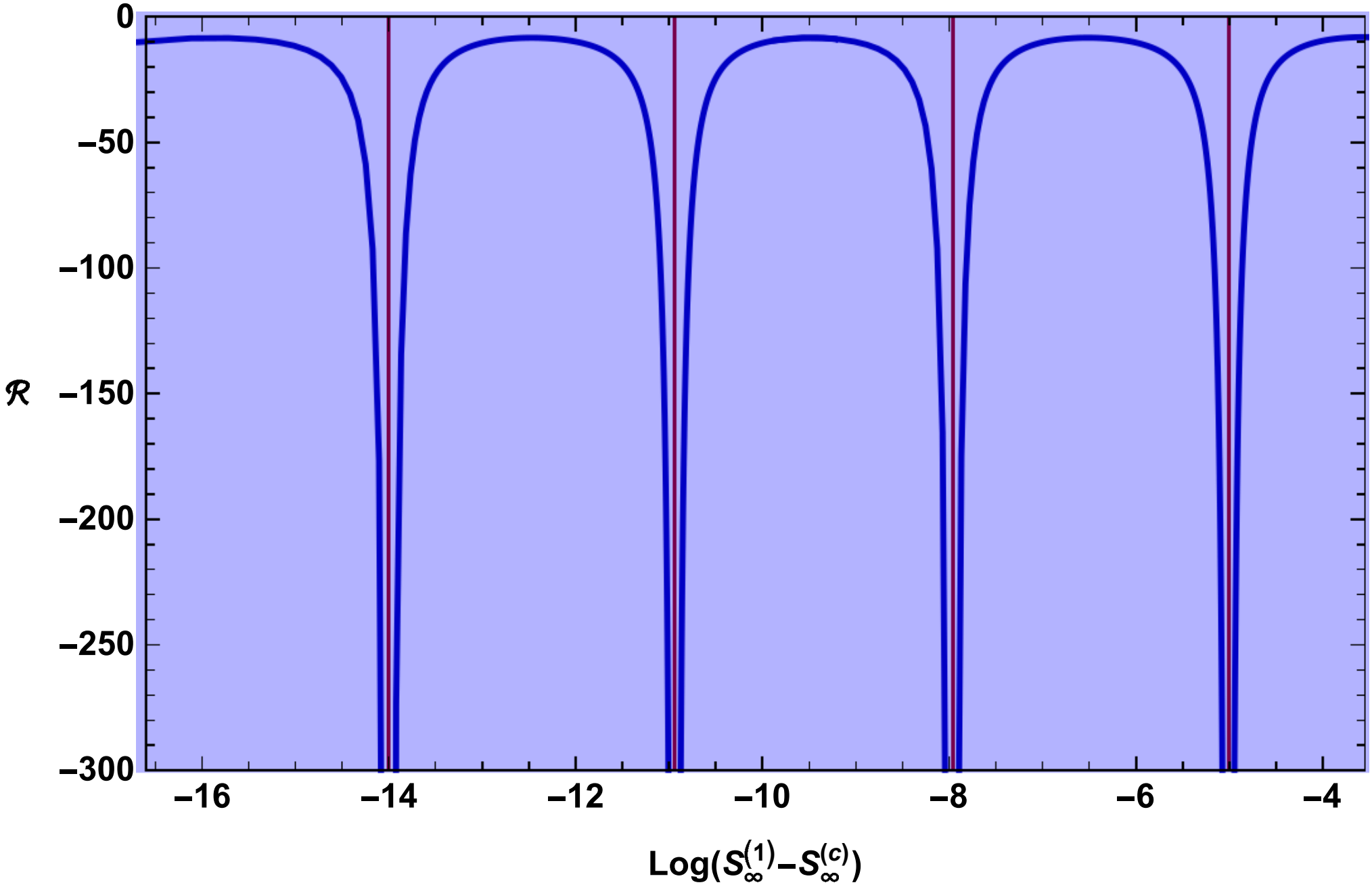
0
−50
−100
−150
−200
−250
−300
ℛ
−16
−14
−12
−10
−8
−6
−4
Log(S∞(1)−S∞(c))

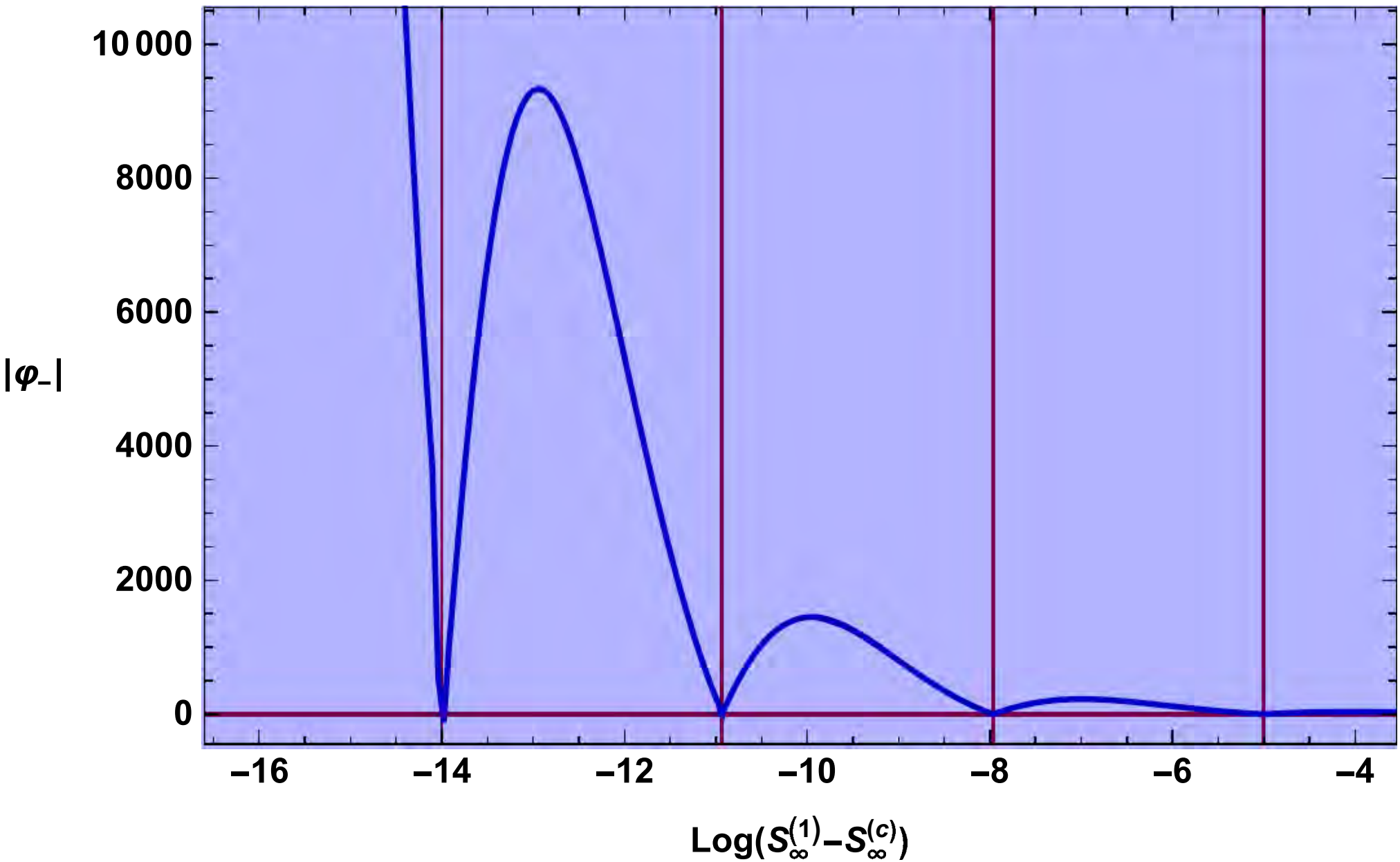
10 000
8000
6000
4000
2000
0
|φ-|
−16
−14
−12
−10
−8
−6
−4
Log(S∞(1)−S∞(c))

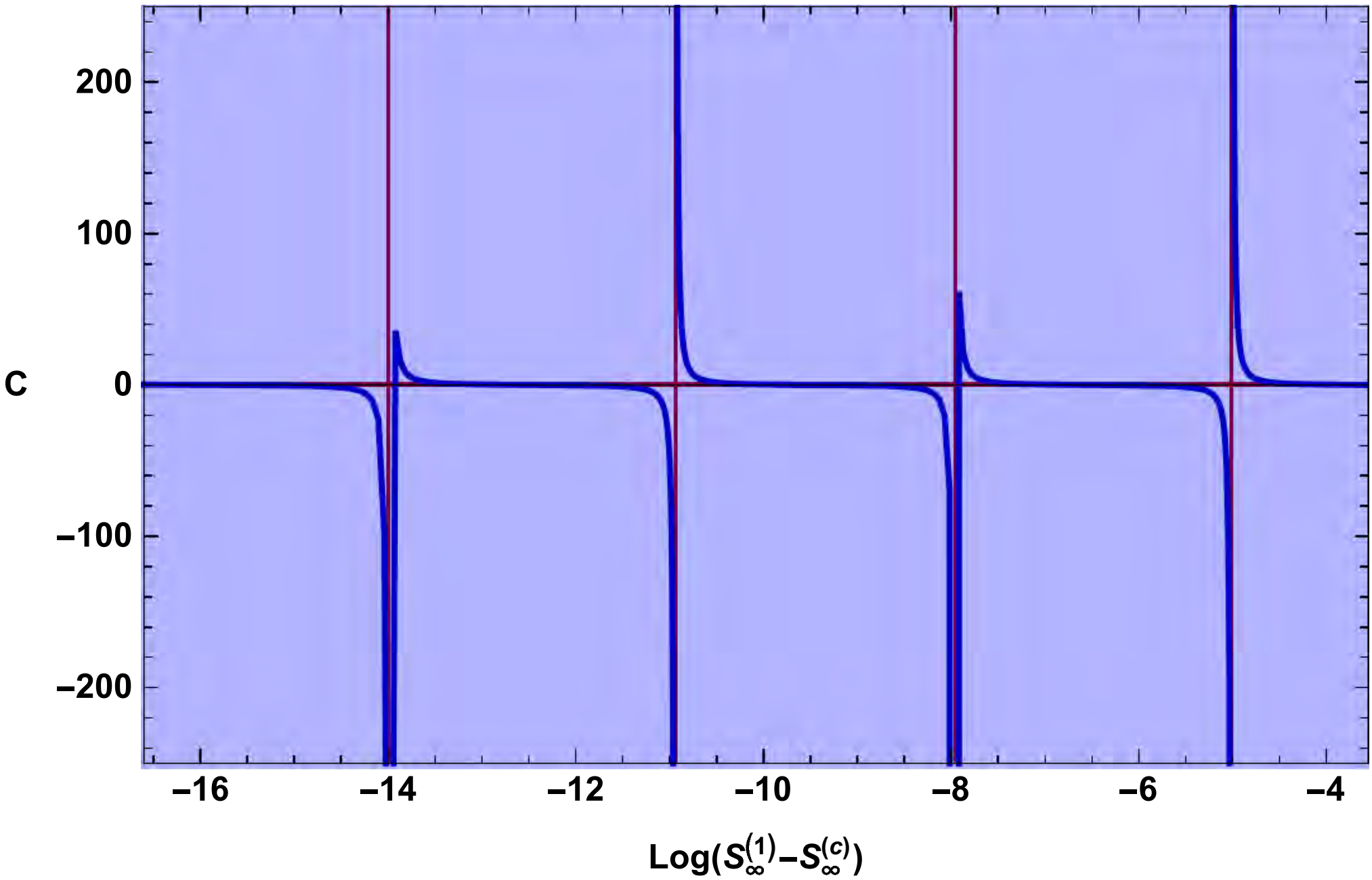
200
100
0
−100
−200
C
−16
−14
−12
−10
−8
−6
−4
Log($S_\infty^{(1)}-S_\infty^{(c)}$)

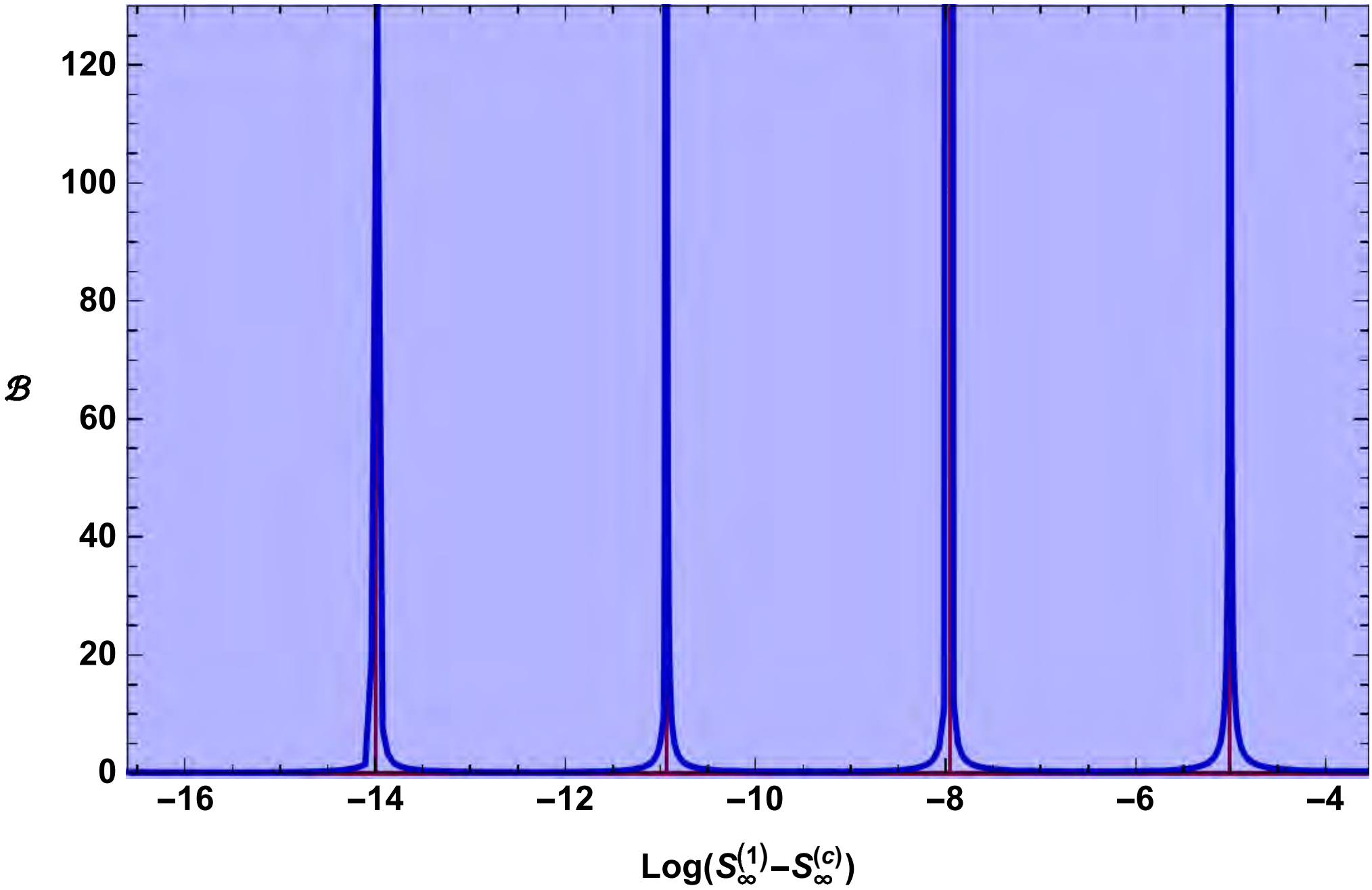

The blue region . The horizontal axis is $\log(S_\infty^{(1)} - S_\infty^{(c)})$, where $S_\infty^{(c)} \approx -1.25$

is the critical value for which we have the UV-Reg solution with infinite numbers of the loops.

Single boundary solutions

- To obtain a single boundary, one can orbifold a symmetric solution.

Aharony+Marolf+Rangamani

- This can be done in the class of solutions we called S. They have $S_0 = 0$ and they are completely symmetric.

- We obtain the half space with $u \in (-\infty, u_0)$.

- We can interpret such solutions by inserting an end-of-the-world brane at u_0.

- But because $\dot{A} = \dot{\Phi} = 0$ at u_0, this brane is both tensionless and chargless.

- However, a look at correlators indicates that conformal invariance is broken (For AdS-sliced AdS).

- In the two boundary case, we have four possible two-point functions $\langle OO \rangle$: $G_{++}, G_{+-}, G_{-+}, G_{--}$

• The symmetric orbifold gives

$$G = G_{++} + G_{+-} = \frac{1}{2^\Delta}\left[\frac{1}{(\cosh L - 1)^\Delta} + \frac{1}{(\cosh L + 1)^\Delta}\right]$$

$$\cosh L = 1 + \frac{(z - z')^2 + |x - x'|^2}{zz'}$$

• The conformal correlator obtained from a Weyl transformation of flat space is the first piece only.

• This may be due to the fact that most boundary conditions break conformal invariance.

• If instead we insert a brane at $u = u_0$ and impose Dirichlet bc we obtain a similar result with a relative minus sign. (The orbibold corresponds to Neumann)

• Are there bc on the brane so that we obtain a conformal correlator?

• Yes, but they are generically non-local on the brane.

Proximity in QFT

- The notion of "proximity" in Quantum Field Theory is an intuitive notion.

- One possible definition of the notion of proximity among CFTs is : can QFT_1 and QFT_2 live in the same Hilbert space?

- If there is flow connecting CFT_1 to CFT_2 we can claim that the two theories can live in the same Hilbert space.

- Another was formulated by van Raamsdonk: the CFT masquerade, mostly relevant for CFT duals.

"When the states of CFT_1 can be approximated by CFT_2?"

or

"Can a suitably chosen state of CFT_1, faithfully encode the space-time dual to a state of CFT_2?"

or

"Can two theories with different operator spectra describe the same bulk geometry?"

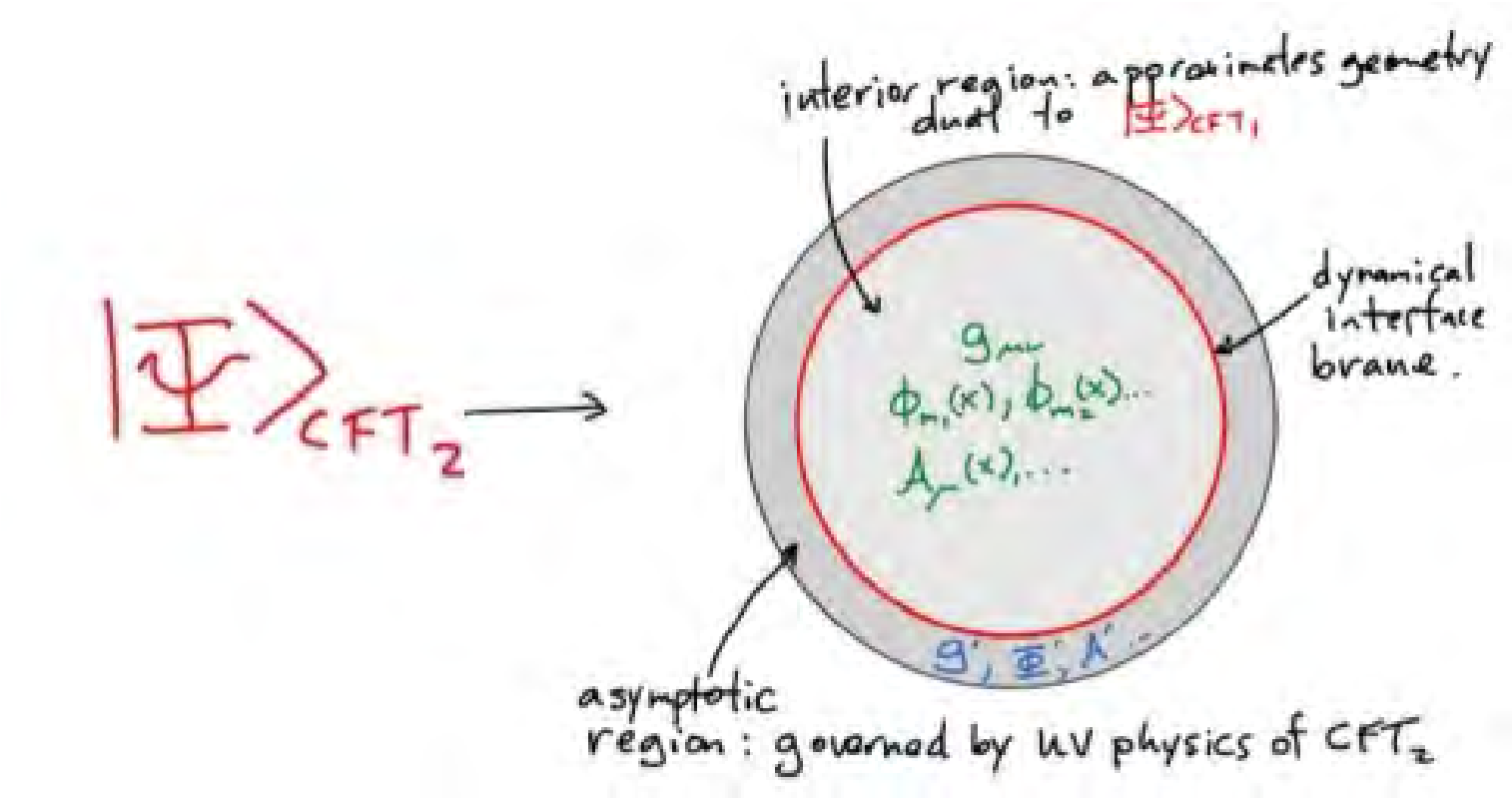

• Van Raamsdonk gave simple solvable examples where the two CFTs are interfaced by a bulk brane.

• This notion is very close to the RG connection, as a continuous version of this setup is a holographic RG flow.

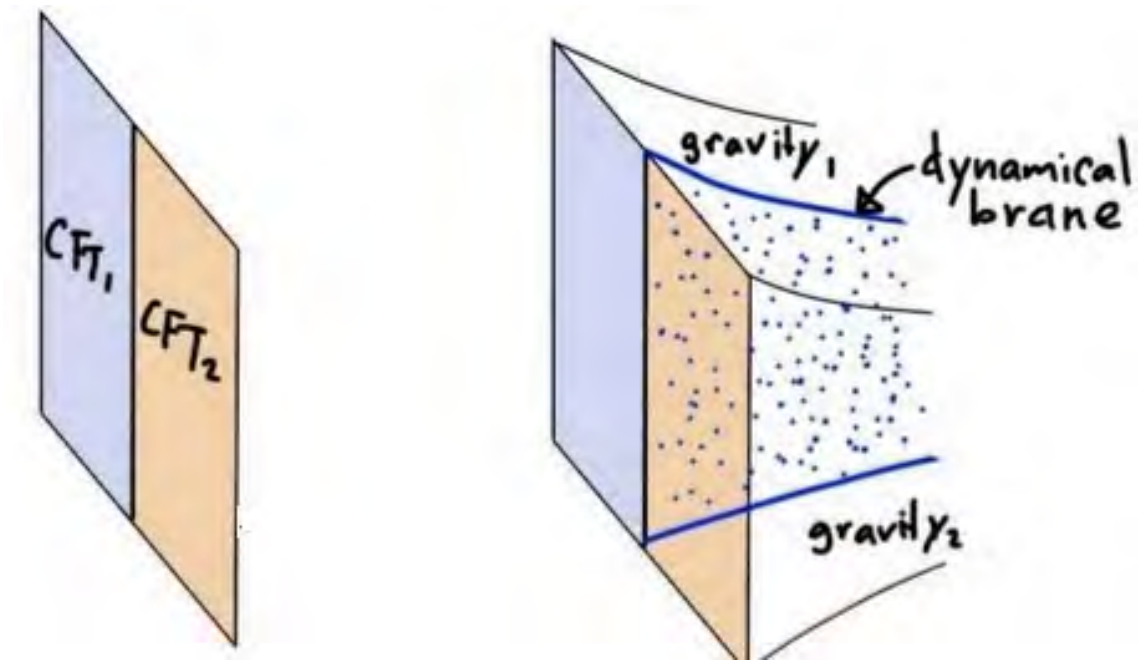

- Another example is theories that can share an inteface.
- They may be generating a bulk brane or

Takayanagi

- They may be like Janus interface geometries.

Bak+Gutperle+Hirano, + many others

The region boundaries and tuned flows

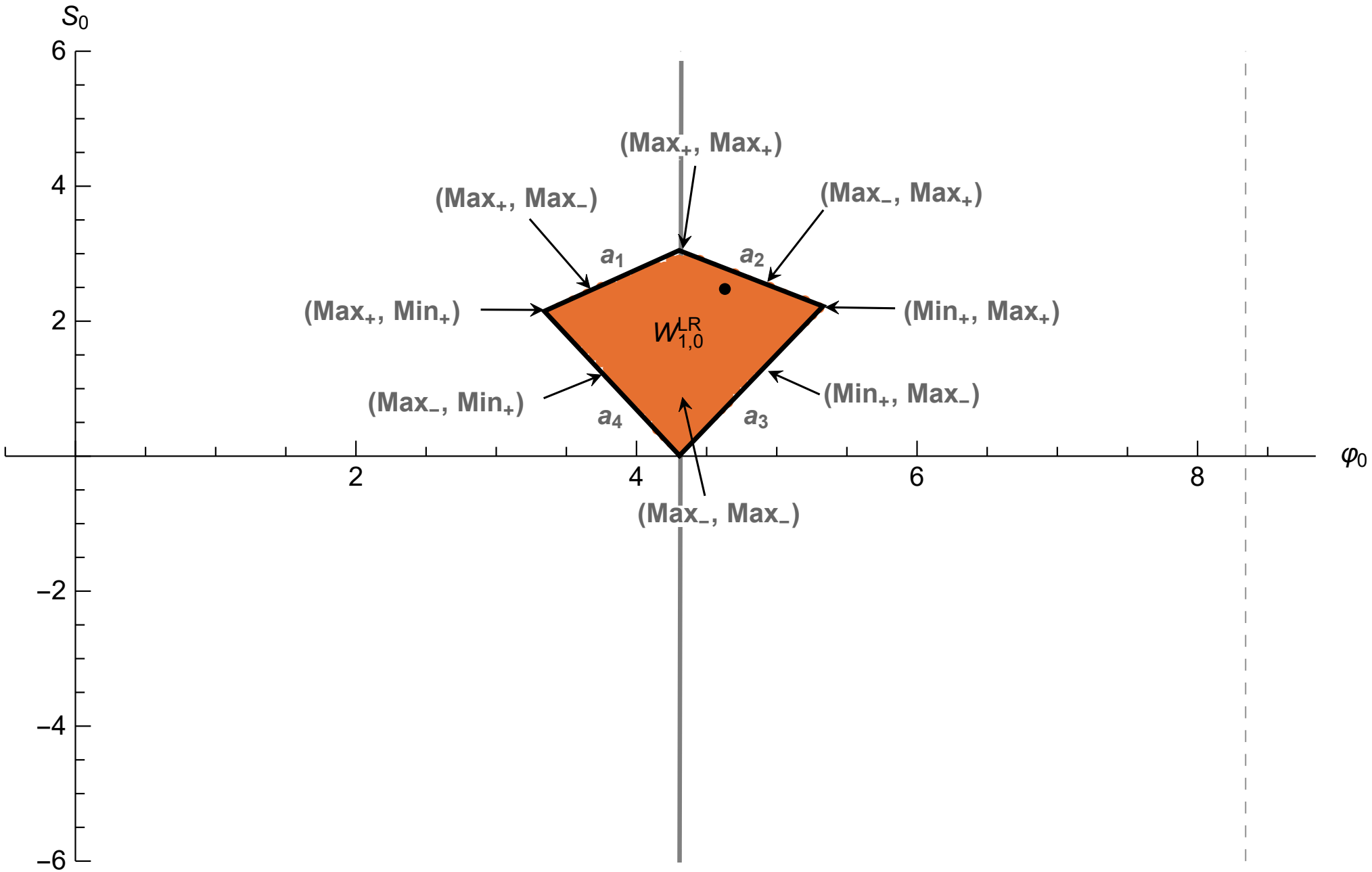

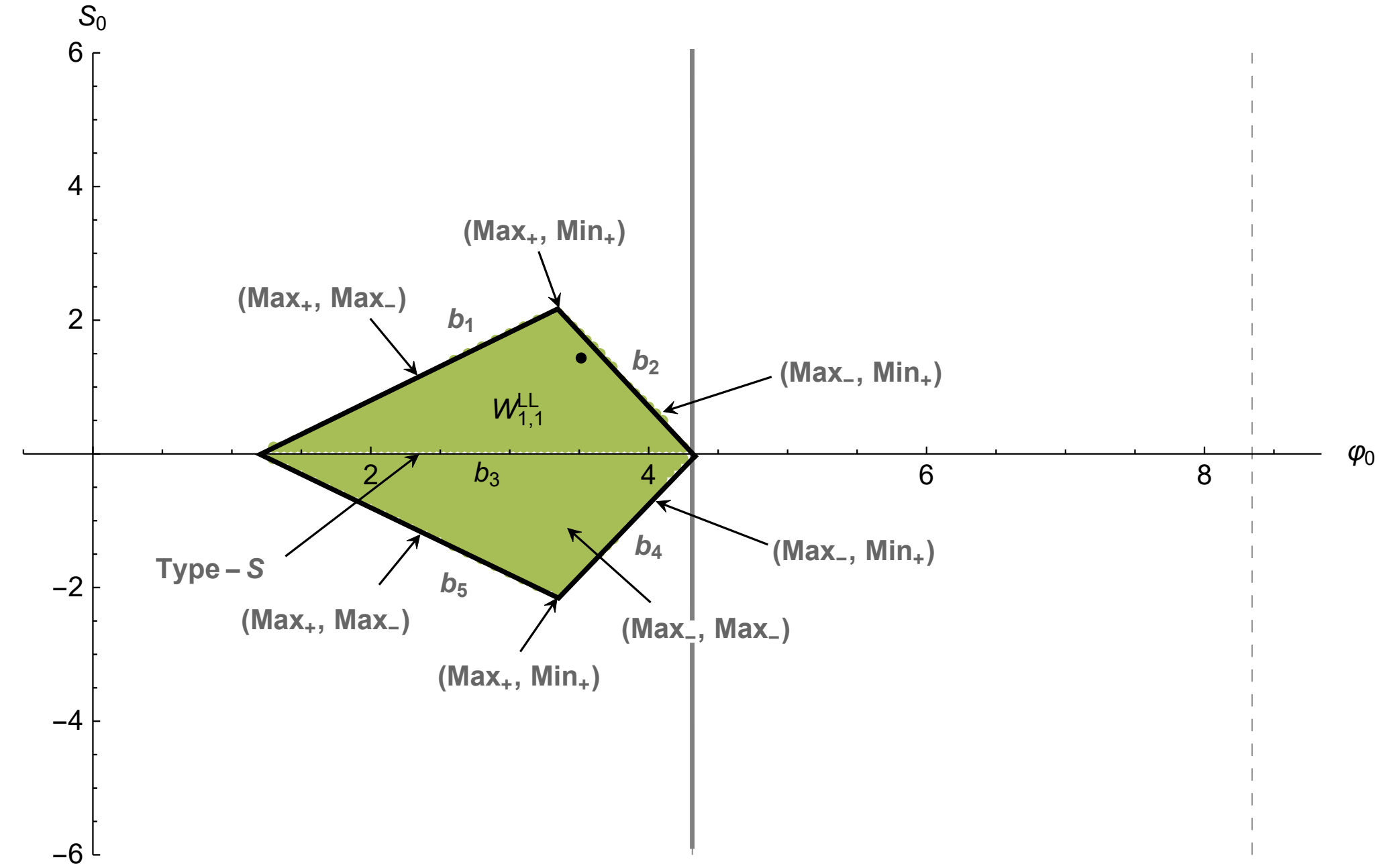
S_0
6
4
2
−2
−4
−6
2
4
6
8
φ_0
$(\mathrm{Max}_+, \mathrm{Min}_+)$
$(\mathrm{Max}_+, \mathrm{Max}_-)$
b_1
b_2
$(\mathrm{Max}_-, \mathrm{Min}_+)$
$W^{\mathrm{LL}}_{1,1}$
b_3
b_4
$(\mathrm{Max}_-, \mathrm{Min}_+)$
$\mathrm{Type}-S$
b_5
$(\mathrm{Max}_+, \mathrm{Max}_-)$
$(\mathrm{Max}_-, \mathrm{Max}_-)$
$(\mathrm{Max}_+, \mathrm{Min}_+)$

Flow fragmentation, walking and emergent boundaries

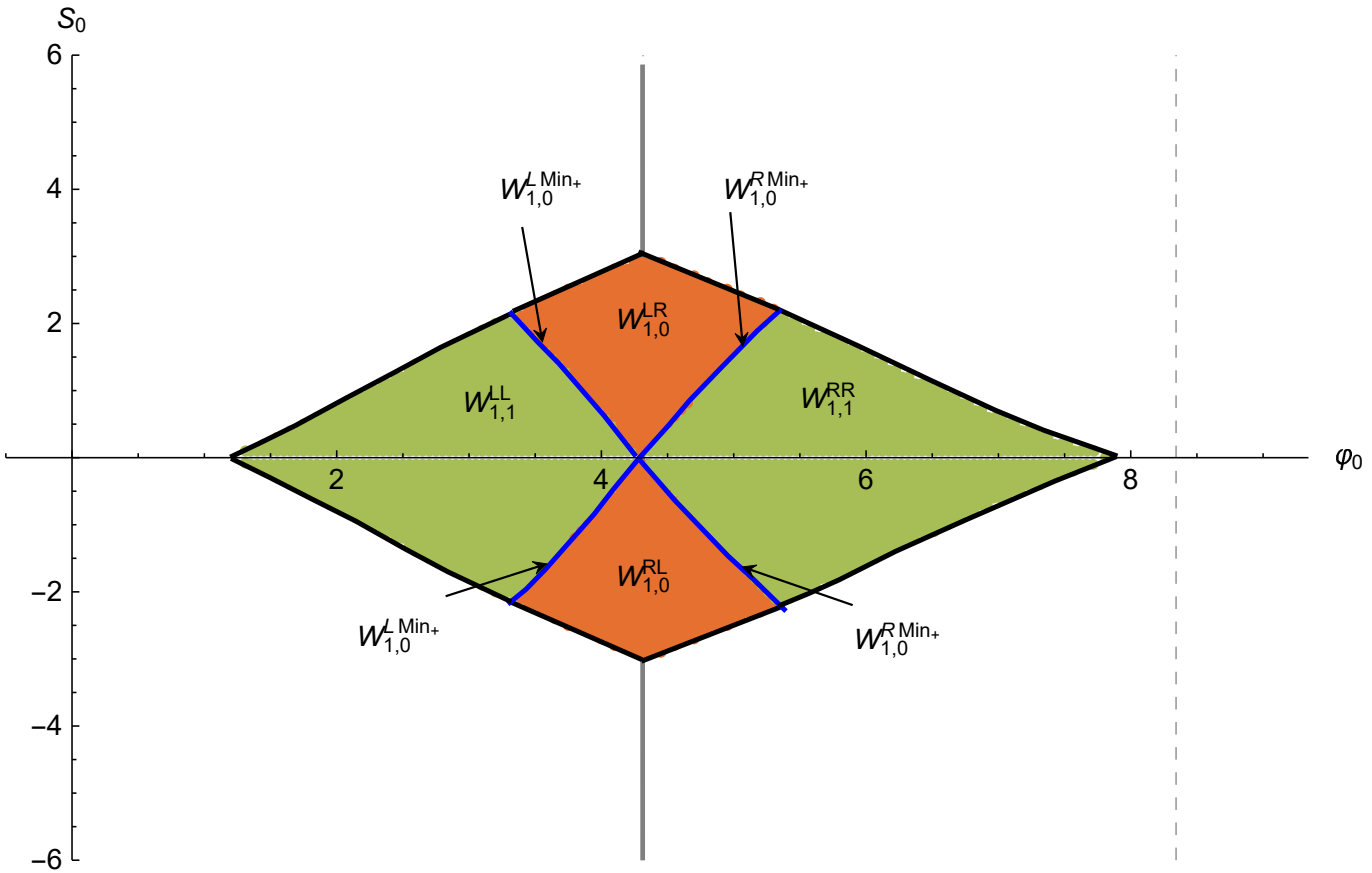

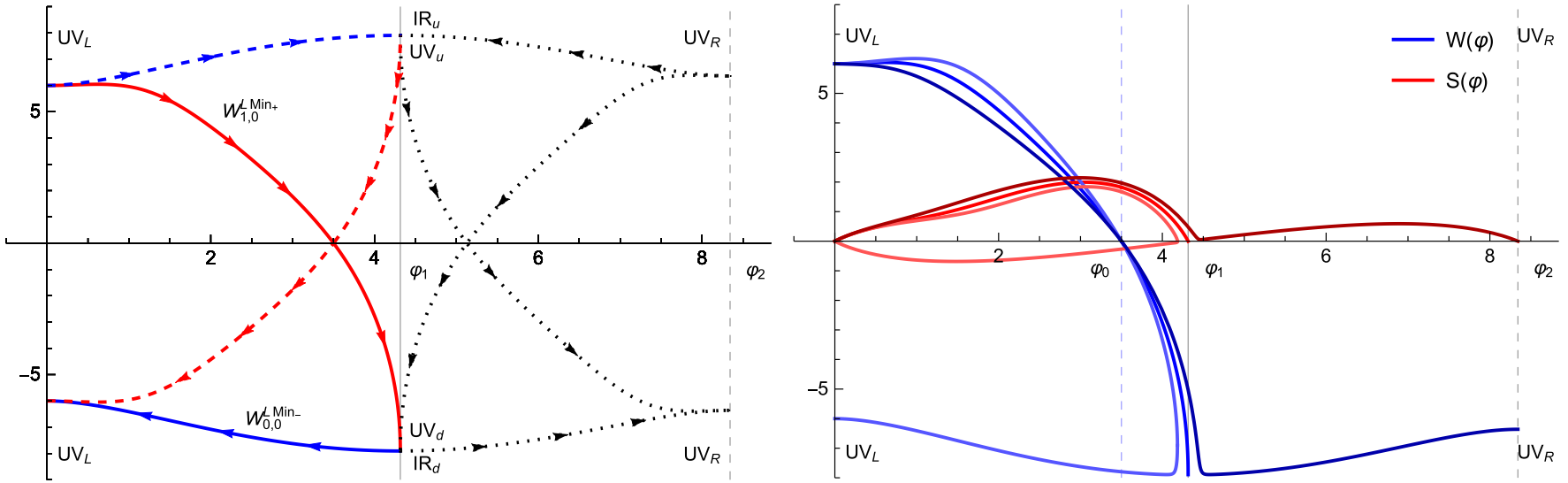

(a): An example of an RG flow between a maximum and a minimum. For the solid curves, (Max_-, Min_+) is a flow between a UV fixed point at maximum $\Phi = 0$ and another UV fixed point at the minimum $\Phi = \Phi_1$. For the (Max_-, Min_-) part of the solution, the minimum is an IR fixed point. The dashed curves show the flipped image of the solid curves. The black dotted curves are other possible RG flows with the same UV fixed points. (b): At a fixed Φ_0 when the value of S_0 is exactly on the border of type $W^{LR}_{1,0}$ and type $W^{LL}_{1,1}$, we have the $W^{LMin_+}_{1,0}$ branch solution (the middle flow). If we increase or decrease the value of S_0 we have the $W^{LR}_{1,0}$ or $W^{LL}_{1,1}$ solutions respectively.

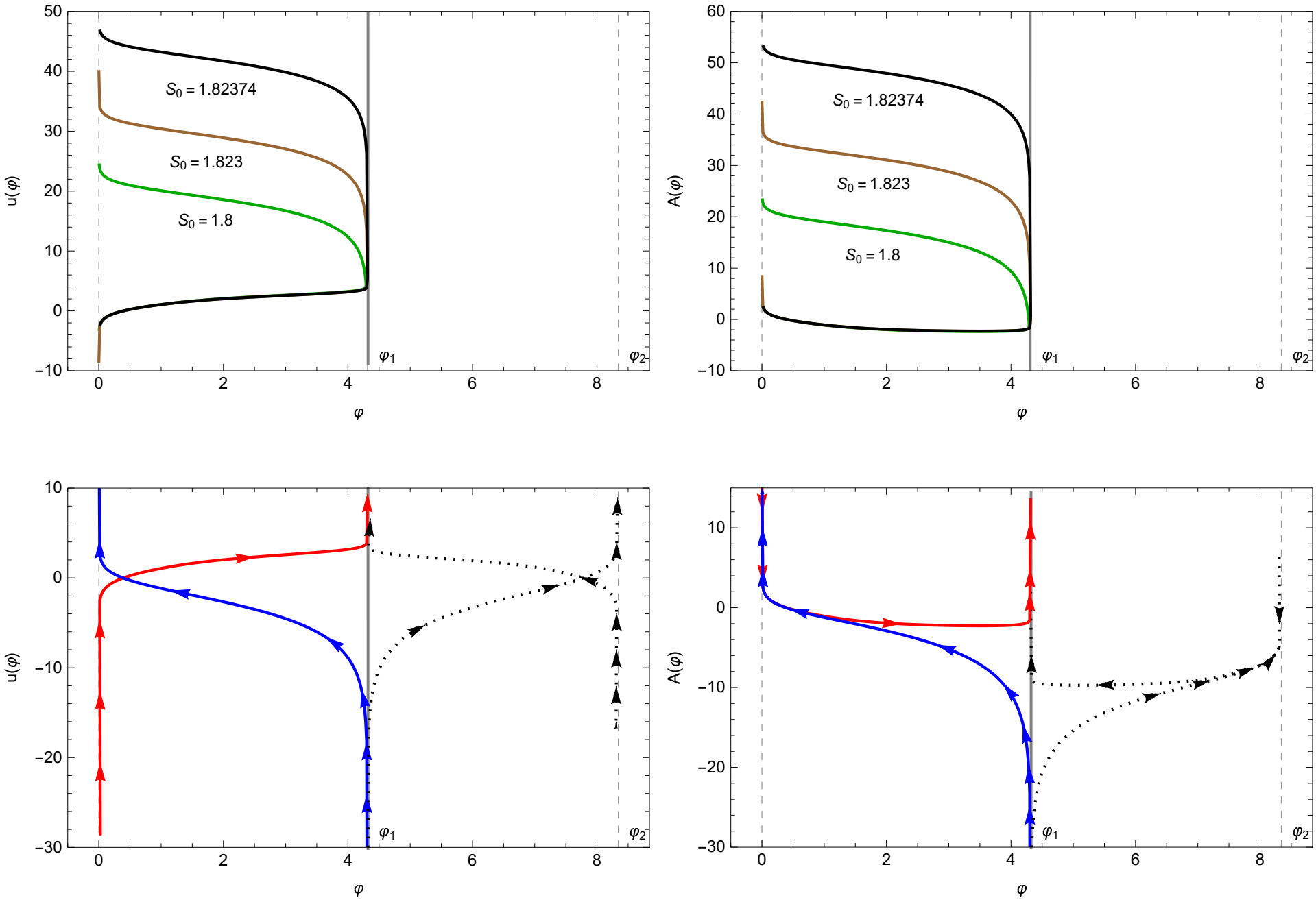

The behavior of the holographic coordinate and scale factor in terms of Φ for the $W_{1,0}^{LMin_+}$ and $W_{0,0}^{LMin_-}$ RG flows. The red curve belongs to $W_{1,0}^{LMin_+}$ and the blue to $W_{0,0}^{LMin_-}$.

• In this limiting region we have an explicit example of solution fragmentation.

• There are two phenomena visible in this example.

♠ Walking. This the phenomenon when an intermediate AdS region appears between the UV and IR, or between UV and UV as is the case here

♠ The emergence of a new boundary.

$$(Max_-, Max_-) \quad \rightarrow \quad (Max_-, Min_-) \quad \oplus \quad (Min+, Max_-)$$

• Such flows can be rotated into cosmological solutions with a cosmological bounce, no singularity and "inflation" at the place of big bag.

Confining Theories on AdS-Critical solutions

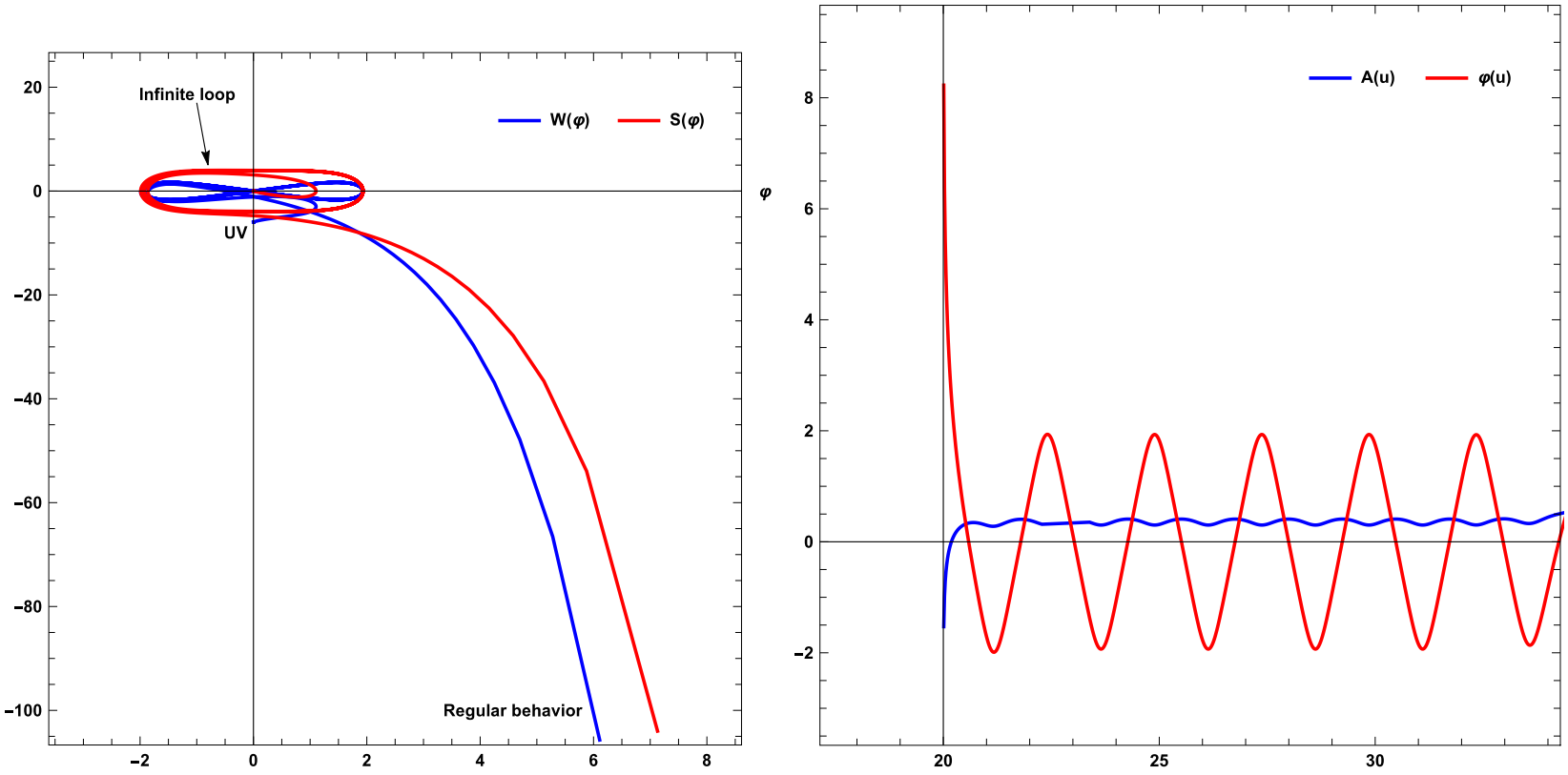

The numerical solutions with an arbitrary number of A and Φ oscillations.

Solutions with many A-loops

The numerical solutions with many oscillations in the scale factor, have two general properties:

• At the oscillation region, the scale factor $A(u)$ has small amplitude oscillations around a fixed value.

• The oscillations of Φ are in a region in which the potential (2) can be approximated by $(0 \leq \Phi \lesssim 2)$

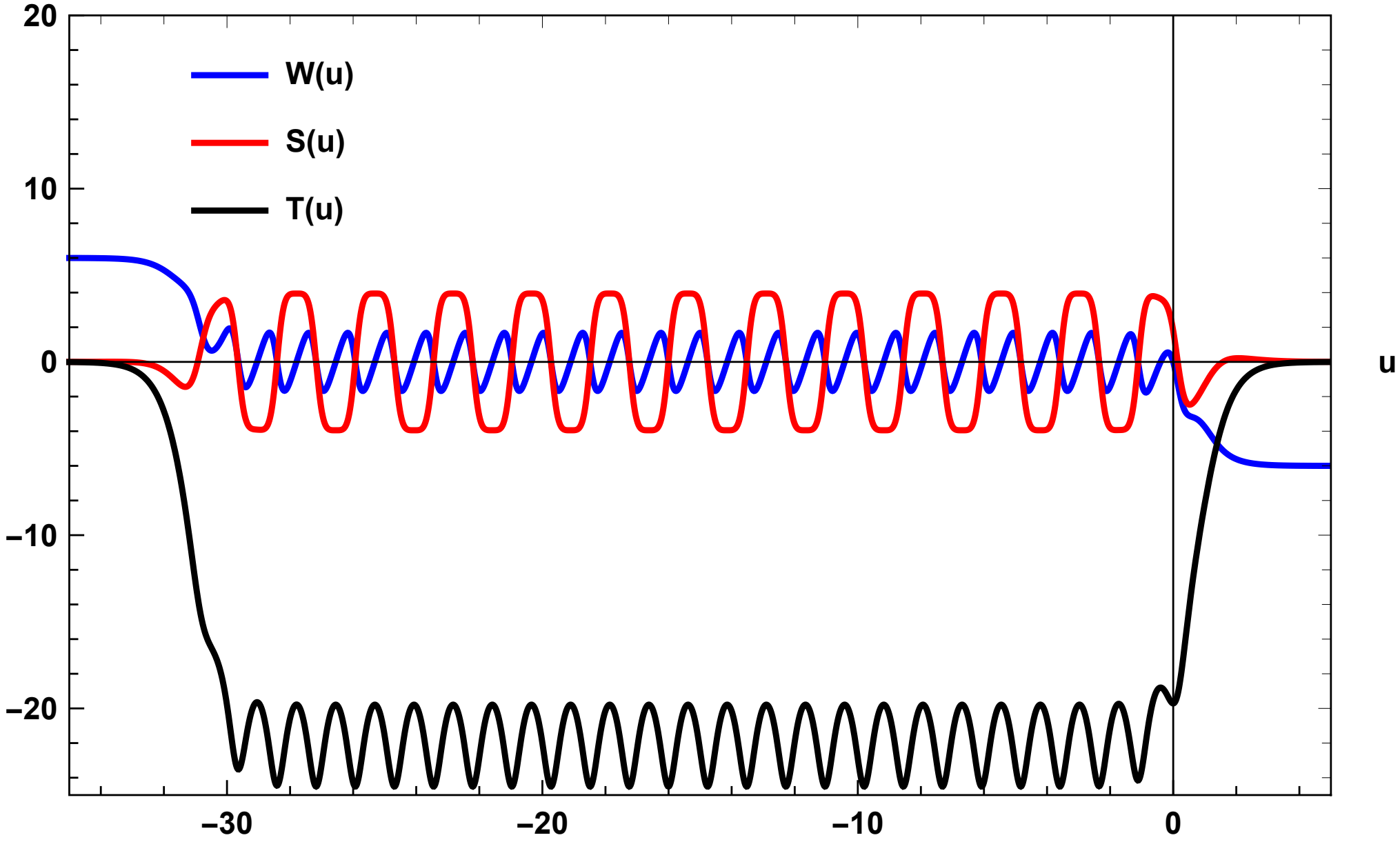
20
10
0
−10
−20
−30
−20
−10
0
u
W(u)
S(u)
T(u)

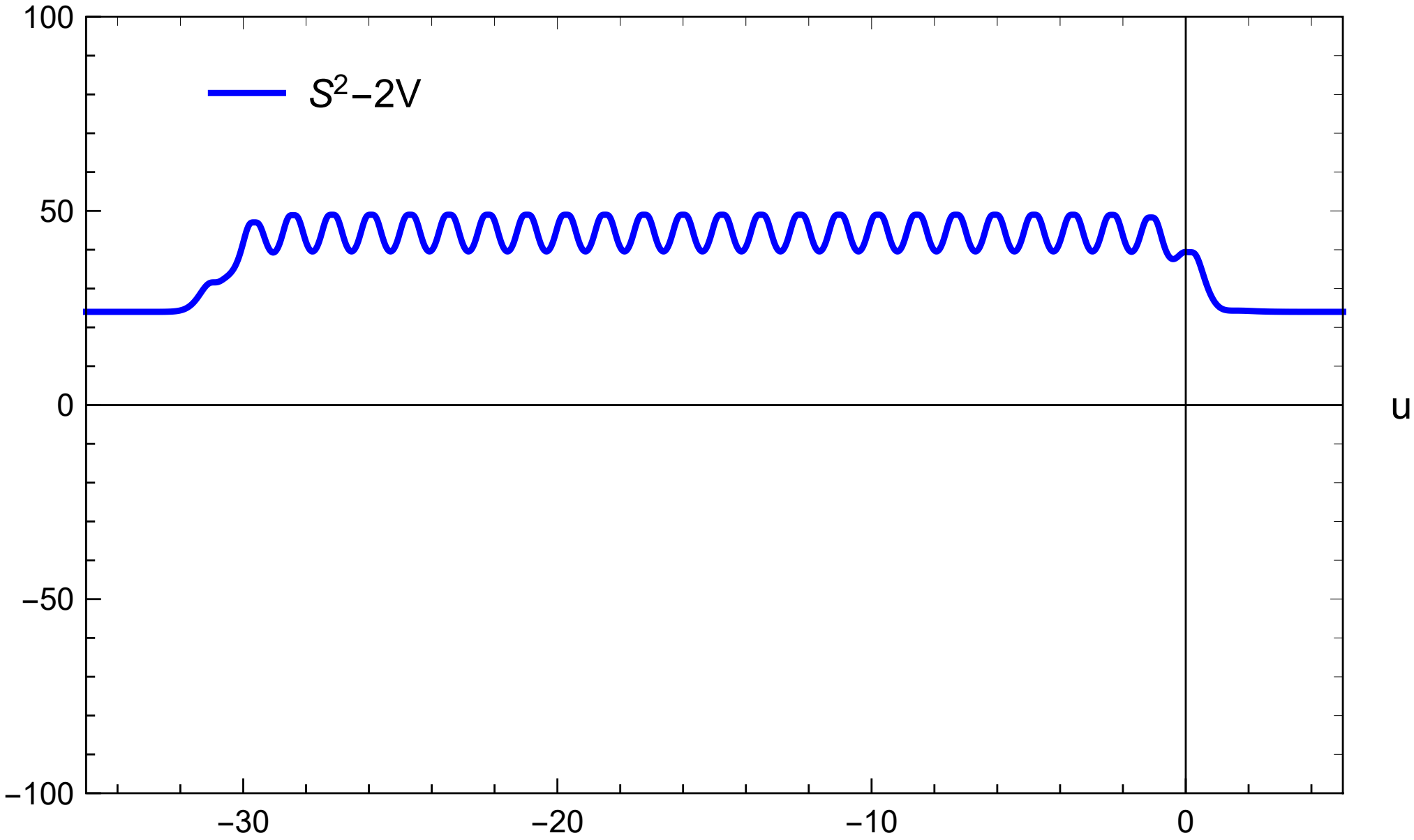
100
50
0
−50
−100
−30
−20
−10
0
u
S^2-2V

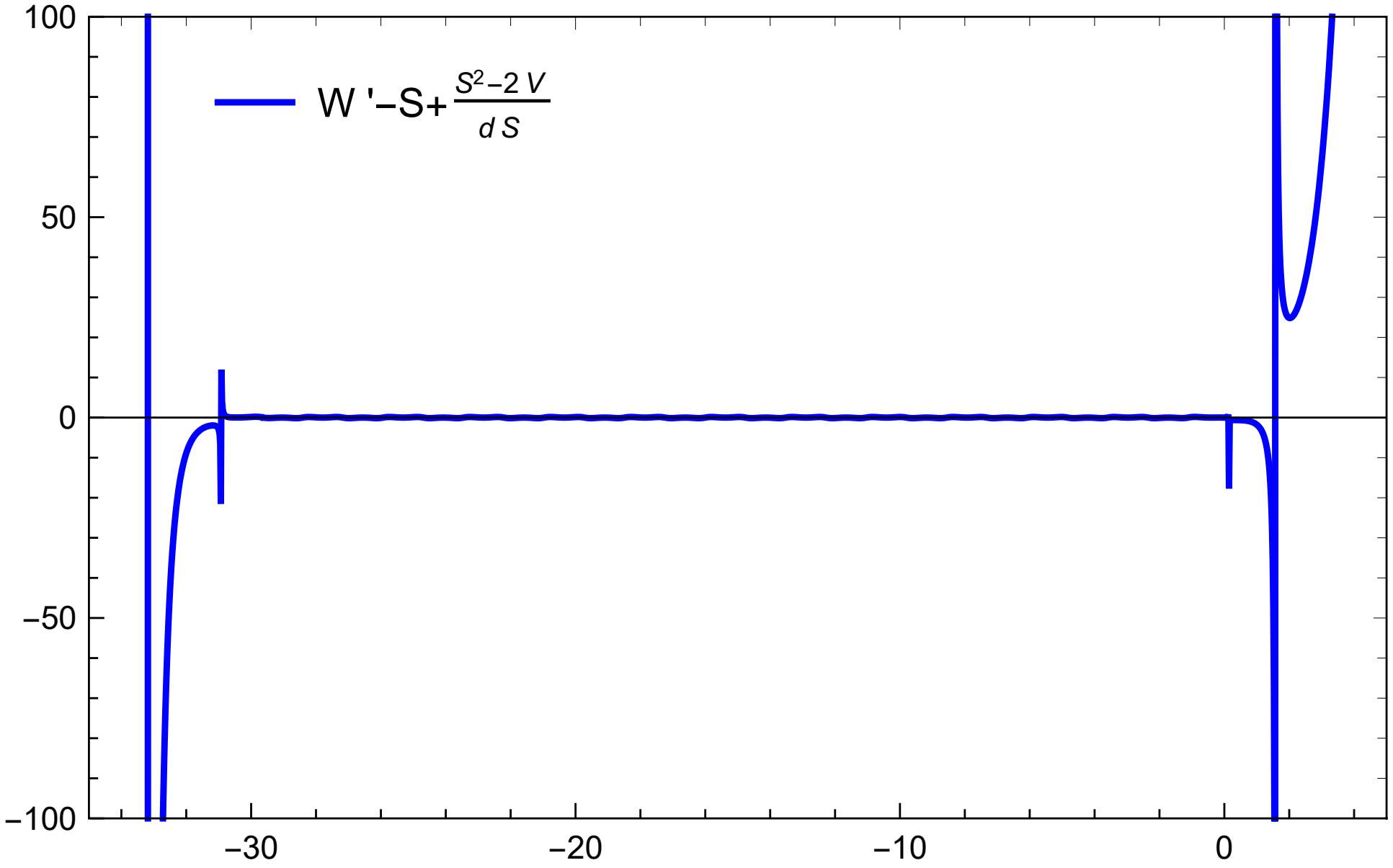

(a) W, S and T as a function of u. (b) Shows the function $S^2 - 2V$ that is nearly constant. $T = W' - S + \frac{S^2-2V}{dS}$ as a function of u. It is approximately zero,

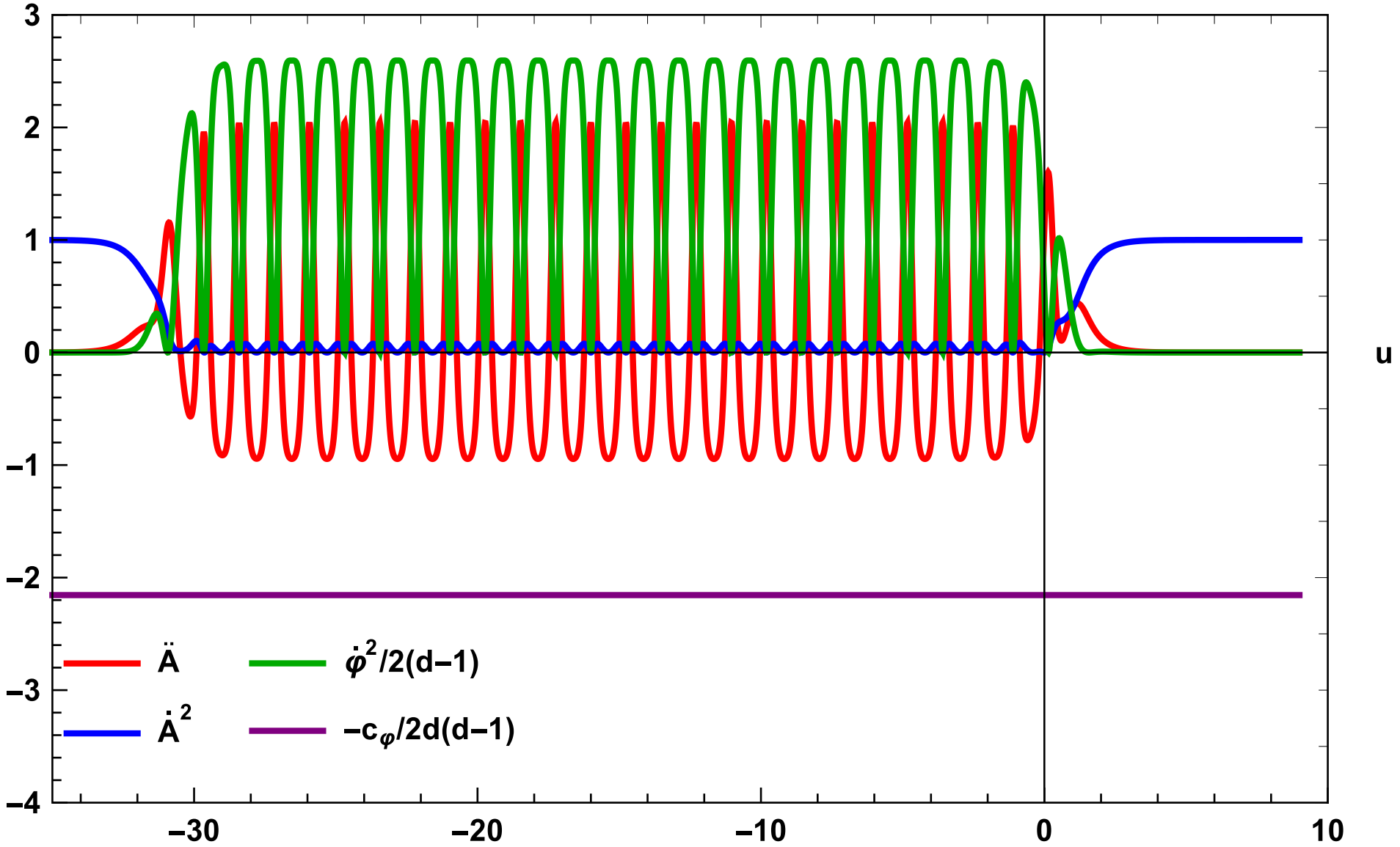

Various terms plotted as a function of the coordinate u. The amplitude of the oscillations of $\dot{A}^2$ is very smaller than the other terms.The horizontal axis is the u coordinate.

Classifying the solutions, Part I

- We pick $d = 4$ and a generic quartic potential

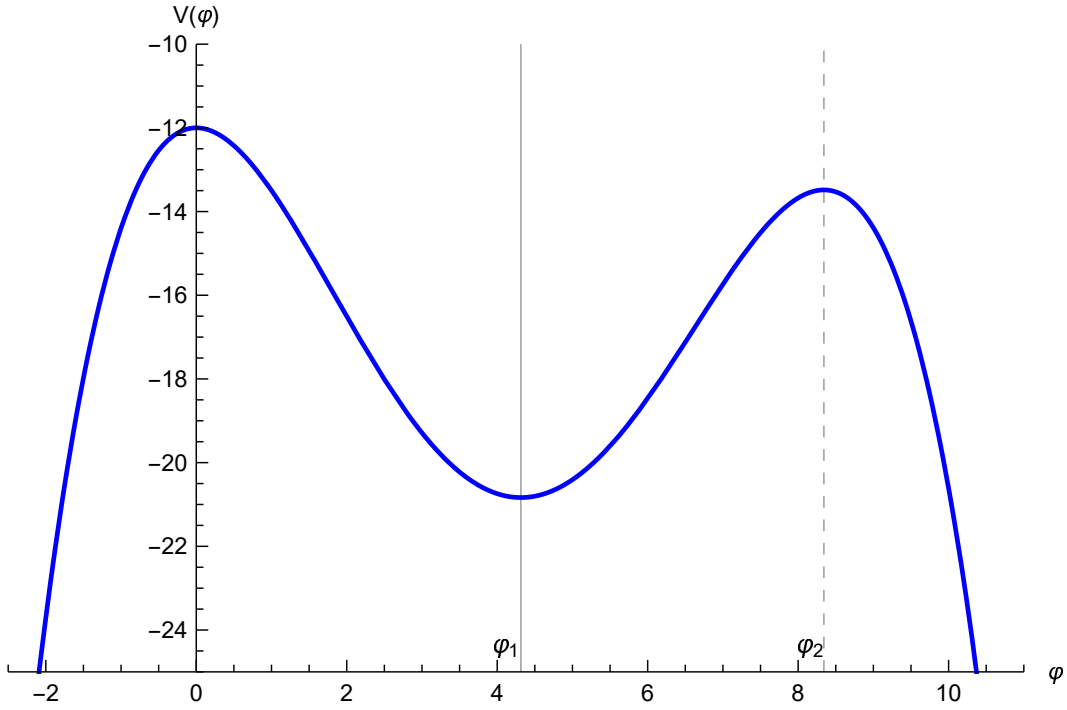

- The left maximum is at $\Phi = 0$.
- The right maximum is at $\Phi_2 = 8.34$.
- The minimum is located at $\Phi_1 = 4.31$.

- "Technical" definitions:

♠ A-bounce is a point where $\dot{A} = 0 \rightarrow W = 0$. It always exists when the slice curvature is negative.

- We denote the position of an A-bounce by Φ_0.

♠ Φ-bounce is a point where $\dot{\Phi} = 0 \rightarrow S = 0$.

• We always start our solution at an A-bounce at $\Phi = \Phi_0$ $(W(\Phi_0) = 0)$and we solve the first order equations

$$\frac{d}{2(d-1)} W^2 + (d-1) S^2 - d S W' + 2V = 0\,,$$

$$S S' - \frac{d}{2(d-1)} S W - V' = 0\,.$$

• We only need an extra "initial" condition: $S_0 \equiv \dot{\Phi}|_{\Phi=\Phi_0} \equiv S(\Phi_0)$.

• The two parameters $(\Phi_0, S_0) \in R^2$ are the complete initial data of the first order system.

• For each pair (Φ_0, S_0) there is a unique solution.

AdS mass spectra

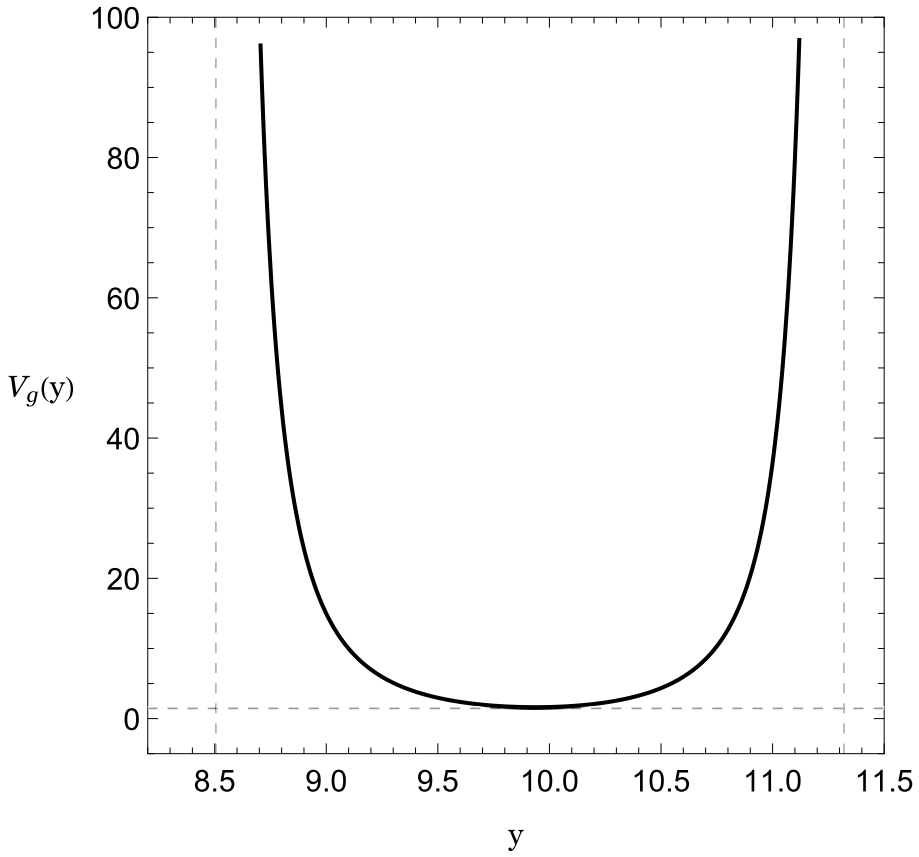

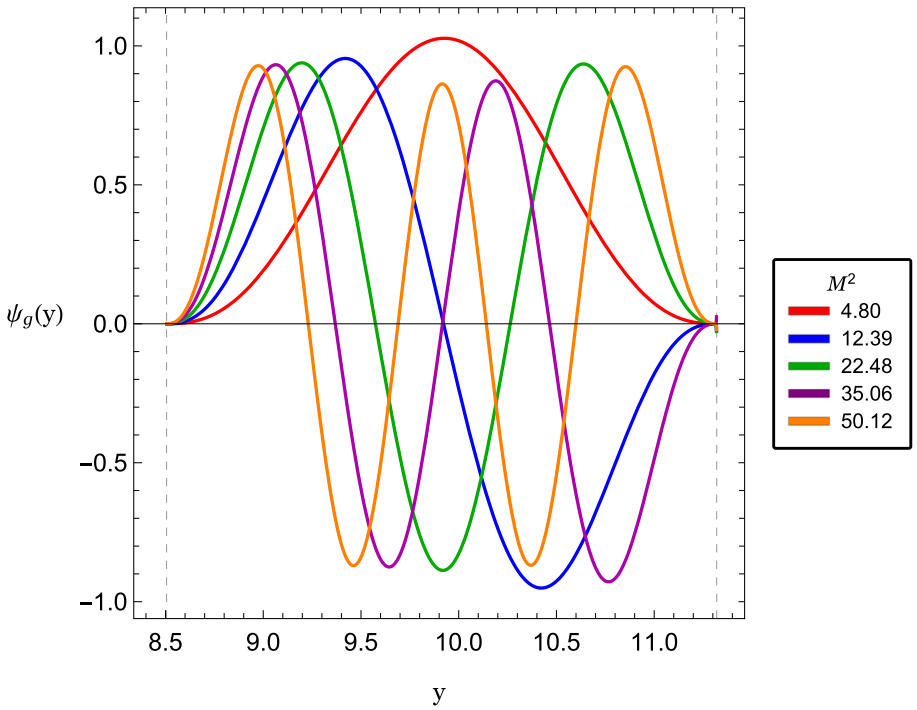

Left: The graviton potential Right): The first five normalizable solutions of the graviton modes. The vertical dashed lines show the locations of the left and right boundaries.

- The expansion of the graviton potential near the UV boundary

$$V_g(y) = \frac{15}{4y^2} + \begin{cases} -\frac{(\Delta_- -2)\Delta_-^2}{(1+2\Delta_-)}\,\varphi_-^2\, y^{2\Delta_- -2} + \mathcal{O}(y^{4\Delta_- -2}), & 0 < \Delta_- < \frac{1}{2} \\ -\frac{(\Delta_- -2)\Delta_-^2}{(1+2\Delta_-)}\,\varphi_-^2\, y^{2\Delta_- -2} + \mathcal{O}(y^0) & \frac{1}{2} \le \Delta_- < 1 \\ \frac{1}{12}\mathcal{R}\,\varphi_-^{2/\Delta_-} + \mathcal{O}(y^{2\Delta_- -2}) & 1 < \Delta_- < 2 \end{cases} .$$

- The leading term for the potential always behaves as $\frac{1}{y^2}$, so for every $UV_L - UV_R$ solution, we should expect a discrete mass spectrum for the gravitons.

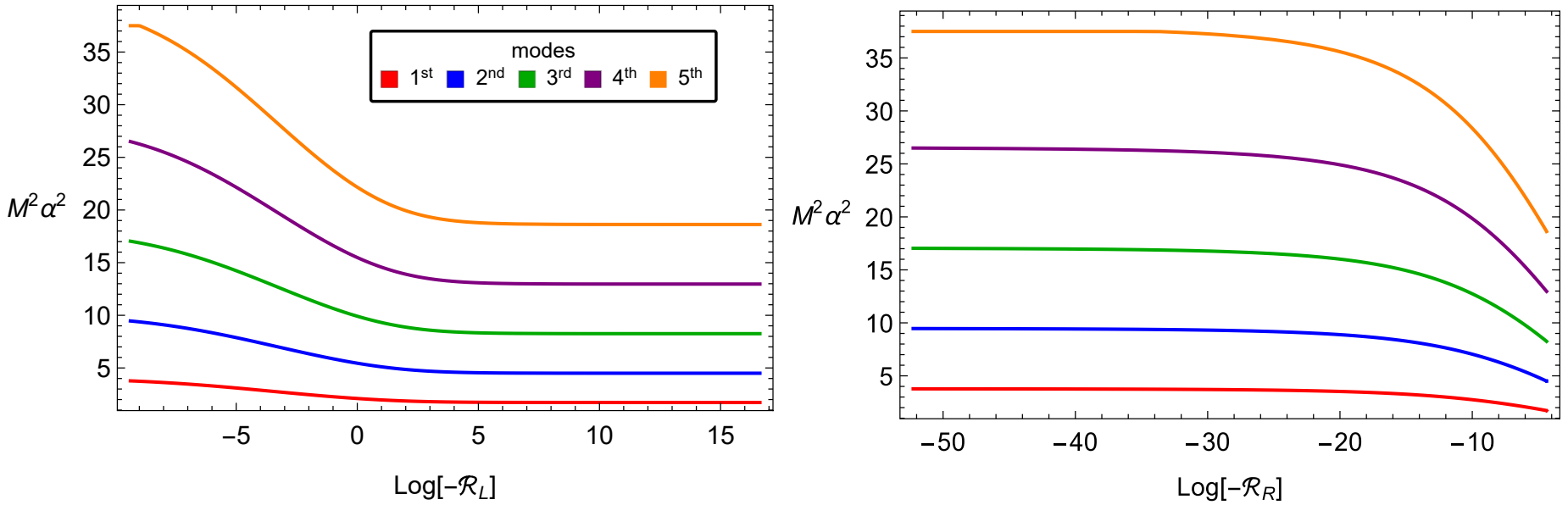

The mass spectrum of the first five graviton modes in terms of dimensionless curvatures for solutions

$$\frac{M^2_{phys}}{R^{UV}} = M^2\alpha^2\,,$$

• In the case of two-boundary solutions that describe conformal interfaces, the two boundaries have different physical curvatures $R^{UV}_{L,R}$.

• Therefore, the only sensible way to define a dimensionless spectrum is via the dimensionless combination $M^2\alpha^2$.

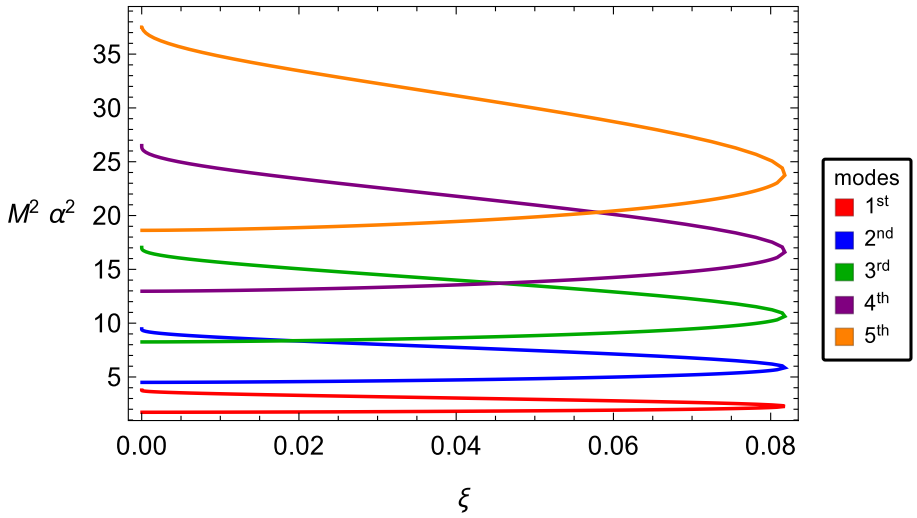

The physical masses as functions of the couplings ξ .

• **Scalar modes**

• For the scalar field, for each mode there is a different potential.

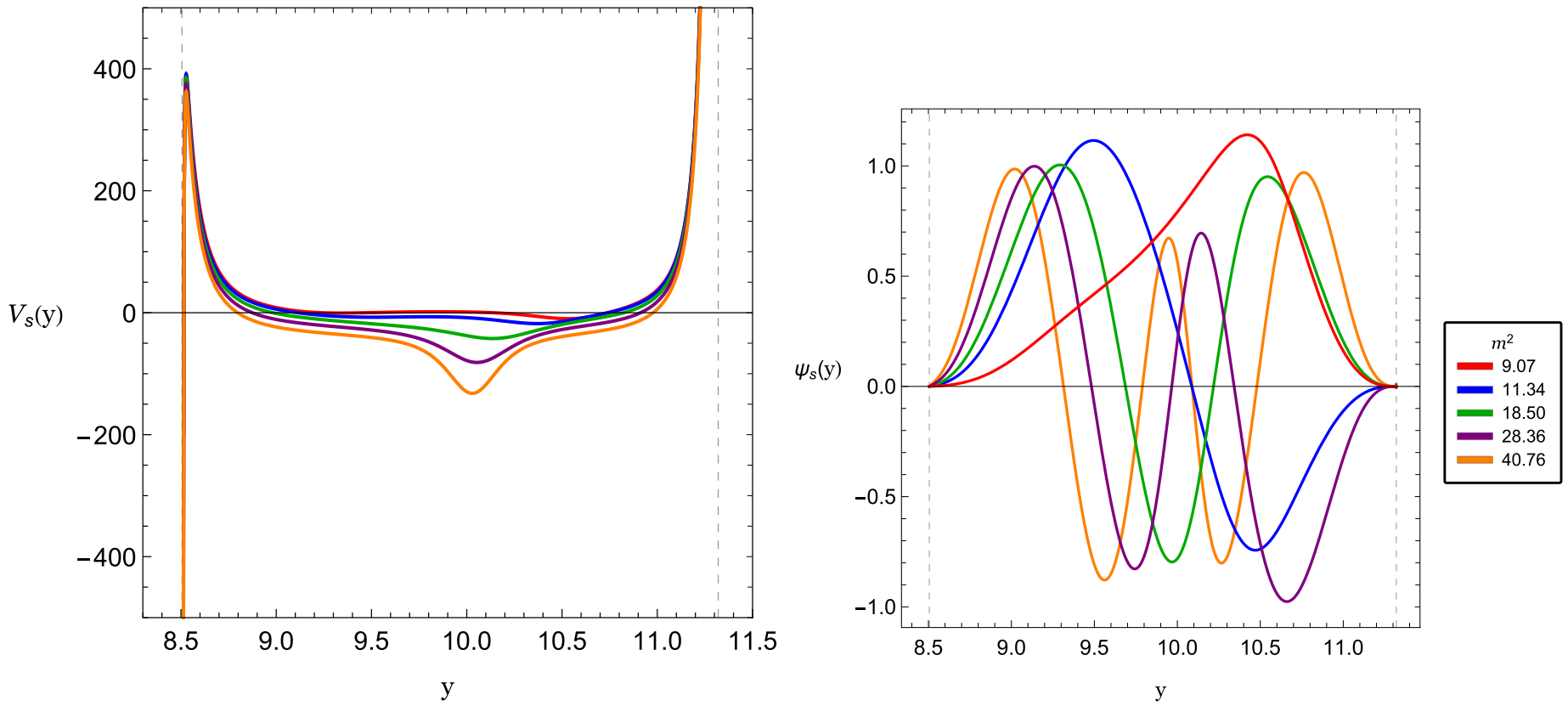

(a) Potentials and (b) wave functions for the first five normalizable modes of the scalar field fluctuations.

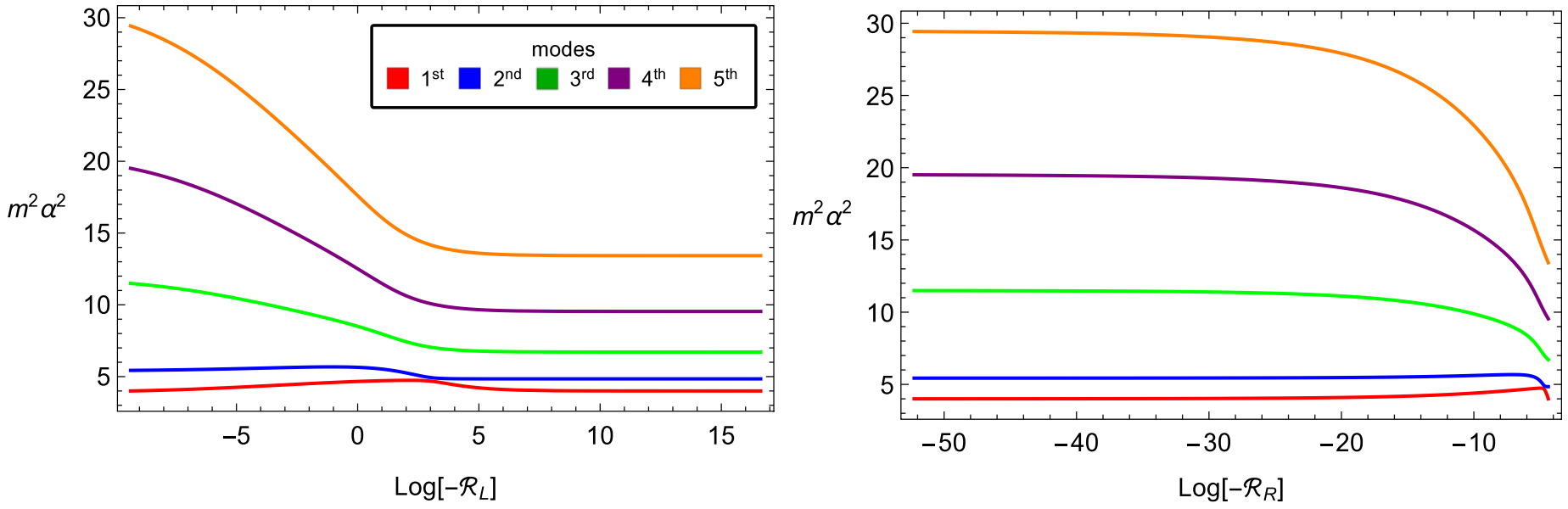

(a), (b): The mass of the first five scalar modes in terms of dimensionless curvatures.

- The expansion of the scalar potential near the UV boundaries is

$$V_s(y) = \frac{1}{4y^2}(2\Delta_- - 5)(2\Delta_- - 3) + \begin{cases} V_1\, y^{2\Delta_- - 2} + \mathcal{O}(y^{4\Delta_- - 2}), & 0 < \Delta_- < \frac{1}{2} \\ V_1\, y^{2\Delta_- - 2} + \mathcal{O}(y^0) & \frac{1}{2} \le \Delta_- < 1 \\ V_2 + \mathcal{O}(y^{2\Delta_- - 2}) & 1 < \Delta_- < \frac{3}{2} \\ V_2 + \mathcal{O}(y^{4-2\Delta_-}) & \frac{3}{2} \le \Delta_- < 2 \end{cases},$$

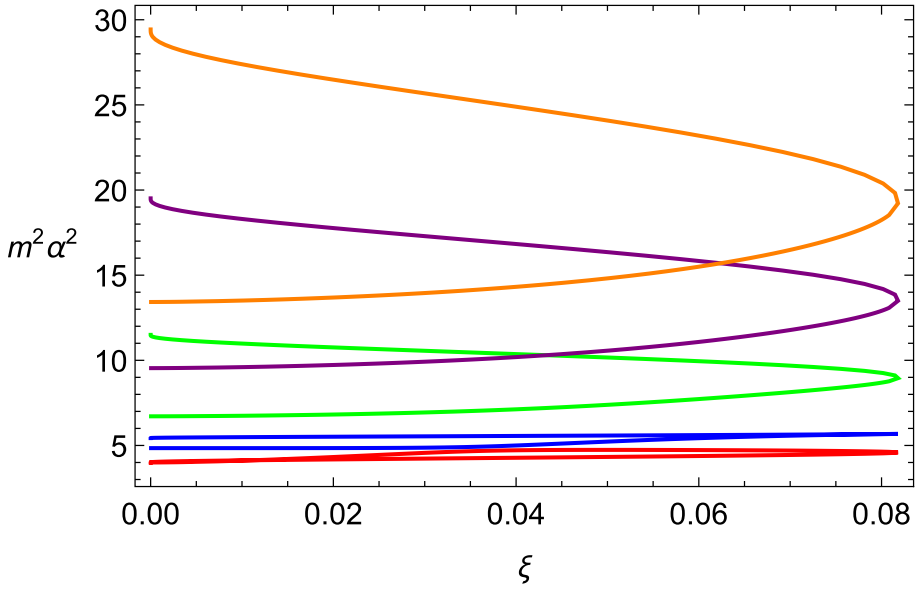

The behavior of the physical mass of the scalar field fluctuations as functions of the couplings ξ

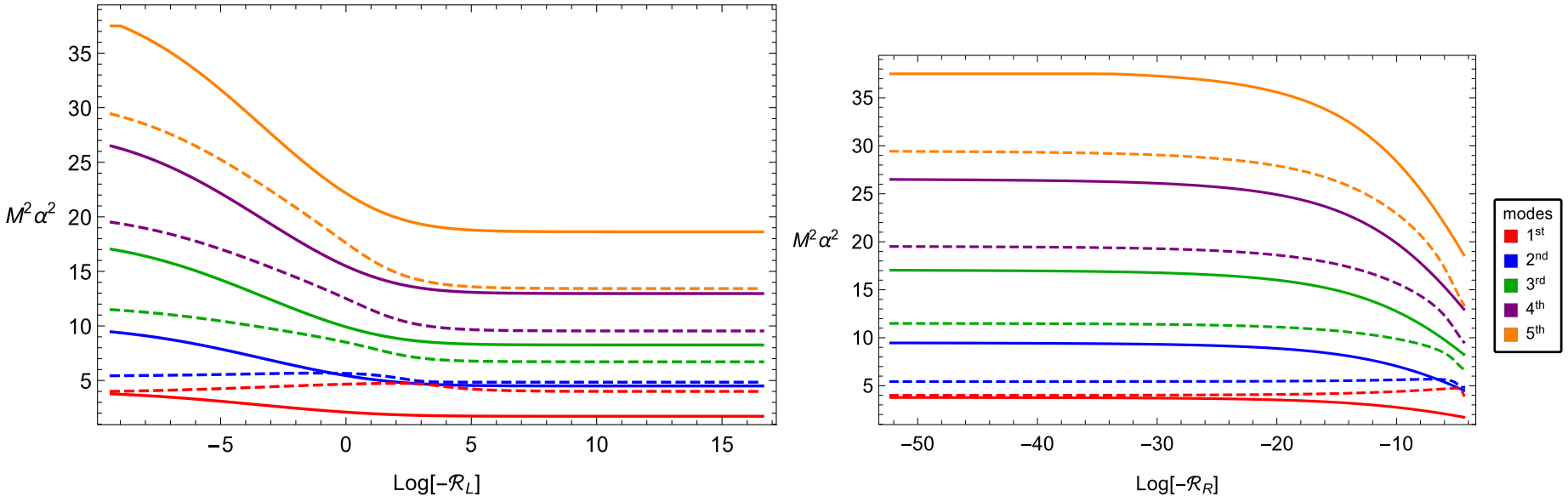

The comparison between the graviton mass (solid curves) and scalar mass (dashed curves).

Skipping fixed points

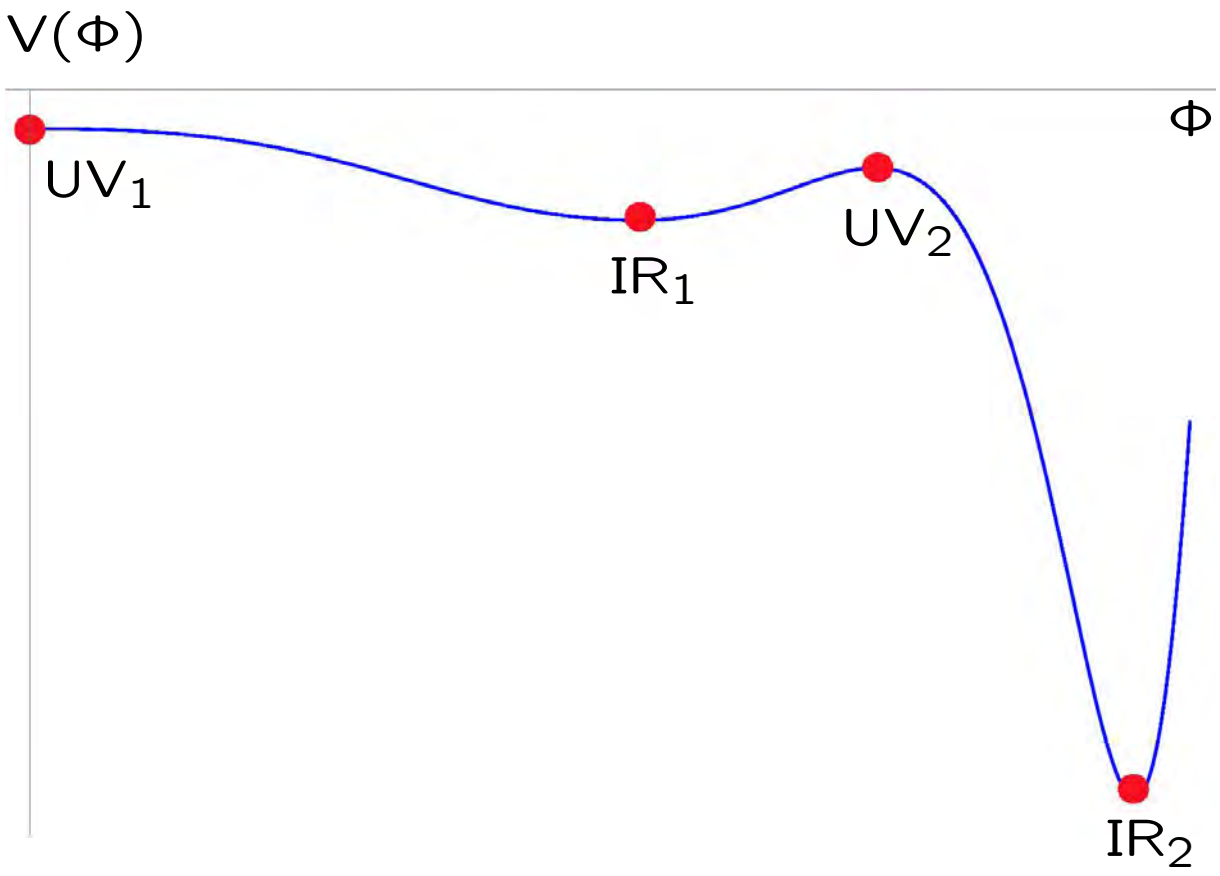

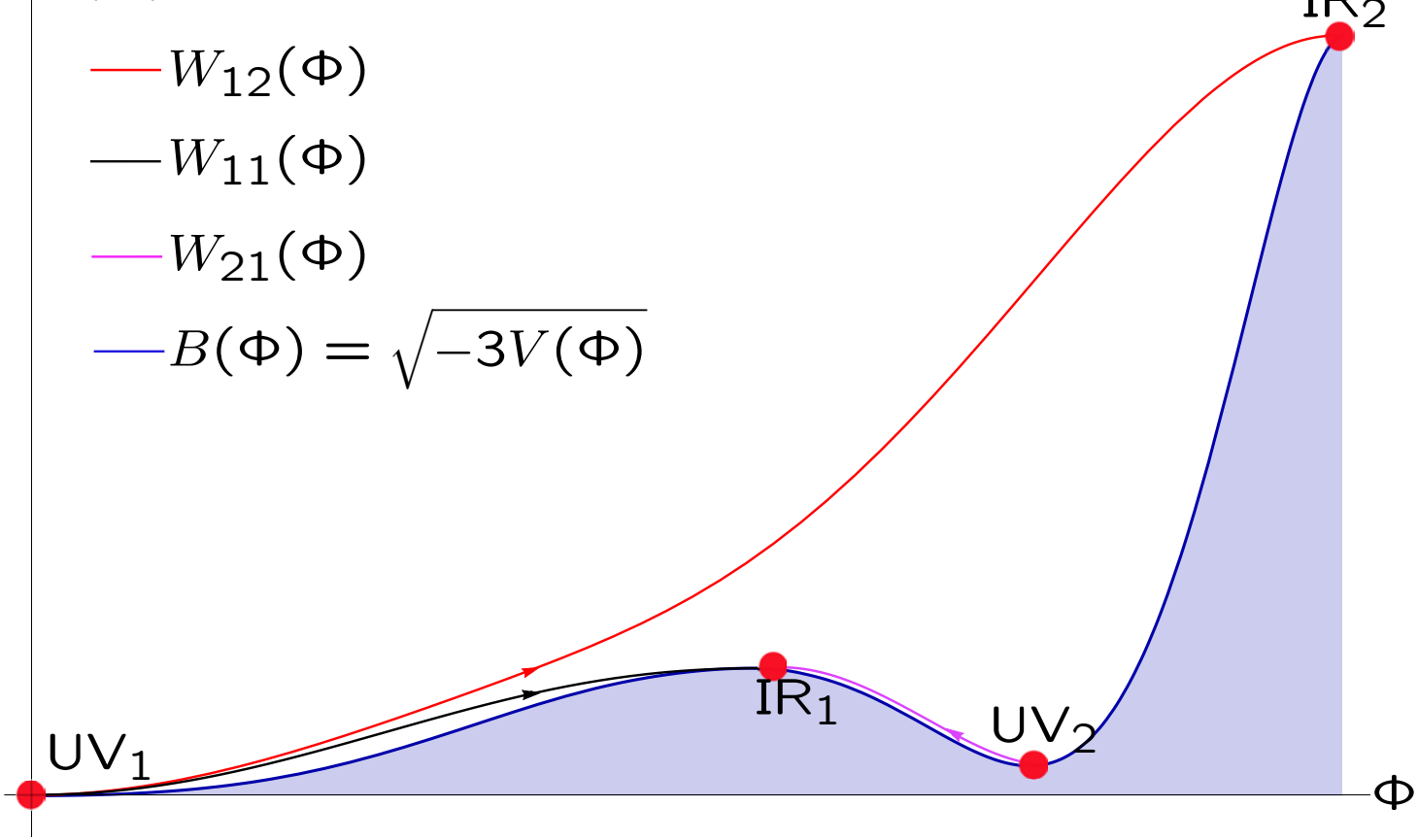

- UV$_2$ is an example of CFT which can be perturbed only on one side (like YM).

- Out of the two flows from UV$_1$ the one towards IR$_2$ has the lowest action.

- This can be shown in general.

Skipping flows at finite curvature

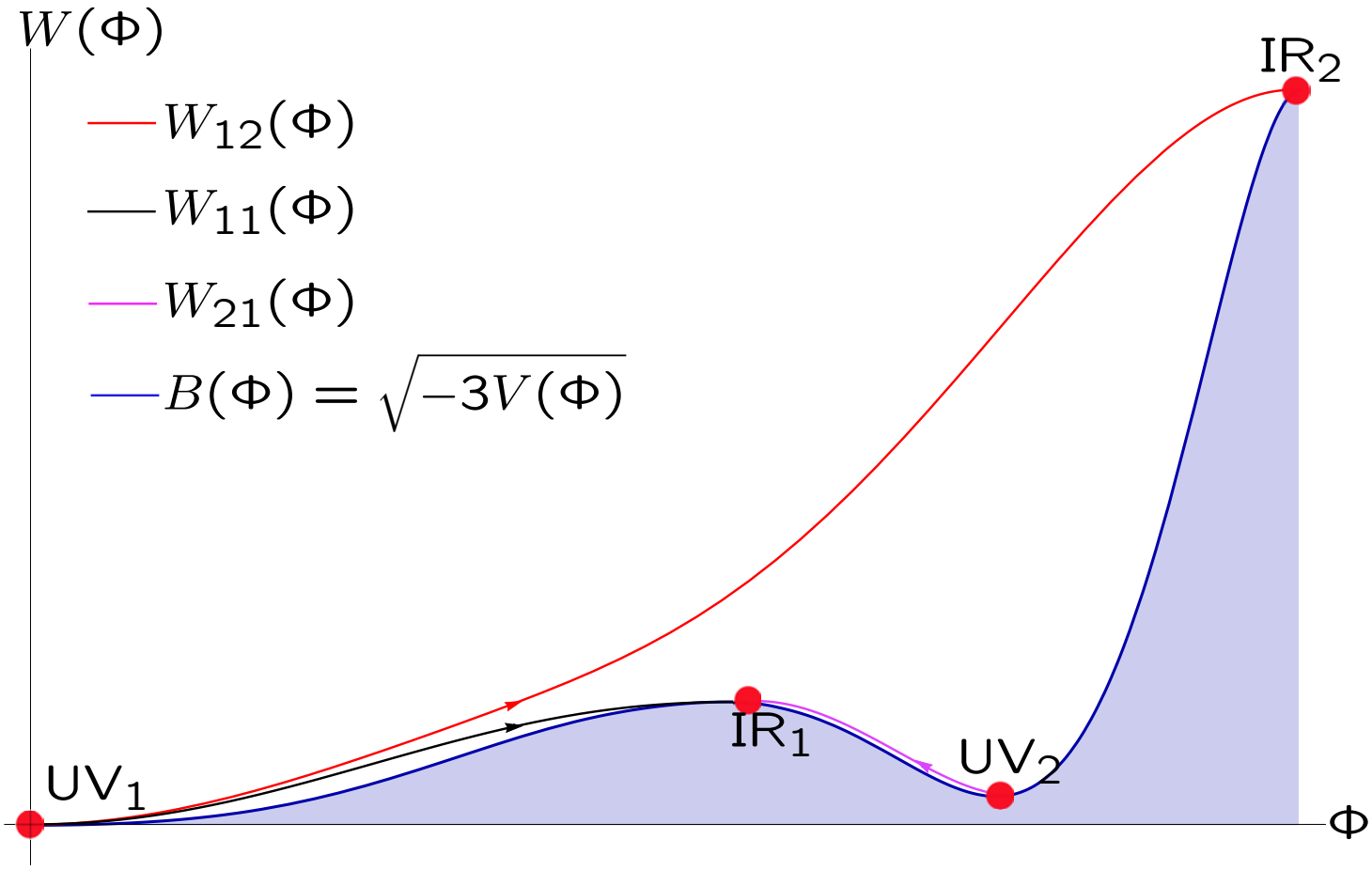

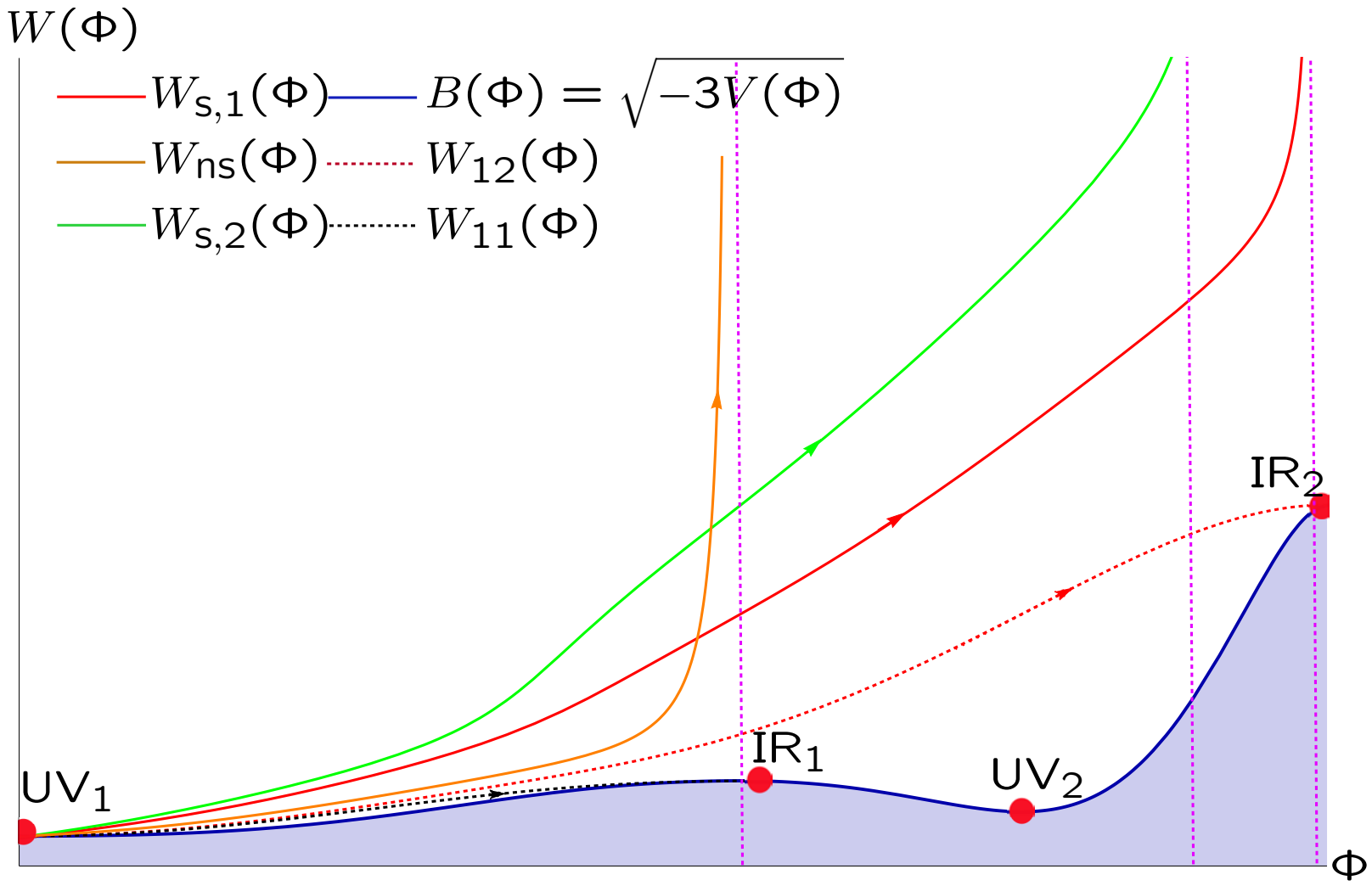

The solid lines represent the superpotential $W(\Phi)$ corresponding to the three different solutions starting from UV_1 which exist at small positive curvature. Two of them (red and green curves) are skipping flows and the third one (orange curve) is non-skipping. For comparison, we also show the flat RG flows (dashed curves)

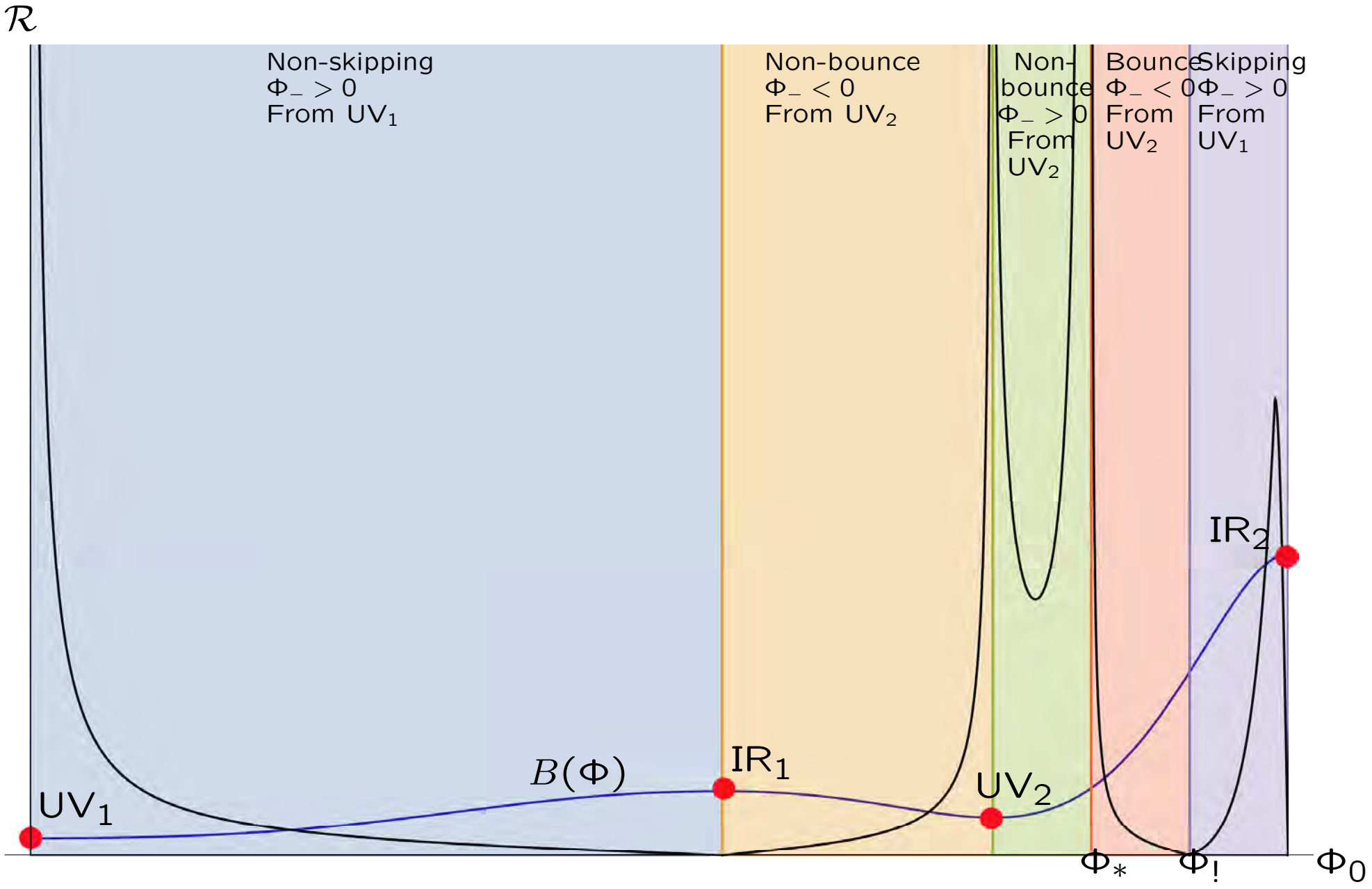
$\mathcal{R}$
Non-skipping
$\Phi_- > 0$
From UV_1
Non-bounce
$\Phi_- < 0$
From UV_2
Non-bounce
$\Phi_- > 0$
From UV_2
Bounce
$\Phi_- < 0$
From UV_2
Skipping
$\Phi_- > 0$
From UV_1
IR_2
$B(\Phi)$
IR_1
UV_2
UV_1
Φ_*
$\Phi_!$
Φ_0

A quantum phase transition for UV_1

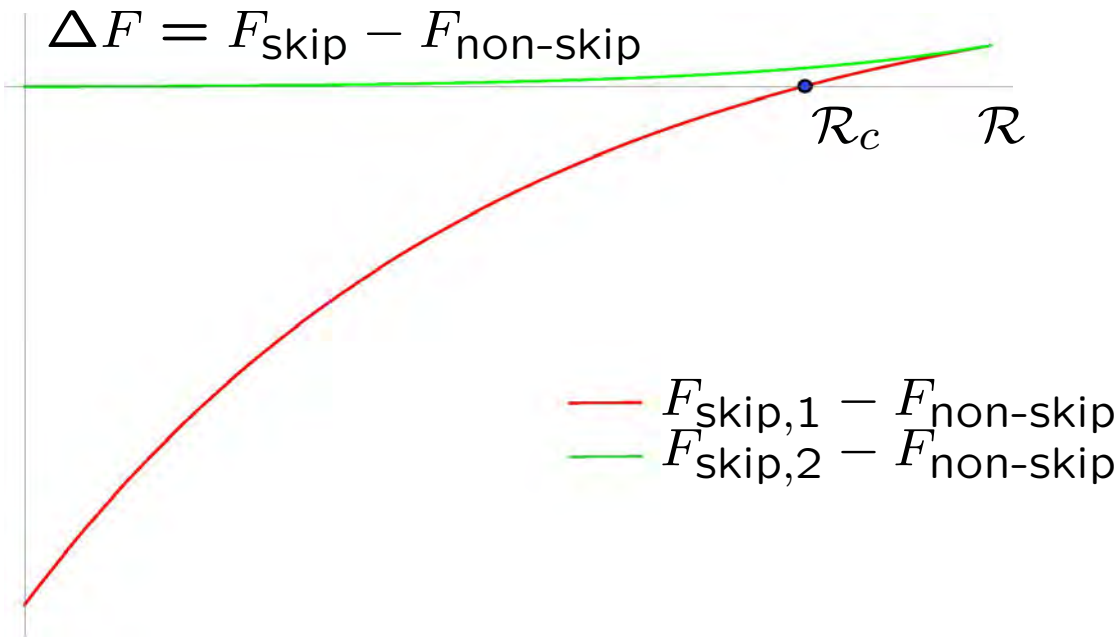

- Free energy difference between the skipping and the non-skipping solution.
- The red curve corresponds to the on-shell action difference between the $W_{s,1}(\Phi)$ solution and the non-skipping solution.

- The green curve corresponds to the on-shell action difference between the $W_{s,2}(\Phi)$ solution and the non-skipping solution $W_{ns}(\Phi)$.

The RG flows from UV_2

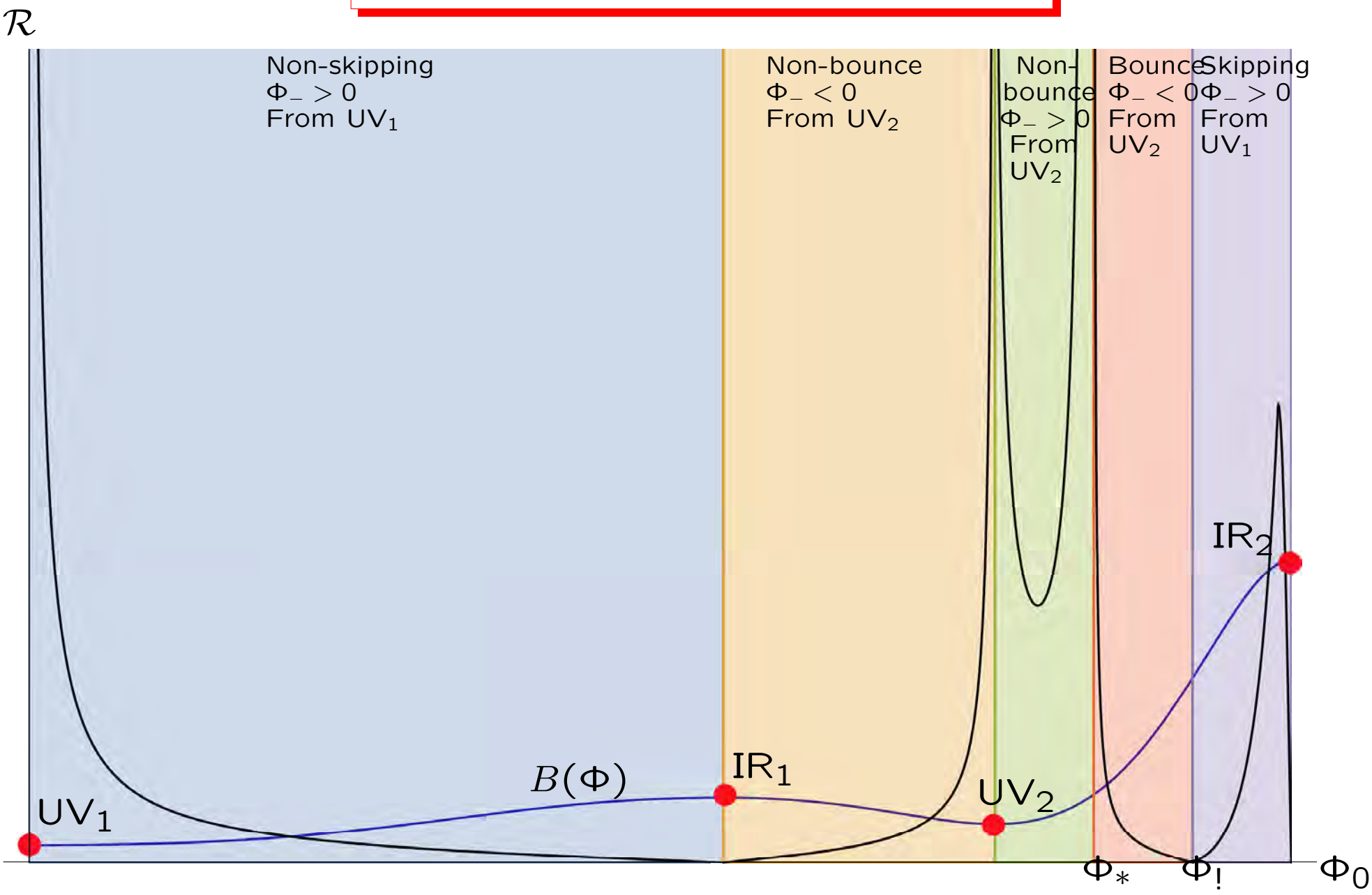

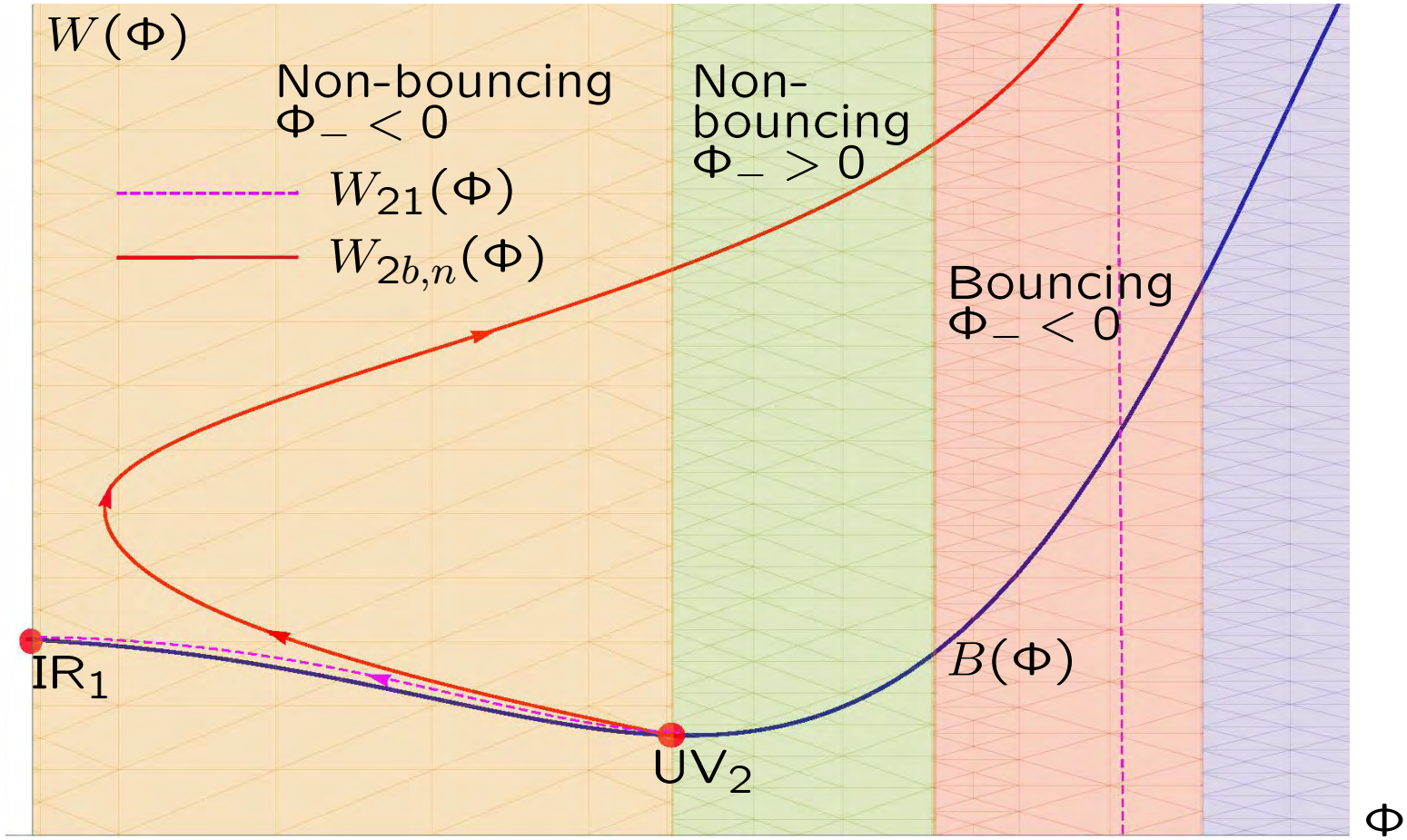
$W(\Phi)$
Non-bouncing
$\Phi_- < 0$
Non-
bouncing
$\Phi_- > 0$
$W_{21}(\Phi)$
$W_{2b,n}(\Phi)$
Bouncing
$\Phi_- < 0$
$B(\Phi)$
IR_1
UV_2
Φ

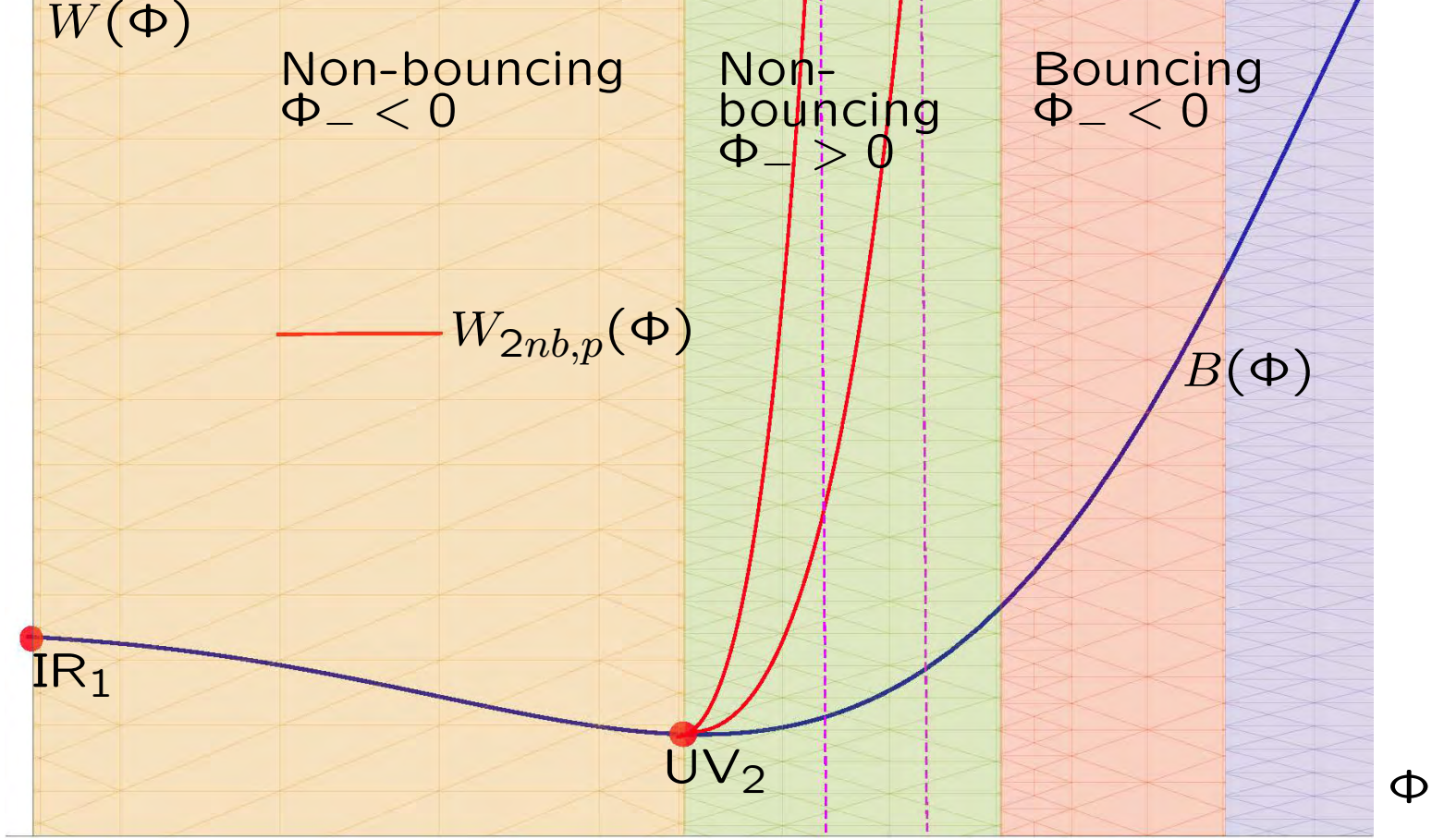
$W(\Phi)$
Non-bouncing
$\Phi_- < 0$
Non-
bouncing
$\Phi_- > 0$
Bouncing
$\Phi_- < 0$
$W_{2nb,p}(\Phi)$
$B(\Phi)$
IR$_1$
UV$_2$
Φ

The on-shell action (free energy)

• A direct computation gives for the unrenormalized on-shell action as a (UV) boundary term:

$$F \equiv S_{\text{on-shell}}(\epsilon) = M_P^{d-1} \int d^d x \sqrt{-\zeta} \left(\left[e^{dA} W \right]_{\text{UV}} + \frac{2R^{\text{uv}}}{d} \int_{\text{UV}}^{\text{IR}} du\, e^{(d-2)A(u)} \right) \Big|_{u=\epsilon}$$

• For positive $\mathcal{R} > 0$, this is the action both for S^d and dS_d.

• It is both UV and IR divergent.

• The UV divergences are well understood since some time.
Hennigson+Skenderis, Skenderis+Papadimitriou

• In the absence of curvature, they can be renormalized at the cost of a single scheme parameter, C_{ct}

$$W(\phi, C_*) \to W(\phi, C_*) - W(\phi, C_{ct})$$

• In the presence of curvature the same procedure for the first terms works similarly.

• The second term contains several divergences as a function of the dimension.

• They need to be subtracted at the cost of a few more scheme parameters.

• In the 3d case that we will specialize, there will be one extra subtraction and therefore another scheme-dependent parameter, B_{ct}.

• Once subtracted, $F^{\text{renormalized}}$ is a function of only $\mathcal{R}$ (cutoff$\to \infty$).

• The renormalized free-energy was conjectured to serve as an $\mathcal{F}$-function in odd dimensions where there are no conformal anomalies.

Jafferis, Jafferis+Klebanov+Pufu+Safdi

• The monotonicity works for CFTs

• But the associated partition function fails to be a monotonic F-function along the the flow.

Klebanov+Pufu+Safdi, Taylor+Woodhead

• Myers and Sinha proposed instead that the entanglement entropy (EE) of an S^2 in R^3 with its complement, can serve as an $\mathcal{F}$-function.

• The proper renormalization of this EE was found by Liu+Mezzei.

• Casini+Huerta+Myers have proved the general monotonicity of this Liu-Mezzei renormalized EE in 3d.

• As the proof does not generalize to other odd dimensions, we would like to understand, in more detail whether there are other $\mathcal{F}$-functions available.

The deSitter entanglement entropy

• Consider a QFT$_d$ on a d-dimensional deSitter space in global coordinates where it is a changing S^{d-1} sphere:

$$ds^2 = -dt^2 + R^2 \cosh^2(t/R)(d\theta^2 + \sin^2\theta \; d\Omega_{d-2}^2)$$

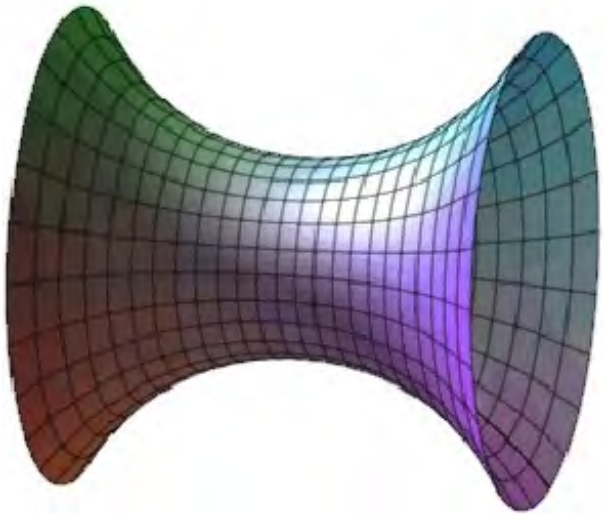

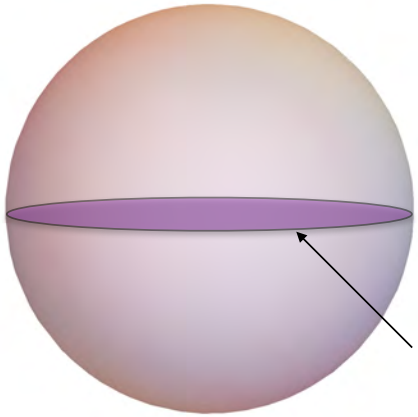

• Consider the entanglement entropy in that theory between two spatial hemispheres that have S^{d-2} as boundary.

• The EE of the two hemispheres can be computed holographically using the Ryu-Takayanagi formula. The result is,

$$S_{EE} = M_P^{d-1} \frac{2R}{d} \int d^d x \sqrt{-\zeta} \int_{\text{UV}}^{\text{IR}} du\, e^{(d-2)A(u)} \,.$$

Ben-Ami+Carmi+Smolkin

• This is precisely the second term that enters the curved on-shell action.

• The dS EE equals the thermal entropy of the static patch in deSitter.

• For a CFT it is also the entanglement entropy for the S^2 in flat space.

Casini+Huerta+Myers

• For the de Sitter entanglement entropy a renormalization à la Liu-Mezzei is still UV-divergent.

Thermodynamics in de Sitter and (entanglement) entropy

• The F-function for 3d CFTs is given by the renormalized "free energy" (or partition function) on the 3-sphere.

Jafferis, Jafferis+Klebanov+Pufu+Safdi

• The interpolating $F-function$ satisfying the F-theorem is given by the S^2 entanglement entropy.

Myers+Sinha, Myers+Casini+Huerta, Liu+Mezzei,Casini+Huerta

• The connection between S^3 partition function and the S^2 entanglement entropy seems puzzling at first.

• We will try to understand it a bit better in our context.

• We will show that there a natural entropy, that is also an entanglement entropy in de Sitter (defined as the analytic continuation of the sphere)

• And that it is related to the "free-energy"/partition function on S^3.

• Consider a QFT$_d$ on a d-dimensional deSitter space in global coordinates where it is a changing S^{d-1} sphere:

$$ds^2 = -dt^2 + R^2 \cosh^2(t/R)(d\theta^2 + \sin^2\theta \; d\Omega_{d-2}^2)$$

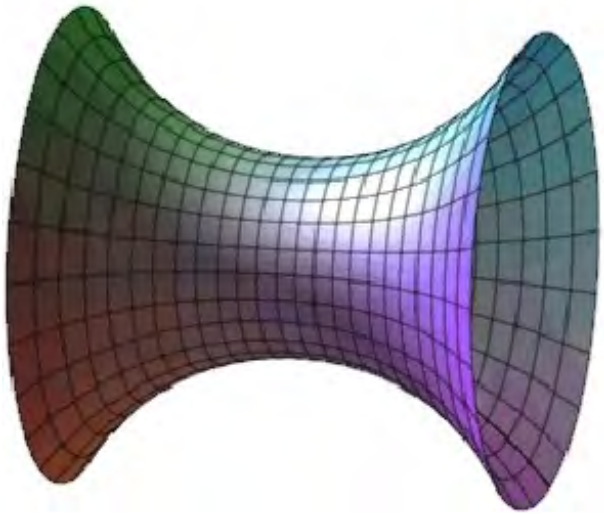

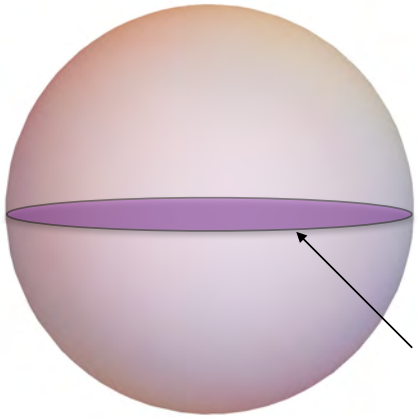

• Consider the entanglement entropy in that theory between two spatial hemispheres that have S^{d-2} as boundary.

• The EE of the two hemispheres can be computed holographically using the Ryu-Takayanagi formula. The result is,

$$S_{EE} = M_P^{d-1} \frac{2R}{d} \int d^d x \sqrt{-\zeta} \int_{\text{UV}}^{\text{IR}} du\, e^{(d-2)A(u)} \,.$$

Ben-Ami+Carmi+Smolkin

• This is precisely the second term that enters the curved on-shell action.

$$F = 2M_p^{d-1} V_d \left[(d-1) \left[e^{dA} \dot{A} \right]_{\text{UV}} + \frac{R}{d} \int_{\text{IR}}^{\text{UV}} du\, e^{(d-2)A} \right] ,$$

• The first term has also a thermodynamical interpretation: we change coordinates on the de Sitter slices and go to static patch coordinates.

Casini+Huerta+Myers

$$ds^2 = du^2 + e^{2A(u)} \left[-\left(1 - \frac{r^2}{\alpha^2}\right) d\tau^2 + \left(1 - \frac{r^2}{\alpha^2}\right)^{-1} dr^2 + r^2 d\Omega_{d-2}^2 \right] .$$

where α is the de Sitter radius and $0 < r < \alpha$.

• Now there is a bulk horizon at $r = \alpha$. The Bekenstein-Hawking entropy can be calculated and it is equal to the dS entanglement entropy, S_{EE}.

- The associated temperature to this horizon is constant

$$T = \frac{1}{2\pi\alpha}$$

- A similar computation of the "energy" U gives

$$\beta U = 2(d-1) M_P^{d-1} \left[e^{dA(u)} \dot{A}(u) \right]_{UV} V_d.$$

- Putting everything together we get a familiar thermodynamic formula

$$F = U - T\ S$$

for the de Sitter free-energy and its S^3 analytic continuation.

- The standard rules of thermodynamics relate our two functions $B(\mathcal{R}), C(\mathcal{R})$.

$$C'(\mathcal{R}) = \frac{1}{2} B(\mathcal{R}) - \mathcal{R} B'(\mathcal{R})$$

- We conclude that de Sitter entanglement entropy and Free energy on S^3 are tightly connected.

- For a CFT, dS S_{EE}, is also the entanglement entropy for the S^2 in flat space.

Casini+Huerta+Myers

The free energy and expectation values

- We can calculate the on-shell action, add counterterms, and remove the cutoff:

$$F_{d=3}^{\text{renorm}}(\mathcal{R}|B_{ct},C_{ct}) = -(M\ell)^2\Omega_3\left[\mathcal{R}^{-\frac{3}{2}}(C(\mathcal{R})-C_{ct})+\mathcal{R}^{-\frac{1}{2}}(B(\mathcal{R})-B_{ct})\right]$$

- B_{ct}, C_{ct} are constants that parametrize the scheme dependence.

- It can be shown that for ANY holographic QFT on dS

$$F = U - T\ S$$

for the de Sitter free-energy and its S^3 analytic continuation.

- The standard rules of thermodynamics relate our two functions $B(\mathcal{R}), C(\mathcal{R})$.

$$C'(\mathcal{R}) = \frac{1}{2}B(\mathcal{R}) - \mathcal{R}B'(\mathcal{R})$$

- in d=4 we have instead

$$C'(\mathcal{R}) = B(\mathcal{R}) - \mathcal{R}B'(\mathcal{R}) + \frac{\mathcal{R}}{96}$$

- For $\mathcal{R} < 0$ the same relation holds, up to constant, branch-wise.

Two-boundary saddle points

- Similarly, the free energy can be calculated for the two-boundary solutions dual to holographic interfaces.

- In this case, the free energy depends on the data of both theories

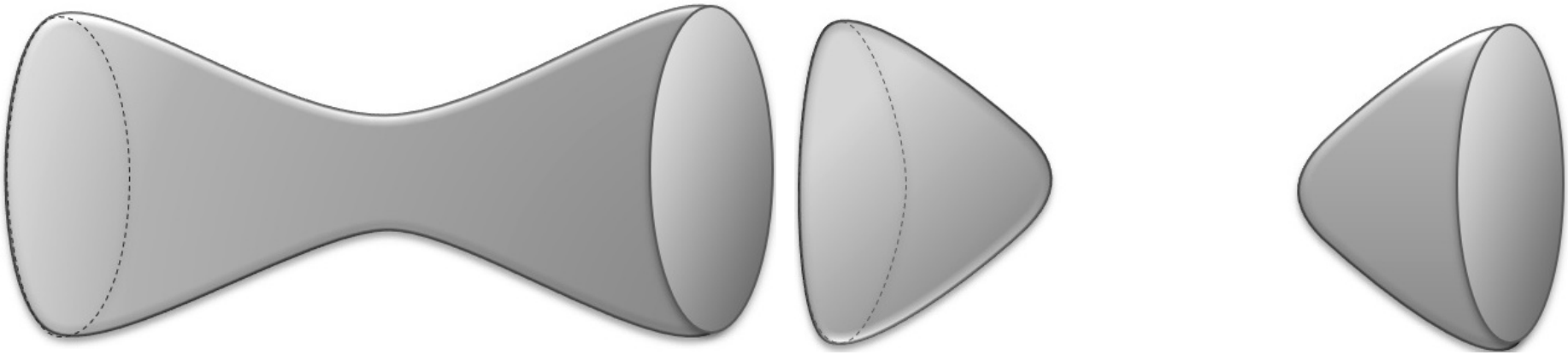

- There is always competition from the factorized solutions.

- The factorized solutions have lower-free energy always.

- This would seem to imply that cross-correlators are exponetially suppressed by $e^{-N_c^2}$.

• However typically there will be perturbatively connected "disconnected" saddle points most probably power-suppressed in N.

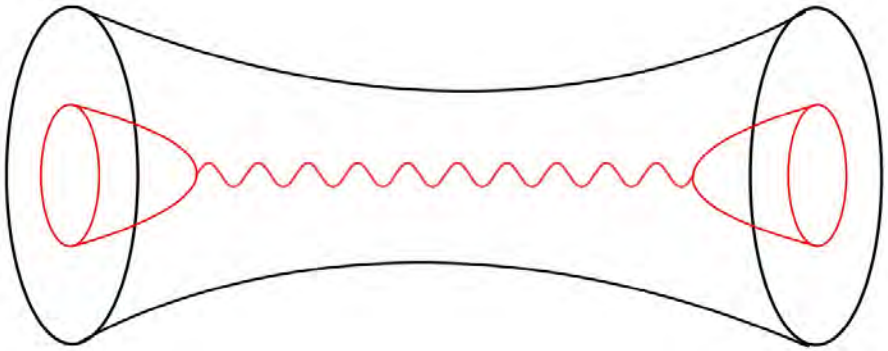

AdS-relation to sources

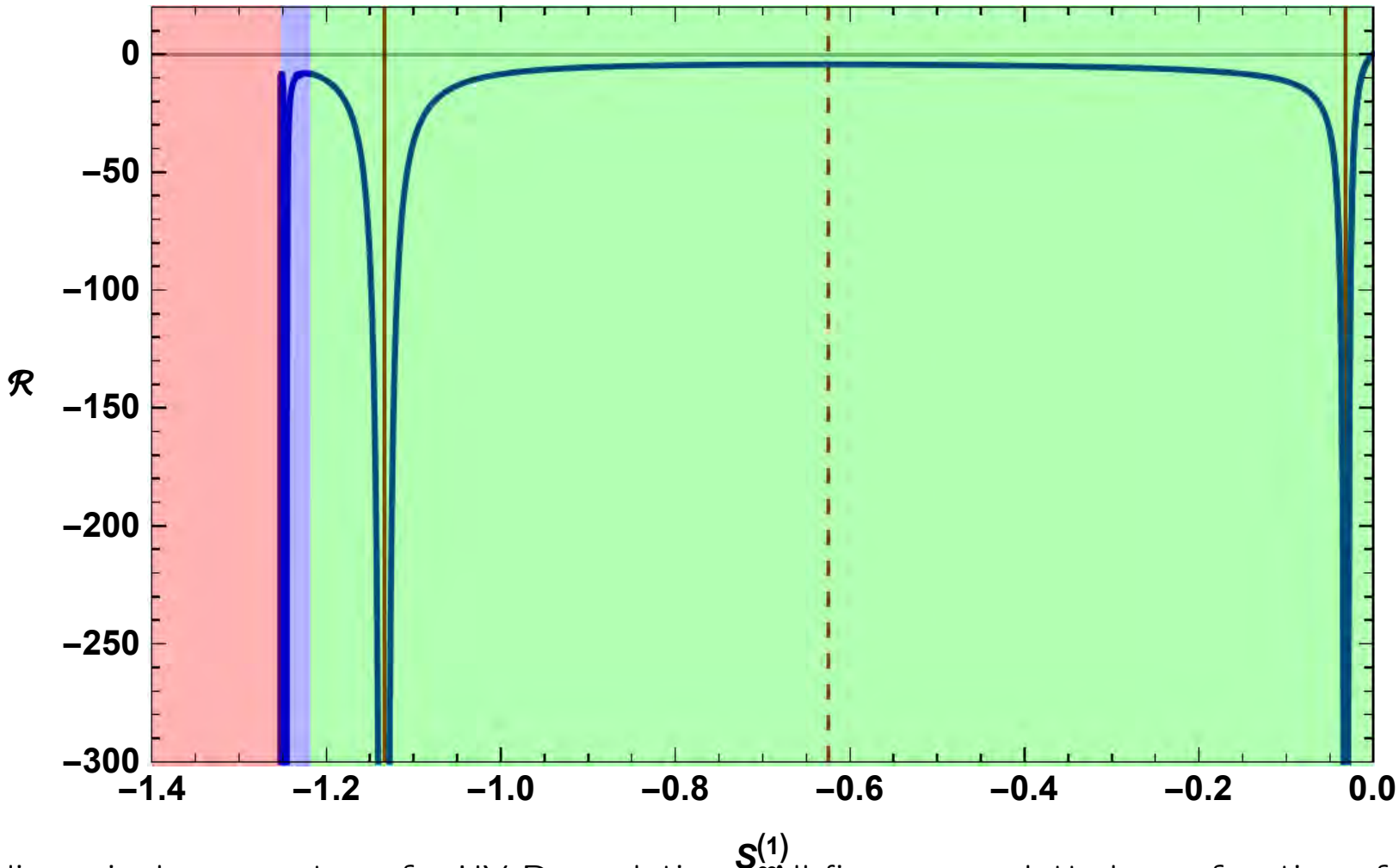

$\mathcal{R}$, the dimensionless curvature, for UV-Reg solutions. All figures are plotted as a function of the free parameter $S_\infty^{(1)}$. In each graph, the green region belongs to the regular solutions without A-bounce and the blue region to solutions with at least one A-bounce. In the red region, we have solutions without boundary. The vertical dashed line in figure (a) corresponds to the global AdS solution in the uplifted theory and the product solution is the solution right before the blue-red boundary.

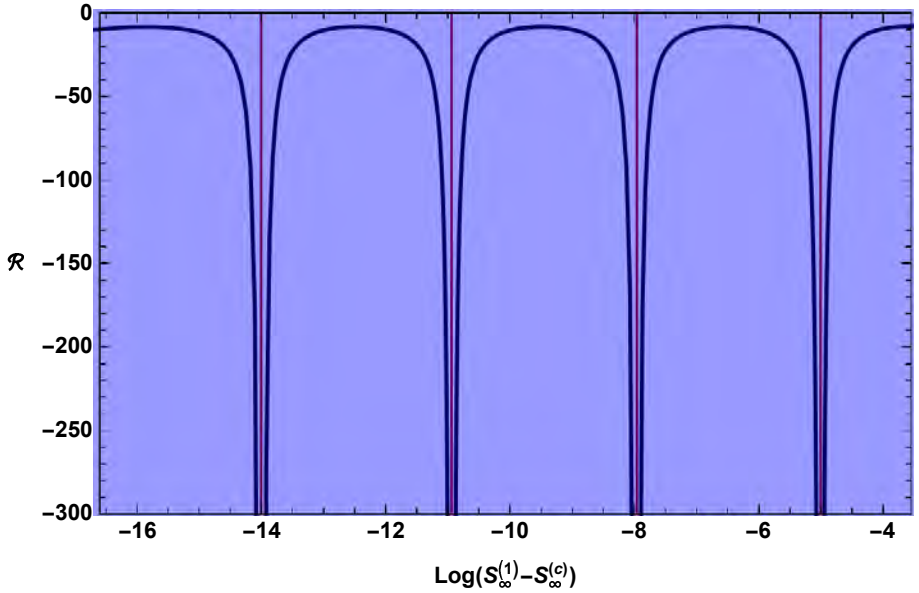

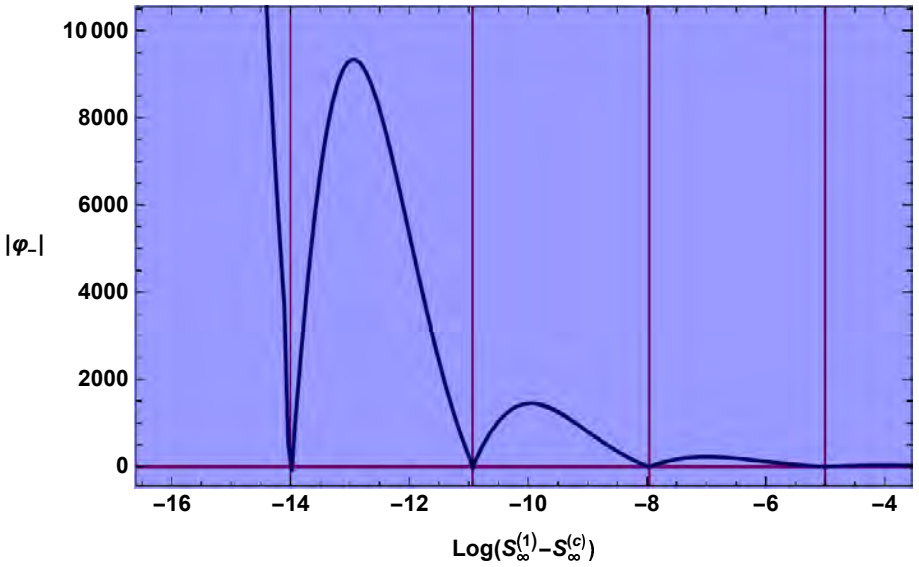

The blue region in detail. The horizontal axis is $\log(S_\infty^{(1)} - S_\infty^{(c)})$, where $S_\infty^{(c)} \approx -1.25$ is the critical value for which we have the UV-Reg solution with infinite numbers of the loops.

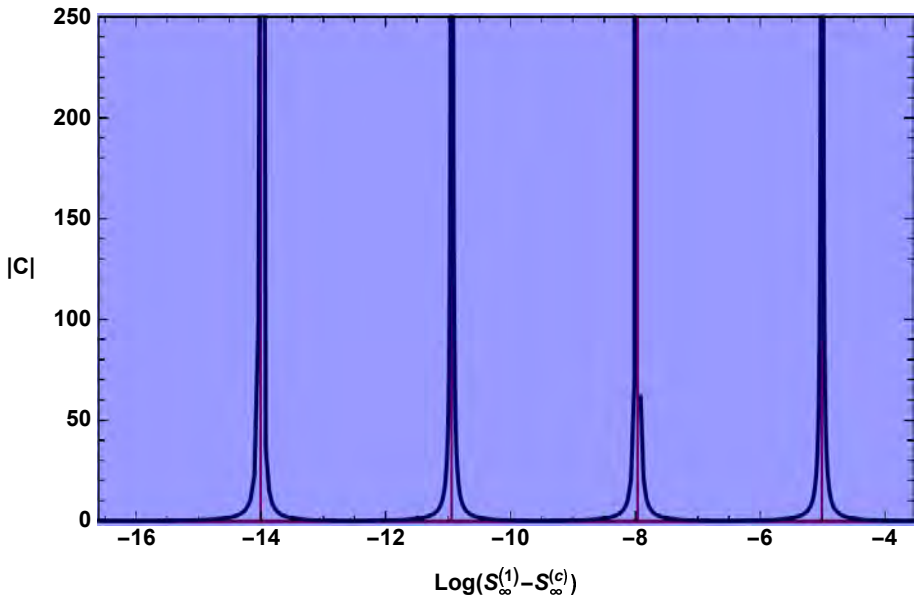
250
200
150
100
50
0
|C|
−16
−14
−12
−10
−8
−6
−4
Log($S_\infty^{(1)}-S_\infty^{(c)}$)

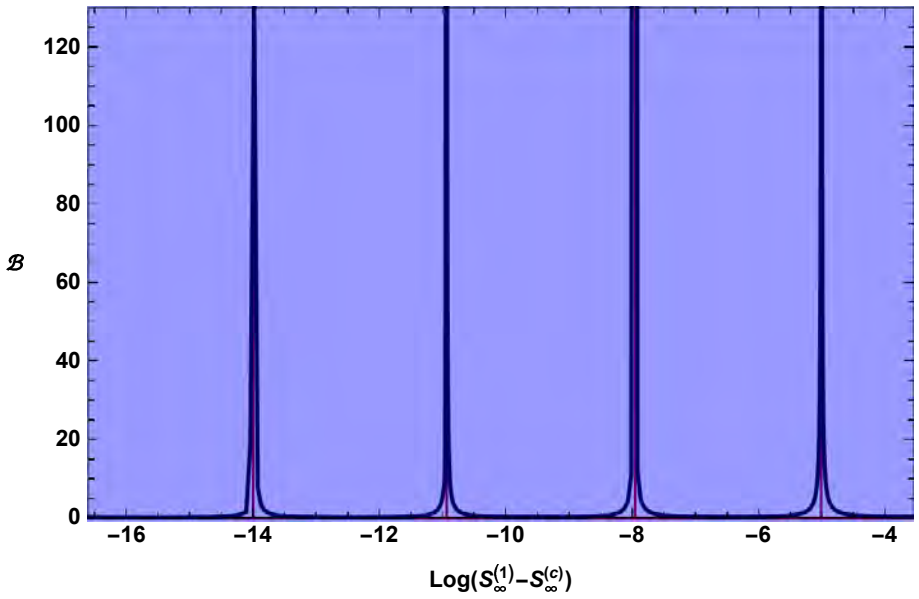
120
100
80
60
40
20
0
ℬ
−16
−14
−12
−10
−8
−6
−4
Log($S_\infty^{(1)}-S_\infty^{(c)}$)

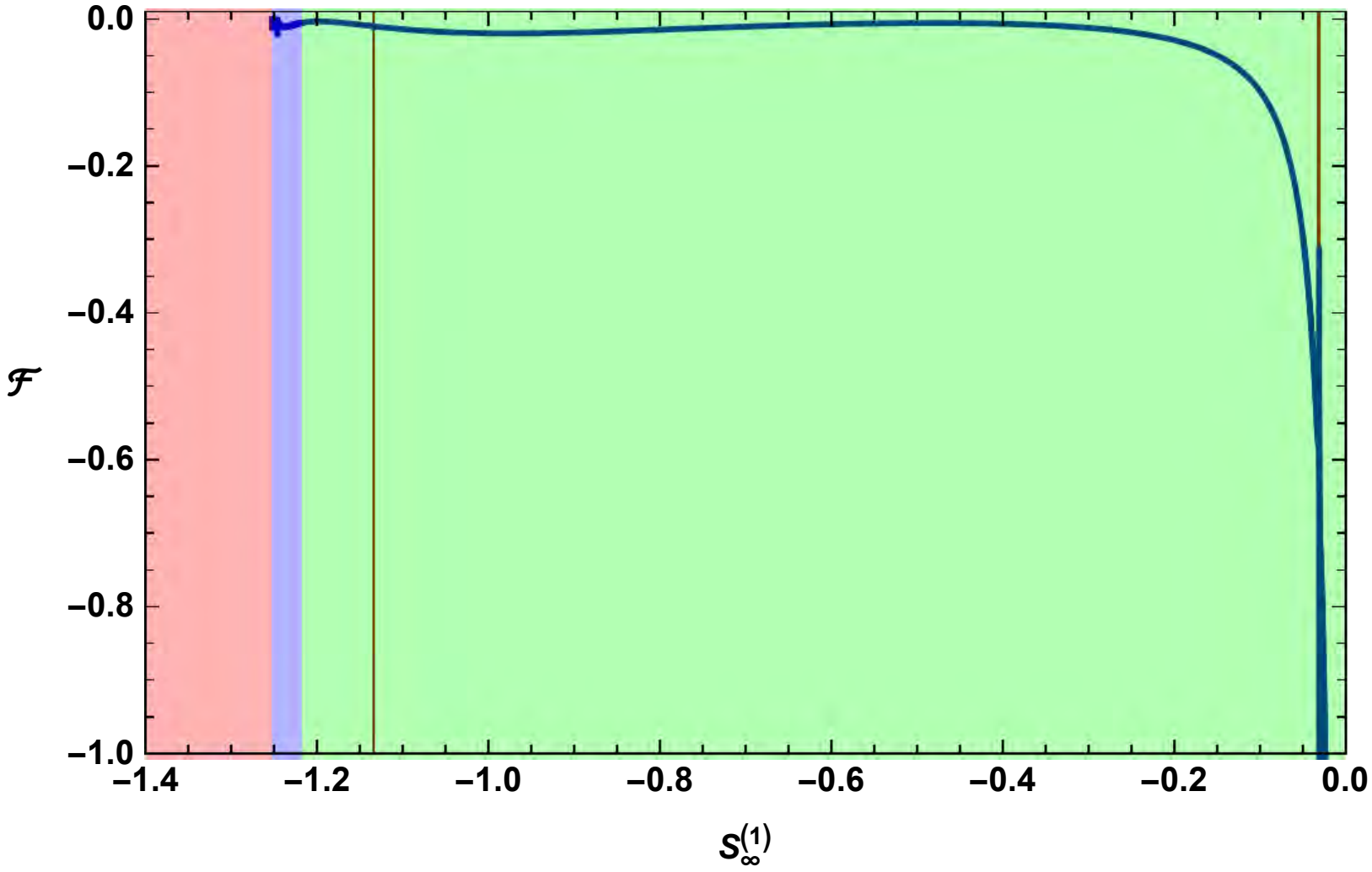

(a): The free energy for UV-Reg solutions living on the black curves. The vertical red lines show the location of Φ-bounces.

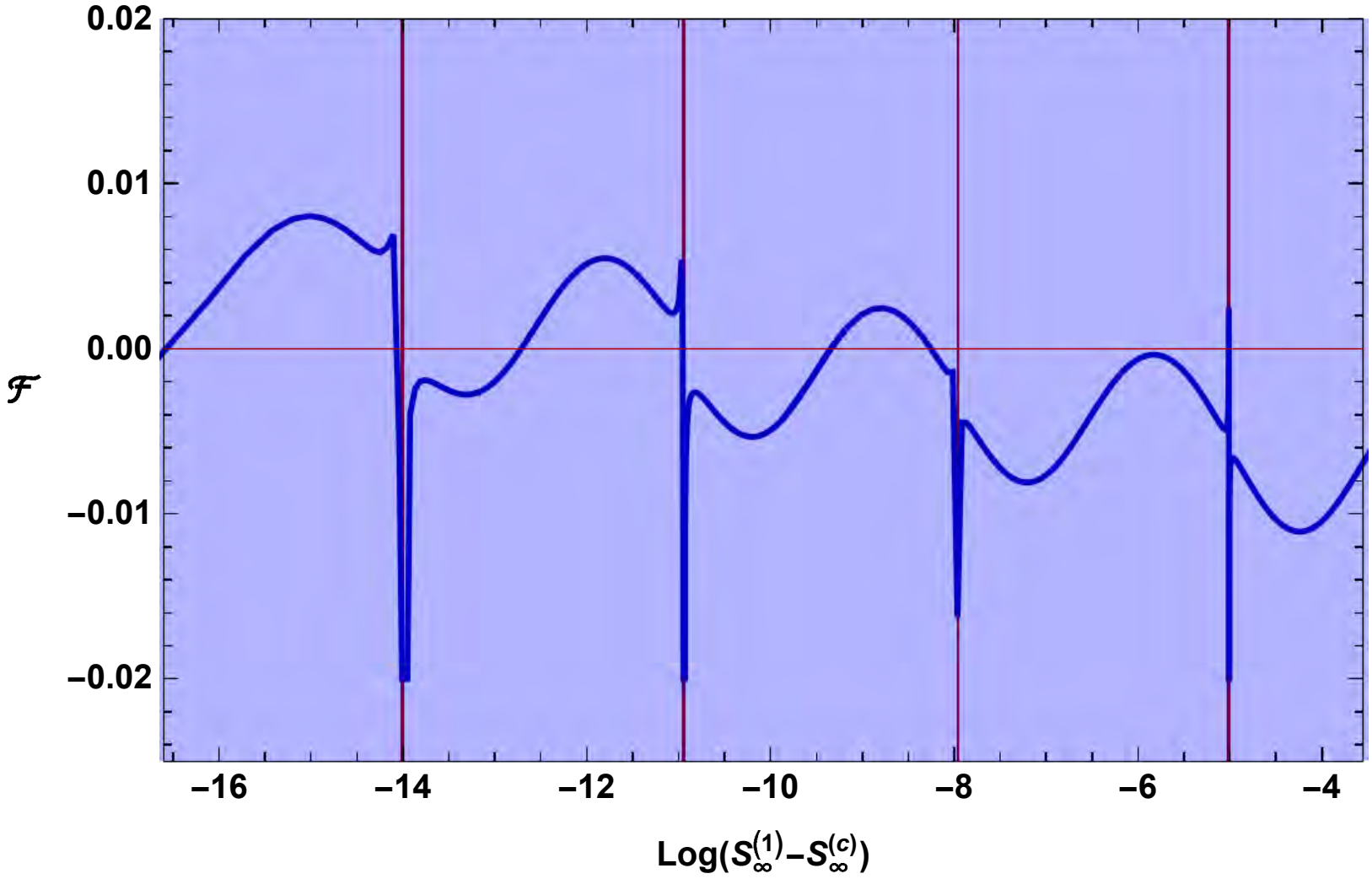

The blue region is zoomed in. The horizontal line is now $\log(S_\infty^{(1)} - S_\infty^{(c)})$, where $S_\infty^{(c)} \approx -1.25$ is the critical value for which we have the UV-Reg solution with infinite numbers of loops. The vertical red lines show the location of Φ-bounces.

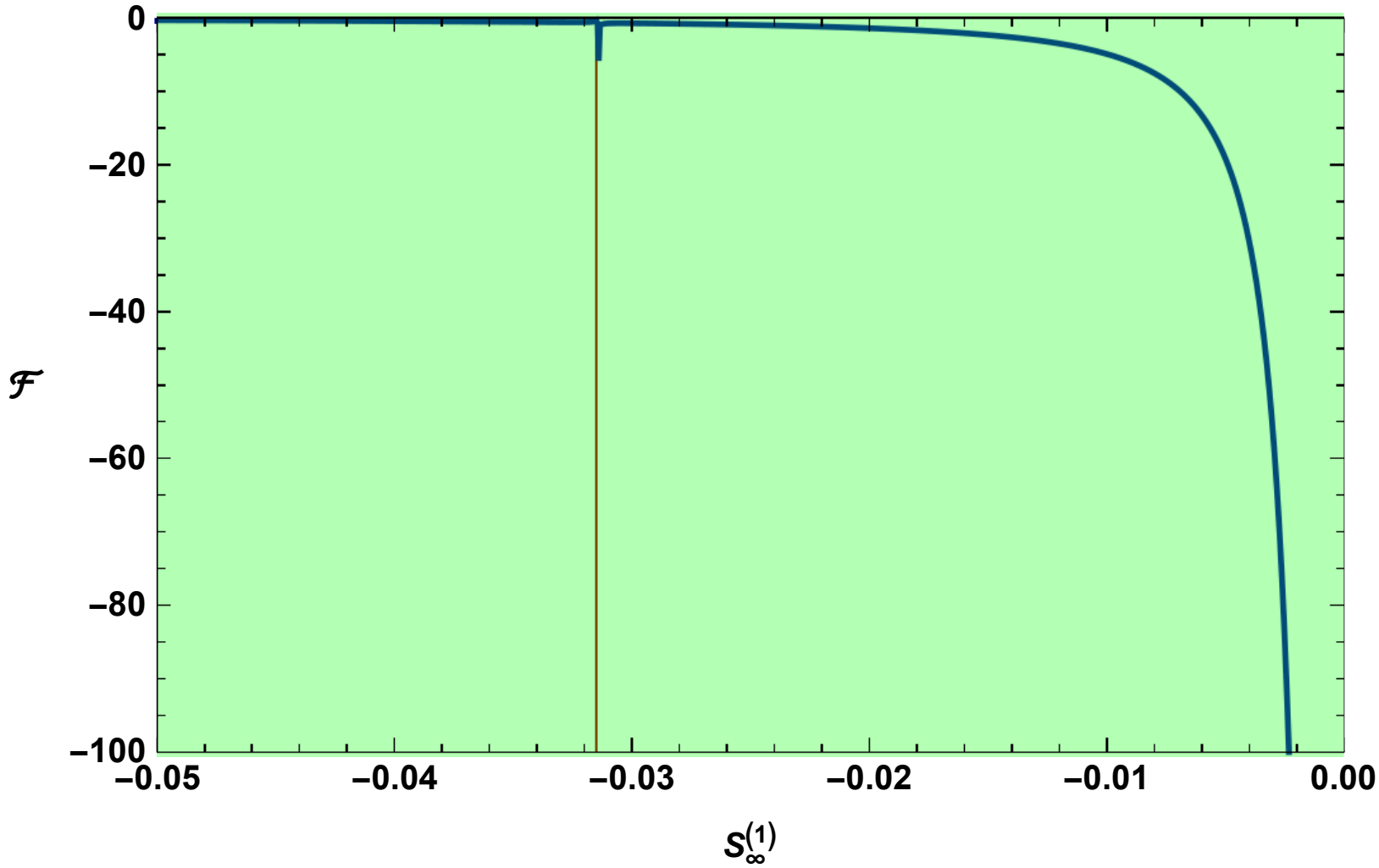

The region near $S_\infty^{(1)} = 0$ is zoomed. The vertical red lines show the location of Φ-bounces.

The AdS free energy

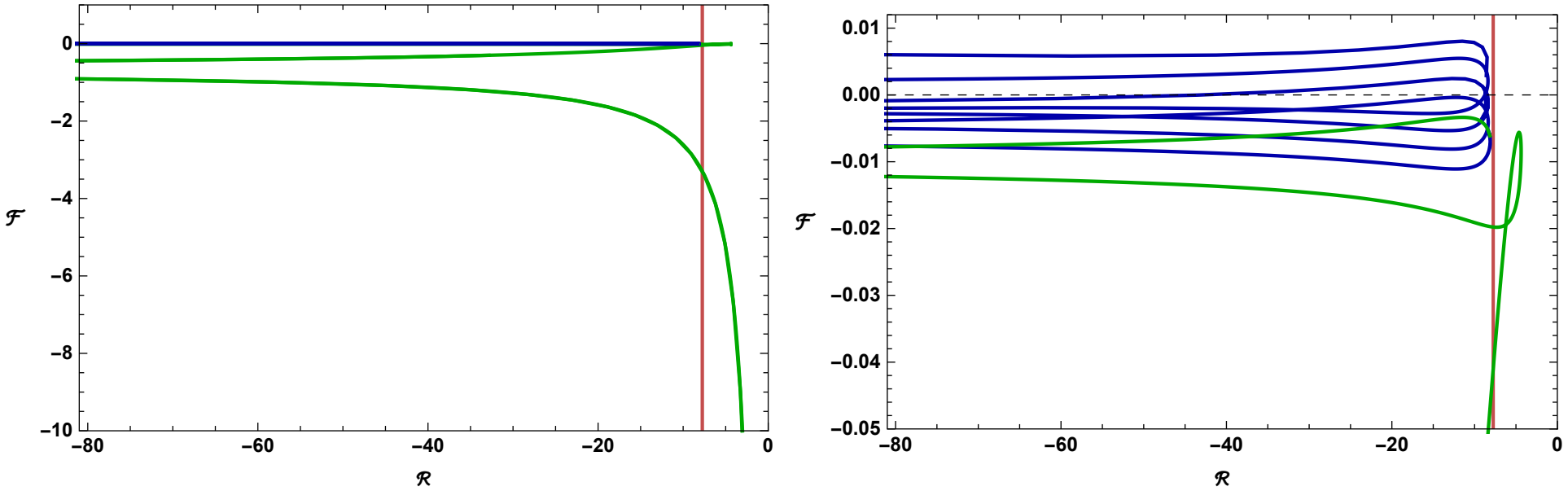

(a): Free energy in terms of dimensionless curvature. The green/blue curves correspond to the green/blue region in previous plots. Figure (b) is the zoomed region near $\mathcal{F} = 0$. The vertical red line shows for $\mathcal{R} \gtrsim -7.7$ only solutions without A-bounce exist.

- The solution with no oscillations has the lowest free energy.
- Is there Efimov scaling here?

Solutions with no AdS$_{d+1}$ boundary

• These are solutions that go from $\Phi = -\infty$ to $\Phi = \pm\infty$, and are classified by the number of Φ-bounces, $n = 0, 1, 2, \cdots$.

• We believe that a reasonable interpretation of such solutions is as interfaces between topological QFTs on each side.

• There are only topological observables in the bulk QFTs.

• If the slices have a (side) boundary, then there are non-trivial correlation functions of interface operators.

• They are associated to linearized solutions around the I_n solutions sourced at the side boundary.

Spectra

- We linearize the theory around the previous solutions.

- The metric g_{AB} in terms of the background metric $g^{(0)}_{AB}$ and its fluctuations h_{AB} becomes

$$ds^2 = a^2(y)\Big[g^{(0)}_{AB} + h_{AB}(y, x^\mu)\Big]dx^A dx^B\,,$$

$$h_{yy} \to 2\phi \quad , \quad h_{\mu y} \to A_\mu \quad , \quad h_{\mu\nu} \to h_{\mu\nu}\,.$$

$$\Phi = \Phi_0(y) + \chi(y, x^\mu)\,.$$

- We do the standard decomposition:

$$A_\mu = \nabla_\mu W + A^T_\mu\,,$$

$$h_{\mu\nu} = 2\zeta_{\mu\nu}\psi + 2\nabla_{(\mu}\nabla_{\nu)}E + 2\nabla_{(\mu}V^T_{\nu)} + h^{TT}_{\mu\nu}$$

with

$$\nabla^\mu A^T_\mu = 0 \quad , \quad \nabla^\mu V^T_\mu = 0 \quad , \quad \nabla^\mu h^{TT}_{\mu\nu} = h^{TT\mu}_{\mu} = 0\,.$$

• After some song and dance we end up with two propagating degrees of freedom as with flat slices:

♠ Transverse traceless spin-2 $\rightarrow$ massive 4d graviton states.

$$h^{TT}_{\mu\nu} = h(y)\ \xi_{\mu\nu}(x) \quad , \quad (\Box_2 - \frac{2}{3}\kappa - M^2)\xi_{\mu\nu} = 0$$

$$h'' + 3\frac{a'}{a}h + M^2 h = 0$$

• This can be mapped as usual into a 1-d Schrodinger equation with a potential.

♠ A single scalar mode satisfying

$$\widehat{\lambda}''_m(y) + A\widehat{\lambda}'_m(y) + B\widehat{\lambda}_m(y) = 0 \qquad , \qquad z \equiv \frac{a\Phi'_0}{a'}\,.$$

$$A = 3\frac{a'}{a} + 6\frac{z'}{z}\frac{3m^2+4\kappa}{(9m^2+12\kappa-\kappa z^2)}\,, B = m^2 + 2\kappa + \frac{2\kappa a z'}{a' z}\frac{3m^2+4\kappa}{(9m^2+12\kappa-\kappa z^2)}\,.$$

• Solving for the eigenvalues of this is harder.

$$(\nabla_\mu \nabla^\mu - \frac{1}{3} s\kappa)\delta h = \begin{cases} -\frac{1}{\alpha^2}(\nu^2 - \frac{9}{4})\delta h & dS \\ -k^2 \delta h & Minkowski\,, \\ \frac{1}{\alpha^2}(\nu^2 - \frac{9}{4})\delta h & AdS \end{cases}$$

$$\nu = \frac{1}{2}\sqrt{(d-1)^2 + 4\mathfrak{m}^2\alpha^2} \quad , \quad \mathfrak{m} = m, M\,.$$

- **Tachyonic stability**

The (4d) mode is tachyon-stable if $\begin{cases} |Re(\nu)| \leq \frac{3}{2}, & dS \\ k^2 \leq 0, & Minkowski \\ Re(\nu) \neq 0, & AdS \end{cases}$

- Independent of the spin, the above relations translate to

$$\text{The mode is tachyon-stable if} \begin{cases} \mathfrak{m}^2 \geq 0, & dS \\ \mathfrak{m}^2 \geq 0, & Minkowski\,, \\ \mathfrak{m}^2 \geq \frac{3}{4}\kappa & AdS \end{cases}$$

- In the dS_4 space-time, in order to have a positive norm state for graviton modes, the mass squared should satisfy

$$M^2\alpha^2 > 2 \quad \Rightarrow \quad M^2 > \frac{2}{3}\kappa\,,$$

which is known as the Higuchi bound.

For each holographic theory the spectra can be calculated numerically.

Flow fragmentation, walking and emergent boundaries

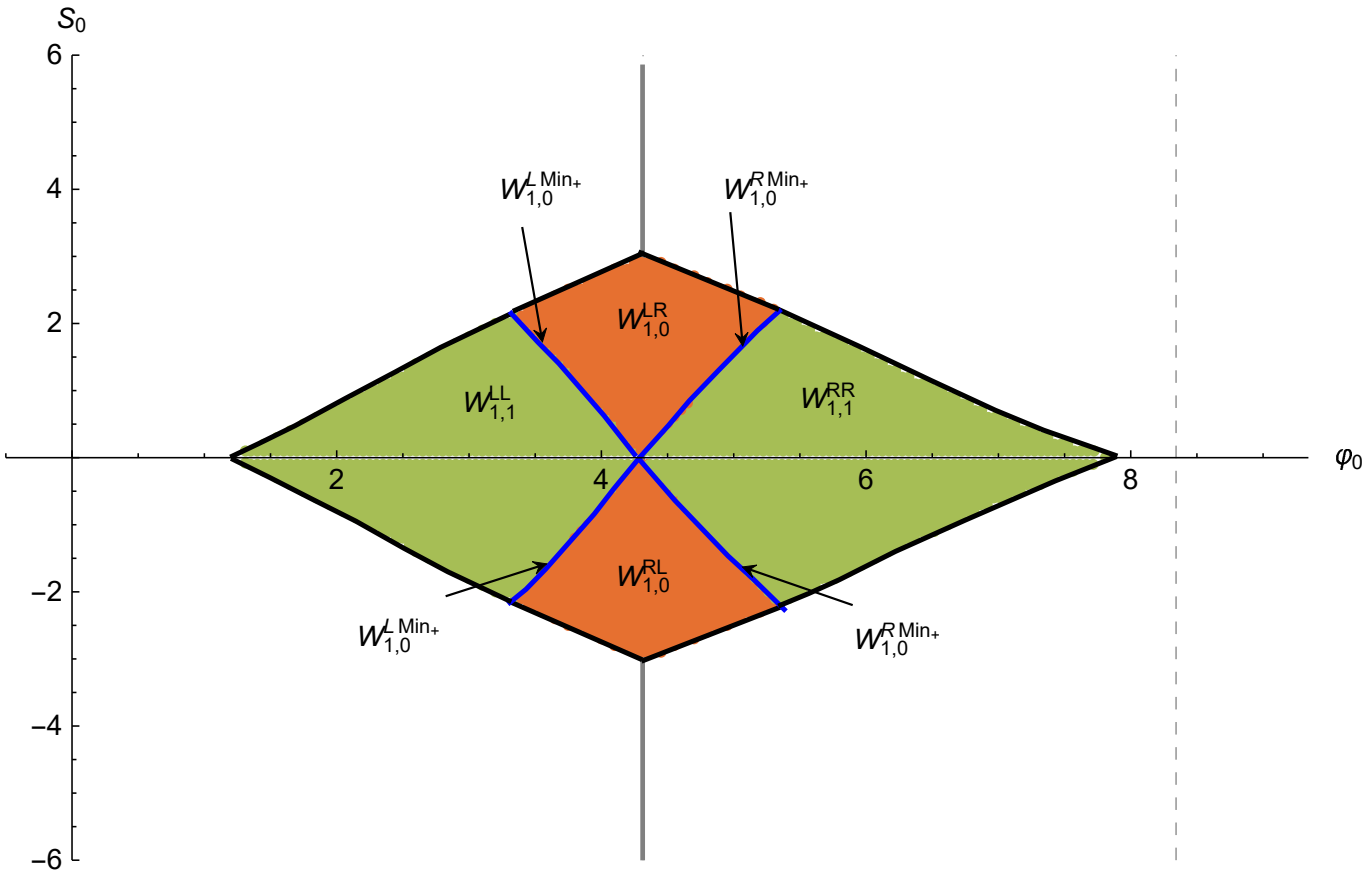

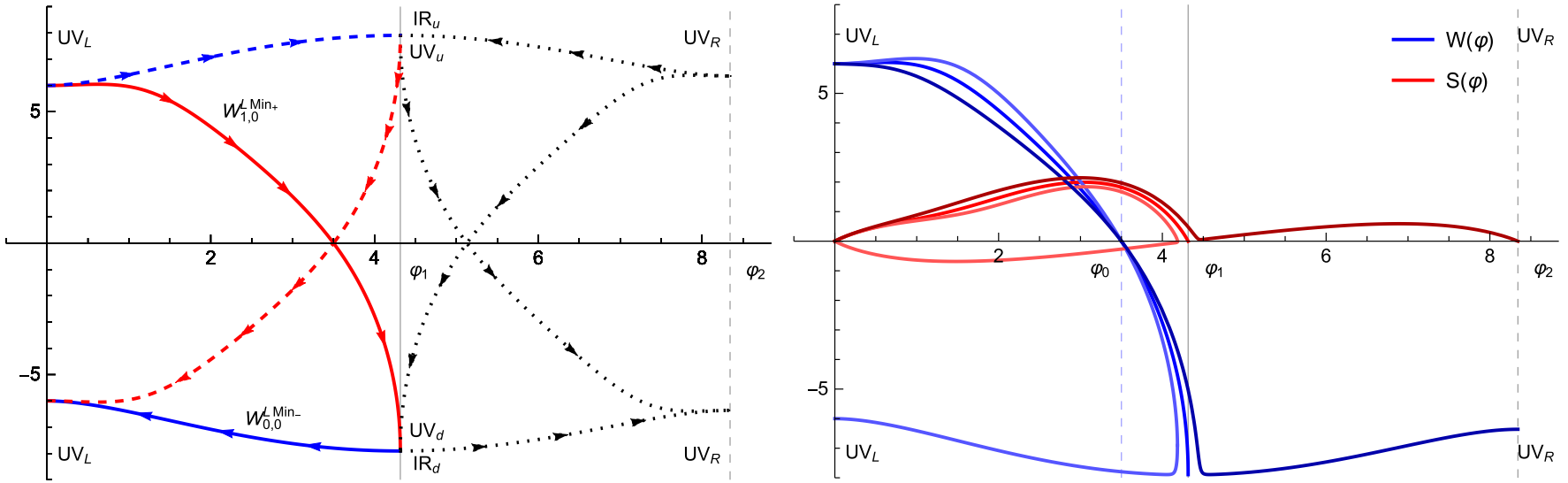

(a): An example of an RG flow between a maximum and a minimum. For the solid curves, (Max_-, Min_+) is a flow between a UV fixed point at maximum $\Phi = 0$ and another UV fixed point at the minimum $\Phi = \Phi_1$. For the (Max_-, Min_-) part of the solution, the minimum is an IR fixed point. The dashed curves show the flipped image of the solid curves. The black dotted curves are other possible RG flows with the same UV fixed points. (b): At a fixed Φ_0 when the value of S_0 is exactly on the border of type $W^{LR}_{1,0}$ and type $W^{LL}_{1,1}$, we have the $W^{LMin_+}_{1,0}$ branch solution (the middle flow). If we increase or decrease the value of S_0 we have the $W^{LR}_{1,0}$ or $W^{LL}_{1,1}$ solutions respectively.

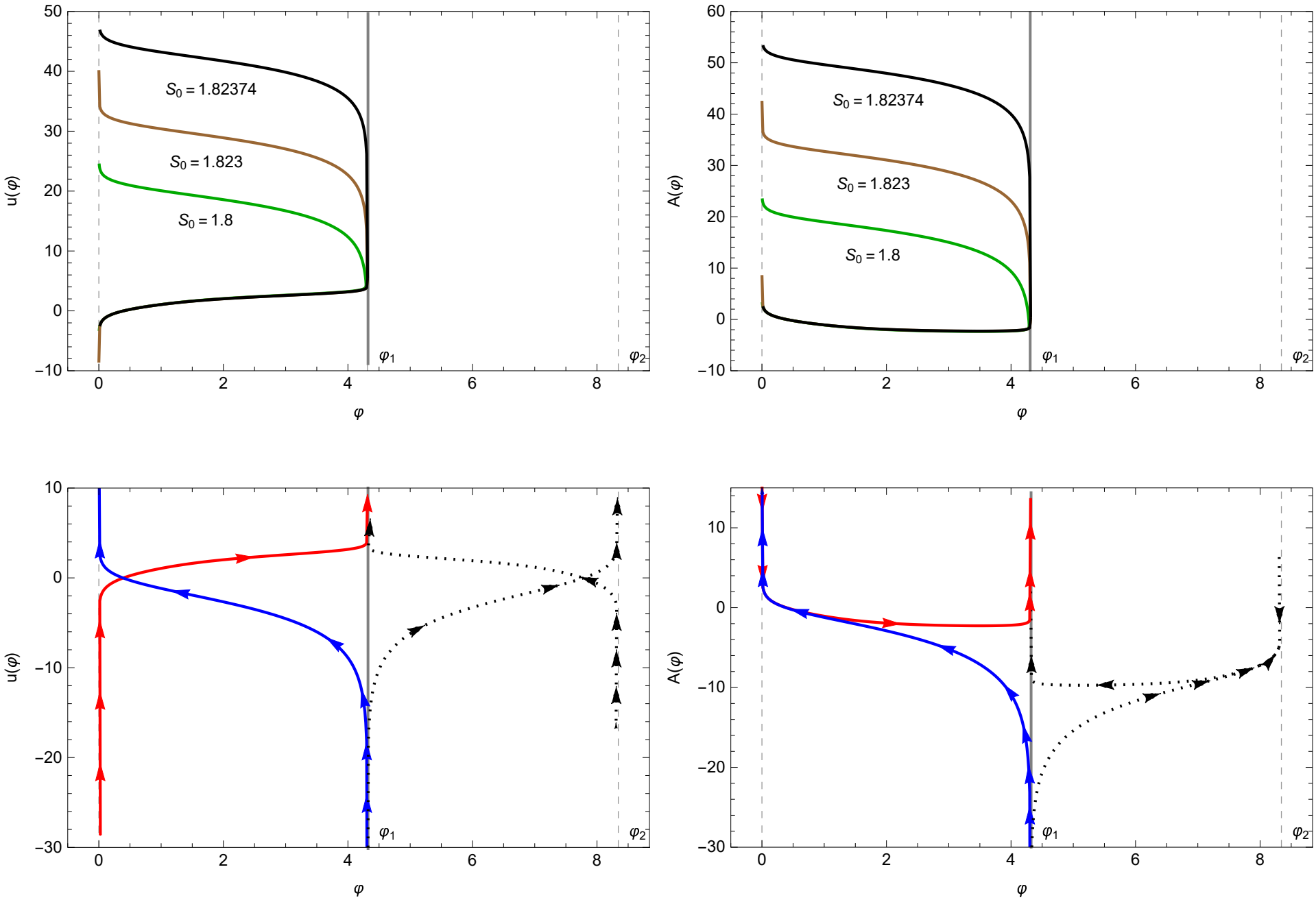

The behavior of the holographic coordinate and scale factor in terms of Φ for the $W_{1,0}^{LMin_+}$ and $W_{0,0}^{LMin_-}$ RG flows. The red curve belongs to $W_{1,0}^{LMin_+}$ and the blue to $W_{0,0}^{LMin_-}$.

• In this limiting region we have an explicit example of solution fragmentation.

• There are two phenomena visible in this example.

♠ Walking. This the phenomenon when an intermediate AdS region appears between the UV and IR, or between UV and UV as is the case here

♠ The emergence of a new boundary.

$$(Max_-, Max_-) \quad \rightarrow \quad (Max_-, Min_-) \quad \oplus \quad (Min+, Max_-)$$

• Such flows can be rotated into cosmological solutions with a cosmological bounce, no singularity and "inflation" at the place of big bag.

Curvature-driven phase transitions and confinement, II

- There is a special value of the asymptotic exponent a in

$$V \simeq -V_\infty e^{2a\Phi} + \cdots ,$$

that we call the *Efimov bound*

$$a = a_{\mathsf{E}} \equiv \frac{2}{\sqrt{(d-1)(9-d)}} ,$$

- There are two regimes:

$$a_C < a < a_{\mathsf{E}} \qquad \text{and} \qquad a_{\mathsf{E}} < a < a_G$$

- $a > a_{\mathsf{E}}$: **Efimov regime.** the vev $\mathcal{C} = \mathcal{C}(\mathcal{R})$ is a multi-valued function of $\mathcal{R}$ exhibiting an Efimov spiral that circles around the critical value $(\mathcal{R}_{\mathsf{C}}, \mathcal{C}_{\mathsf{C}})$ of the type I solution.

• In this case the curvature-driven transition is first order.

• $a < a_{\rm E}$: **Monotonic regime.** There is no Efimov spiral, but there are two qualitatively possible behaviors in which the order of the phase transition is different.

♠ In the first case, the vev $\mathcal{C} = \mathcal{C}(\mathcal{R})$ is multi-valued and exhibits a single swing (instead of a spiral) as it passes through $(\mathcal{R}_{\rm C}, \mathcal{C}_{\rm C})$.

• The free energy contains a swallow tail and the transition is first-order.

♠ In this second case, the vev $\mathcal{C} = \mathcal{C}(\mathcal{R})$ is single-valued and there is a single regular solution for each value of $\mathcal{R}$.

• In this case, we show that the transition is at least second-order, but it may also be higher-order.

$$\text{order of the transition} = 1 + \lceil \delta \rceil \geq 3 \quad , \quad \delta = \frac{(d-1)\,a + 2\sqrt{1-(a/a_{\rm E})^2}}{(d-1)\,a - 2\sqrt{1-(a/a_{\rm E})^2}} > 1$$

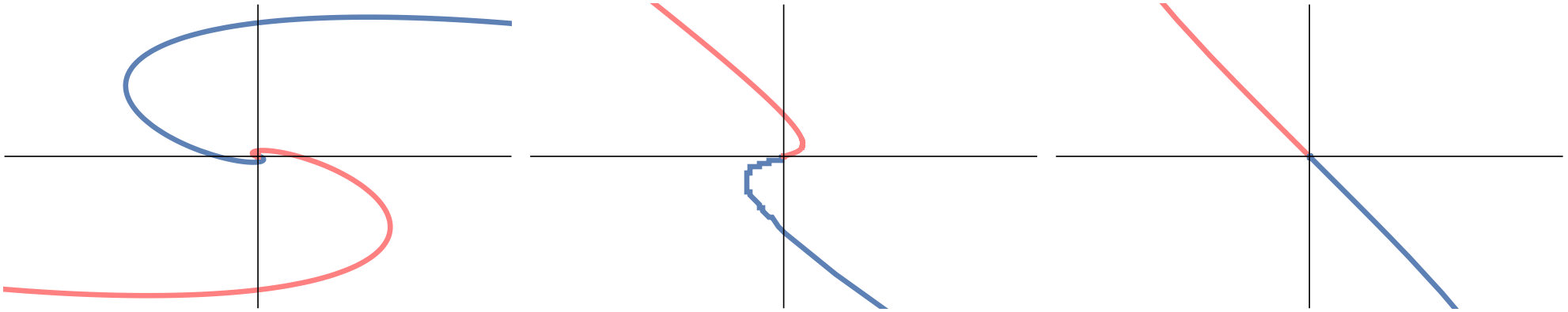

Parameters in IHQCD

- We have 3 initial conditions in the system of graviton-dilaton equations:

♠ One is fixed by picking the branch that corresponds asymptotically to $\lambda \sim \frac{1}{\log(r\Lambda)}$

♠ The other fixes $\Lambda \to \Lambda_{QCD}$.

♠ The third is a gauge artifact as it corresponds to a choice of the origin of the radial coordinate.

- We parameterize the potential as

$$V(\lambda) = \frac{12}{\ell^2}\left\{1 + V_0\lambda + V_1\lambda^{4/3}\left[\log\left(1 + V_2\lambda^{4/3} + V_3\lambda^2\right)\right]^{1/2}\right\},$$

- We fix the one and two loop β-function coefficients:

$$V_0 = \frac{8}{9}b_0 \quad , \quad V_2 = b_0^4\left(\frac{23 + 36b_1/b_0^2}{81V_1^2}\right)^2 , \quad \frac{b_1}{b_0^2} = \frac{51}{121}.$$

and remain with two leftover arbitrary (phenomenological) coefficients.

Fit and comparison

	HQCD	lattice $N_c = 3$	lattice $N_c \to \infty$	Parameter
$[p/(N_c^2T^4)]_{T=2T_c}$	**1.2**	**1.2**	-	$V1 = 14$
$L_h/(N_c^2T_c^4)$	**0.31**	0.28 (Karsch)	**0.31** (Teper+Lucini)	$V3 = 170$
$[p/(N_c^2T^4)]_{T\to+\infty}$	$\pi^2/45$	$\pi^2/45$	$\pi^2/45$	$M_p\ell = [45\pi^2]^{-1/3}$
$m_{0^{++}}/\sqrt{\sigma}$	**3.37**	3.56 (Chen)	**3.37** (Teper+Lucini)	$\ell_s/\ell = 0.15$
$m_{0^{-+}}/m_{0^{++}}$	**1.49**	**1.49** (Chen)	-	$c_a = 0.26$
χ	$(191MeV)^4$	$(191MeV)^4$ (DelDebbio)	-	$Z_0 = 133/4$
$T_c/m_{0^{++}}$	0.167	-	0.177(7)	
$m_{0^{*++}}/m_{0^{++}}$	1.61	1.56(11)	1.90(17)	
$m_{2^{++}}/m_{0^{++}}$	1.36	1.40(4)	1.46(11)	
$m_{0^{*-+}}/m_{0^{++}}$	2.10	2.12(10)	-	

- G. Boyd, J. Engels, F. Karsch, E. Laermann, C. Legeland, M. Lutgemeier and B. Petersson, *"Thermodynamics of SU(3) Lattice Gauge Theory,"* Nucl. Phys. B **469**, 419 (1996) [arXiv:hep-lat/9602007].

- B. Lucini, M. Teper and U. Wenger, *"Properties of the deconfining phase transition in SU(N) gauge theories,"* JHEP **0502**, 033 (2005) [arXiv:hep-lat/0502003];
"SU(N) gauge theories in four dimensions: Exploring the approach to $N = \infty$," JHEP **0106**, 050 (2001) [arXiv:hep-lat/0103027].

- Y. Chen *et al.*, *"Glueball spectrum and matrix elements on anisotropic lattices,"* Phys. Rev. D **73** (2006) 014516 [arXiv:hep-lat/0510074].

- L. Del Debbio, L. Giusti and C. Pica, *"Topological susceptibility in the SU(3) gauge theory,"* Phys. Rev. Lett. **94**, 032003 (2005) [arXiv:hep-th/0407052].

The pressure from the lattice at different N

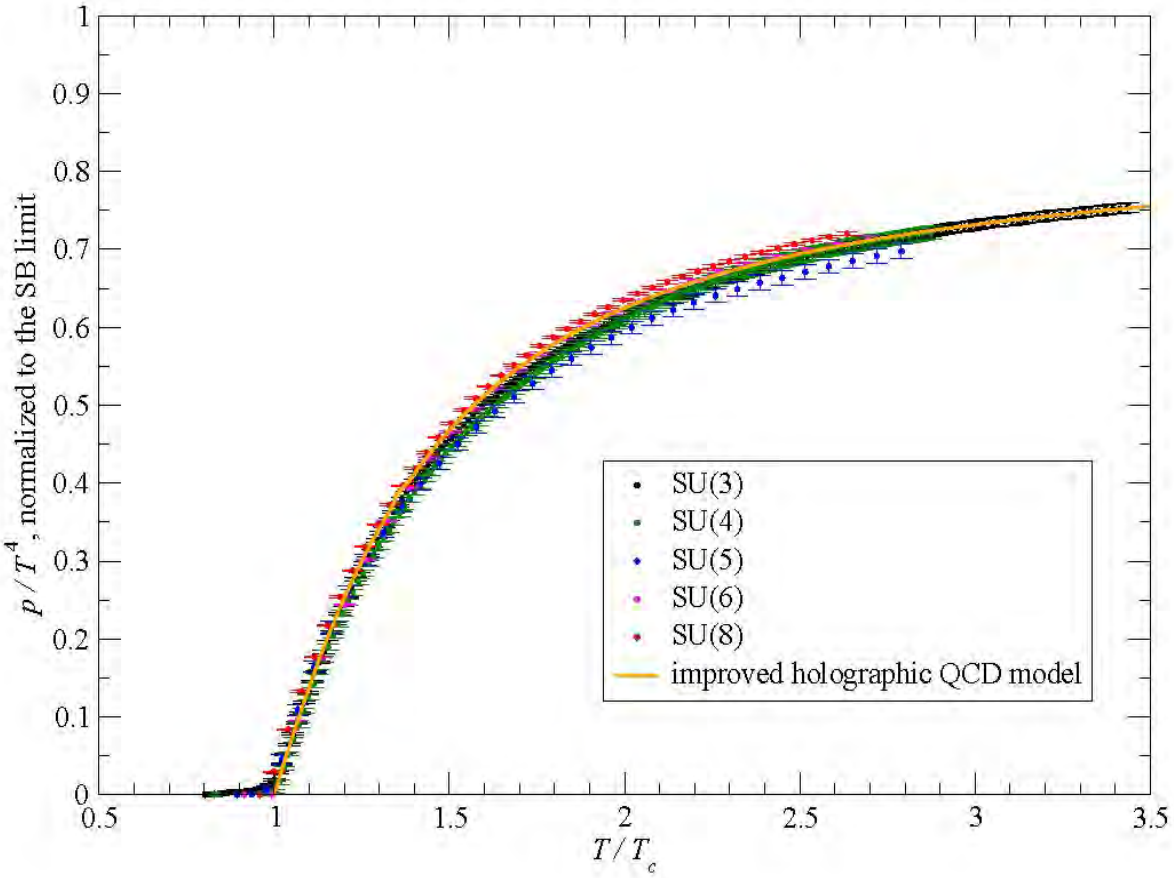

Figure 1: (Color online) The dimensionless ratio p/T^4, normalized to the lattice SB limit $\pi^2(N^2-1)R_I(N_t)/45$, *versus* T/T_c, as obtained from simulations of SU(N) lattice gauge theories on $N_t = 5$ lattices. Errorbars denote statistical uncertainties only. The results corresponding to different gauge groups are denoted by different colors, according to the legend. The yellow solid line denotes the prediction from the improved holographic QCD model from ref. [75] (with a trivial, parameter-free rescaling to our normalization).

Marco Panero arXiv: 0907.3719

The entropy from the lattice at different N

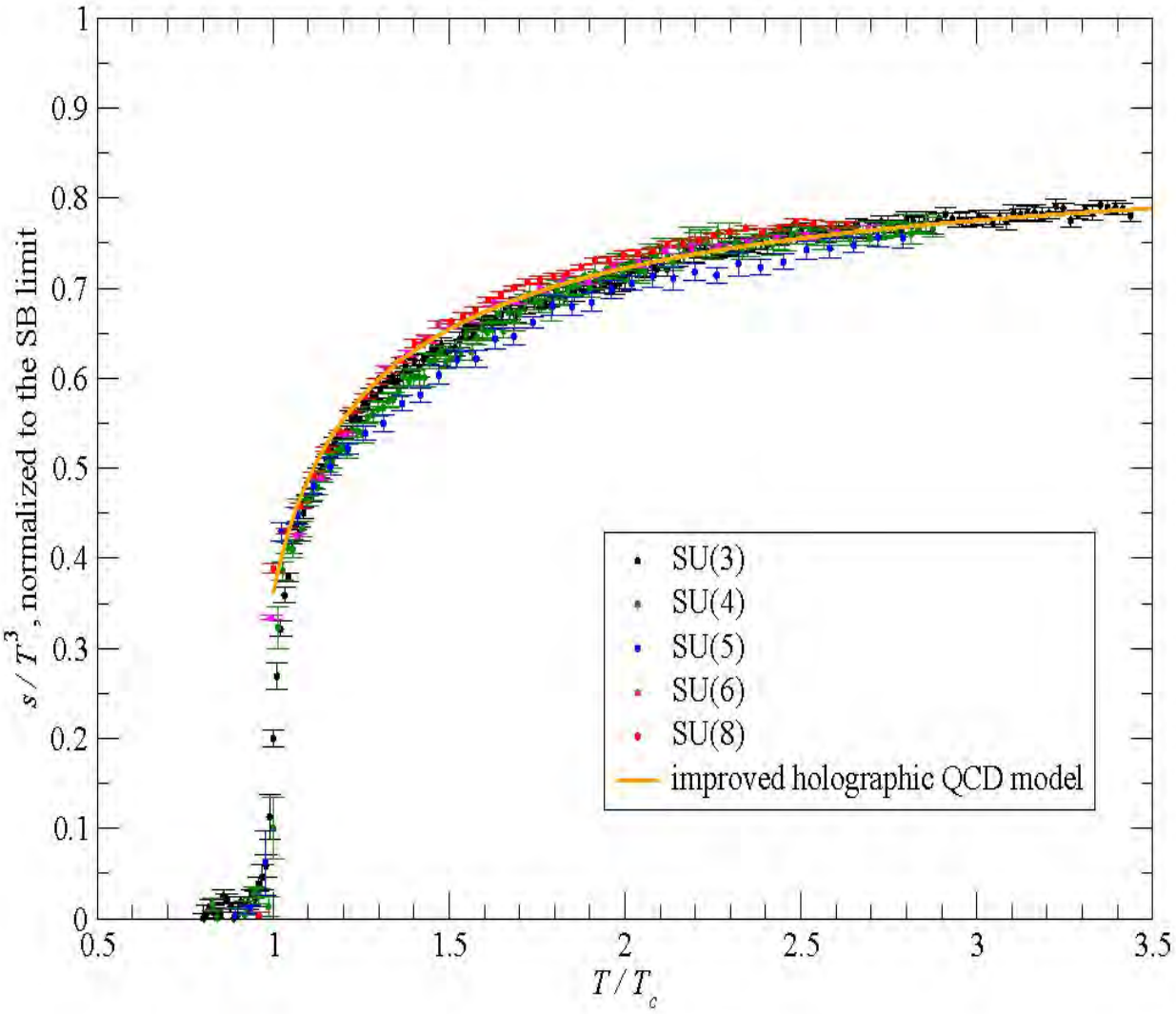

Figure 4: (Color online) Same as in fig. 1, but for the s/T^3 ratio, normalized to the SB limit.

Marco Panero arXiv: 0907.3719

The trace from the lattice at different N

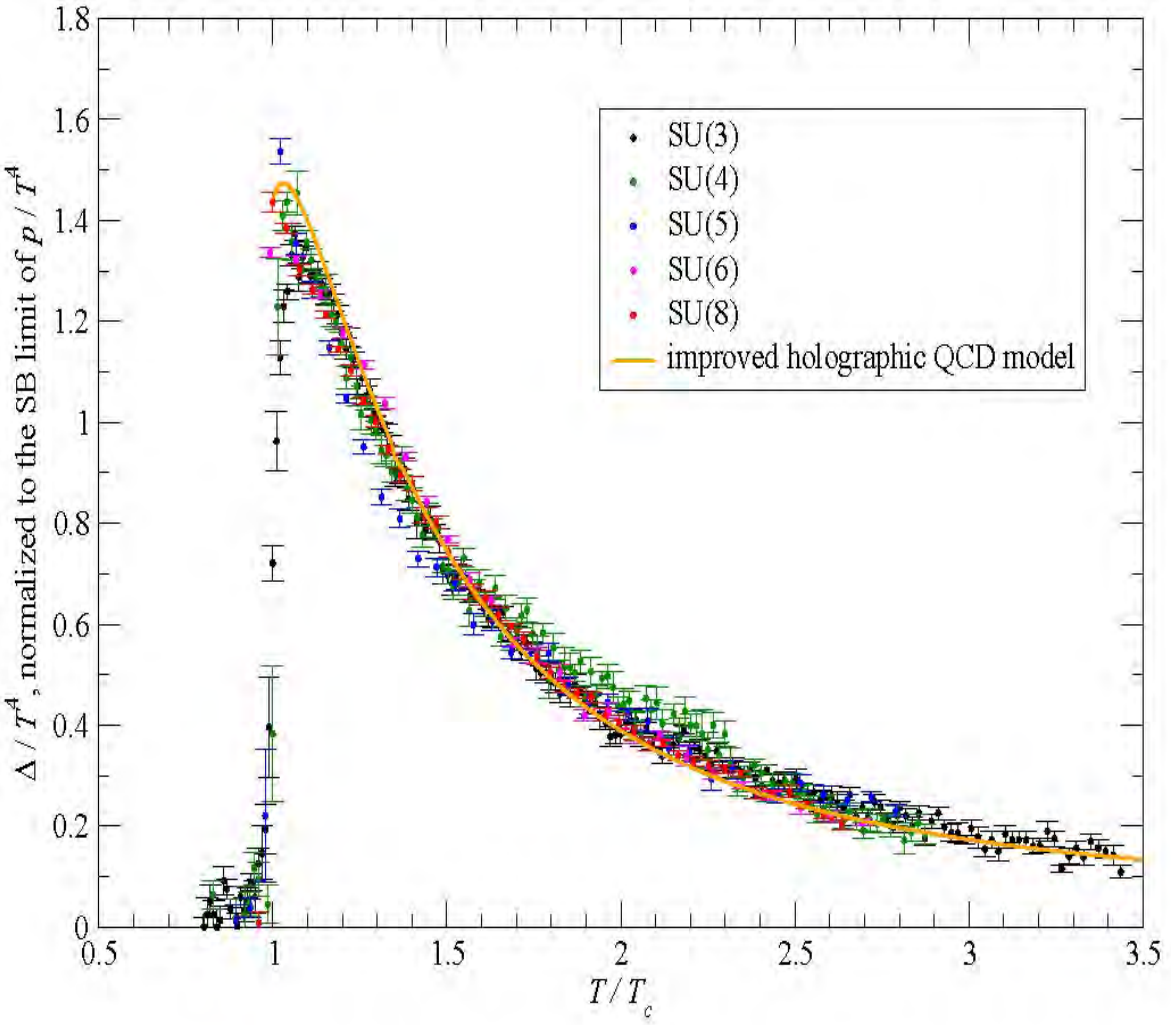

Figure 2: (Color online) Same as in fig. 1, but for the Δ/T^4 ratio, normalized to the SB limit of p/T^4.

Marco Panero arXiv: 0907.3719

The speed of sound

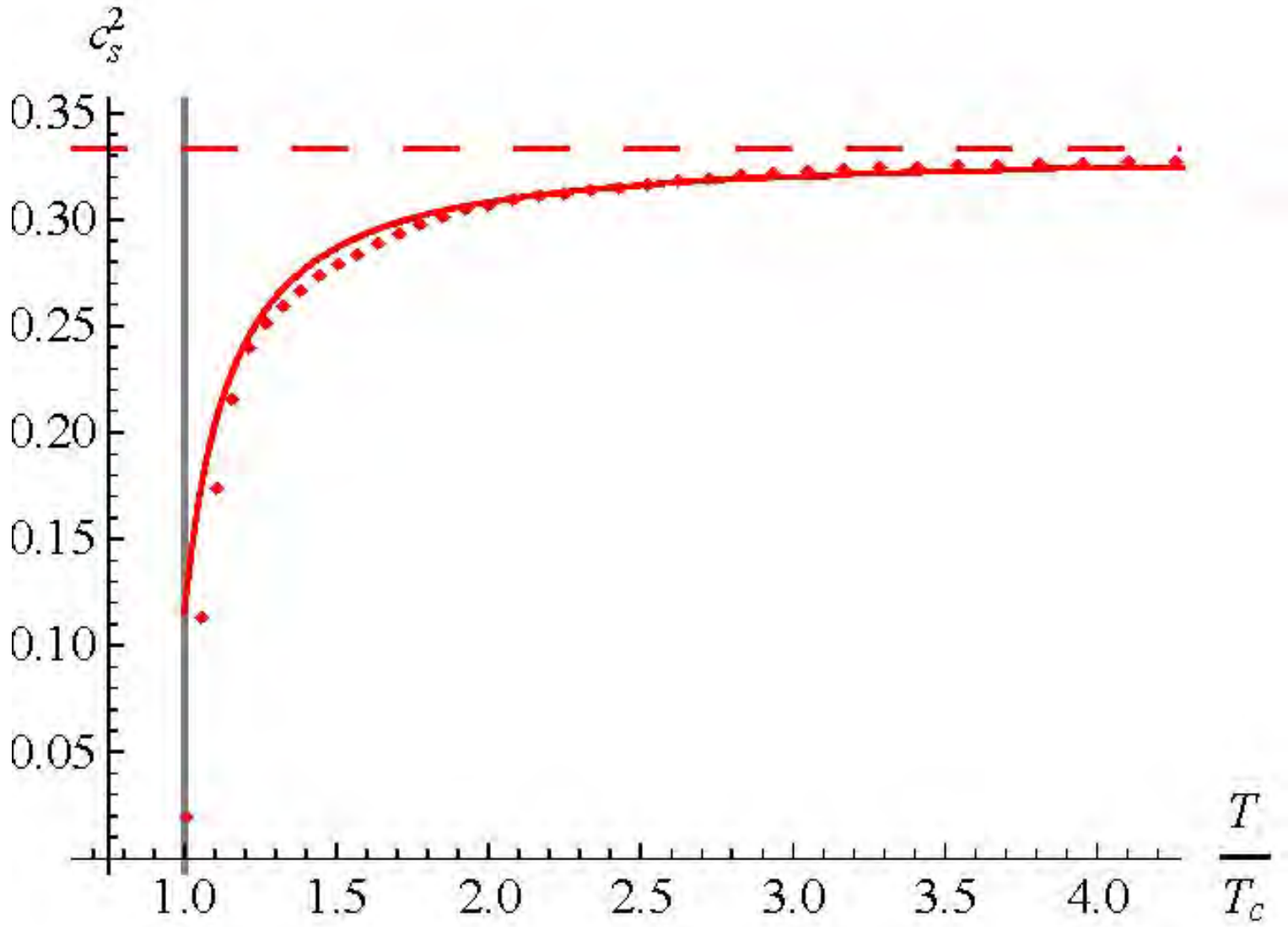

The bulk viscosity in IHQCD

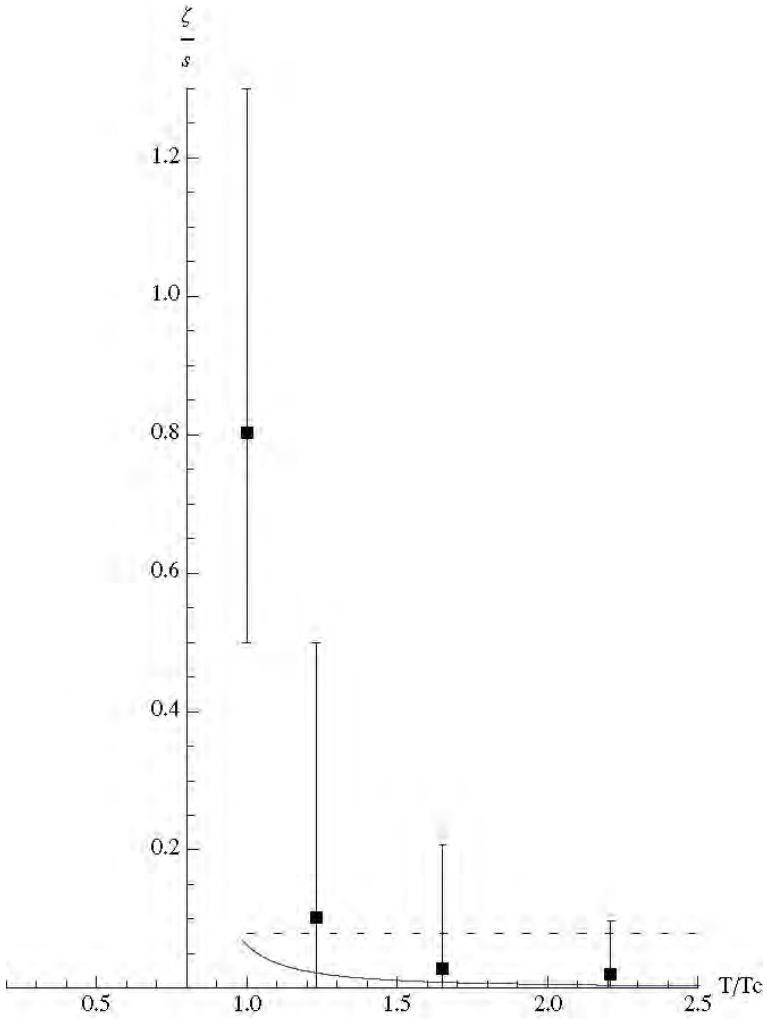

Gursoy+Kiritsis+Michalogiorgakis+Nitti, 2009

- Pure glue only. Calculations with other potentials show robustness. *Gubser*

Detailed plan of the presentation

- Title page 0 minutes
- Bibliography 0 minutes
- Introduction 2 minutes
- QFT on AdS 3 minutes
- The holographic picture 5 minutes
- Interfaces 6 minutes
- Holographic Interfaces 9 minutes
- The curved-sliced RG Flows 14 minutes
- The bulk Einstein equations 15 minutes
- The first order formalism 16 minutes
- The bulk integration constants 19 minutes
- Asymptotics near potential extrema 25 minutes
- Classification of complete flows $\mathcal{R} = 0$ 28 minutes
- Classification of complete flows $\mathcal{R} > 0$ 31 minutes
- Classification of complete flows $\mathcal{R} < 0$ 34 minutes

- Classifying the solutions, $\mathcal{R} < 0$ 38 minutes
- Flow fragmentation, walking and emergence of boundaries 40 minutes
- The dS RG Flows 42 minutes
- Confining Theories on curved manifolds 43 minutes
- Confining Theories on curved manifolds, II 45 minutes
- Confining Theories on AdS-The space of solutions 49 minutes
- Relation to Sources 50 minutes
- The Free energy 51 minutes
- Curvature-driven phase transition and confinement 53 minutes
- IHQCD-like theories 56 minutes
- Conclusions 58 minutes
- Open ends 59 minutes

- QFT on AdS 61 minutes
- Conformal Theories on AdS_4 64 minutes
- A Confining Gauge Theory on AdS 67 minutes
- Rigid Holography 70 minutes
- BCFT 71 minutes
- Proximity in QFT 72 minutes
- Holographic QFT_d on AdS_d 73 minutes
- Holographic Conformal Defects 76 minutes
- The bulk integration constants in the two-boundary case 81 minutes
- Classifying the solutions, II 86 minutes
- The QFT couplings 87 minutes
- Three parameter solutions 88 minutes
- $W_{1,1}^{LL}$ 89 minutes

- $W_{1,2}^{LL}$ 90 minutes
- $W_{1,1}^{LR}$ 91 minutes
- A (3,3) (A-bounce,Φ-bounce) solution 92 minutes
- The behavior of relevant couplings 93 minutes
- The $a_3 \cup a_4$ solution: triple fragmentation 94 minutes
- Interface Correlators 97 minutes
- Details of the Confining Potential 100 minutes
- Vevs 103 minutes
- Single boundary solutions 105 minutes
- Proximity in QFT 107 minutes
- The region boundaries and tuned flows 109 minutes
- Flow fragmentation, walking and emergence of boundaries 113 minutes
- Confining Theories on AdS-Critical Solutions 114 minutes
- Solutions with many A loops 115 minutes
- Classifying the solutions, Part I 119 minutes
- AdS mass spectra 120 minutes

- Skipping fixed points 121 minutes
- Skipping flows at finite curvature 122 minutes
- A quantum phase transition for UV_1 123 minutes
- The RG flows from UV_2 124 minutes
- The on-shell action 125 minutes
- The dS entanglement entropy 126 minutes
- The dS thermodynamics 127 minutes
- The free energy and expectation values 128 minutes
- Two-boundary solutions 130 minutes
- AdS-relation to sources 132 minutes
- AdS-The free energy 134 minutes
- Solutions with no boundary 136 minutes
- Spectra 138 minutes
- Flow fragmentation, walking and emergent boundaries 140 minutes
- Curvature-driven phase transitions and confinement, II 142 minutes
- Parameters in IHQCD 144 minutes
- Fit and comparison 146 minutes

- The pressure from the lattice at different N 148 minutes
- The entropy from the lattice at different N 150 minutes
- The trace from the lattice at different N 152 minutes
- The speed of sound in IHQCD 154 minutes
- The bulk viscosity in IHQCD 156 minutes